TWO-DIMENSIONAL MASS DISPERSION IN RIVERS

by

Forrest M. Holly, Jr.

September 1975

TABLE OF CONTENTS

TABLE OF CONTENTS (Cont.)

LIST OF SYMBOLS (Cont.)

Symbol	Definition	Symbol	Definition
RR	= tracer recovery ratio (dimensionless)	V_o	= volume of tracer injection solution (L^3)
R_1, R_2	= numerical conversion coefficients for diffusion and dispersion (dimensionless)	W	= weight of tracer mass in a control volume (F)
R_h	= hydraulic radius (L)	x	= longitudinal coordinate axis (L)
$R_{I,J}, S_{I,J}$	= constant convection coefficients defined by Eq. 2.40 (dimensionless)	x_o	= location of simulation peak centerline concentration, or longitudinal coordinate of instantaneous point source (L)
r	= Courant number, $u\Delta t/\Delta x$ (dimensionless)	x_i	= coordinate axis in the ith direction (L)
S	= surface of control volume, (L^2) or energy slope (dimensionless)	Δx	= distance step in finite difference solution (L)
T	= period of Fourier Series component (T)		
$\underline{T}$	= diffusive tracer transport vector (L/T)	y	= vertical coordinate axis (L)
t	= time (T)	y_o	= vertical coordinate of instantaneous point source (L)
t_o	= time of passage of peak concentration at measured section, or time of injection of instantaneous point source (T)	z	= transverse coordinate axis (L)
Δt	= time step in finite-difference solution (T)	z_o	= reference transverse coordinate, or transverse coordinate of instantaneous point source (L)
U	= constant longitudinal velocity (L/T)	z_1	= shifted coordinate of transverse position (L)
U_o	= longitudinal velocity at $z = 0$ in uniform shear flow (L/T)	z_L, z_R	= transverse coordinate of left and right channel boundaries (L)
U_a	= cross-sectional average longitudinal velocity (L/T)	β_m	= frequency of Fourier Series component (1/T)
U_c	= convective velocity of tracer cloud (L/T)	Γ_y, Γ_z	= vertical and transverse velocity gradients, respectively (1/T)
U_*	= cross-sectional average shear velocity (L/T)	γ	= weight of solute per unit volume (F/L^3)
u, v, w	= local velocities in the x, y, and z directions (L/T)	∇	= vector gradient operator (1/L)
u^y, w^y, c^y	= local deviations from depth-averaged values of longitudinal velocity, transverse velocity (L/T) and concentration (dimensionless)	ε_m	= molecular diffusivity (L^2/T)
u''	= local deviation of the time-averaged longitudinal velocity from the cross-sectional longitudinal velocity (L/T)	ε_N	= artificial (numerical) diffusivity (L^2/T)
$\underline{u}$	= velocity vector (L/T)	ε_t	= eddy viscosity (L^2/T)
u_o	= siphon tube entrance velocity (L/T)	$\varepsilon_x, \varepsilon_z$	= depth-averaged diffusivities, x and z-directions (L^2/T)
u_i	= local velocity in the ith direction (L/T)	$\bar{\varepsilon}_i$	= scalar turbulent diffusivity, i^{th} direction (L^2/T)
u_i'	= instantaneous deviation of the ith direction velocity from the time average at a point (L/T)	ζ	= transverse coordinate of a continuous line source (L)
		η	= dummy distance variable (L)
V	= control volume (L^3)	θ	= general complex number (varies)

vi

Symbol	Definition	Symbol	Definition
κ	= von Karman's constant (dimensionless)	σ_{huC}^2	= transverse variance of tracer flux (L^2)
λ	= cross-sectional average of $\epsilon_z h^2 u (L^5/T^2)$	$\sigma_x^2, \sigma_y^2, \sigma_z^2$	= variances of concentration distribution in x,y,z directions, respectively (L^2)
ρ	= fluid density (M/L^3)	τ_o	= bed shear stress (F/L^2)
σ_m	= wave number of Fourier Series component (1/L)	ϕ	= transverse diffusivity function (L^2/T)
σ_a^2	= longitudinal variance of cross-sectional average concentration (L^2)	ψ	= peak centerline concentration ratio (dimensionless)

ACKNOWLEDGMENTS

ABSTRACT

The design of waste treatment facilities and the establishment of environmentally-acceptable effluent standards for rivers require that the dilution attributable to natural turbulence be estimated for particular rivers and particular disposal sites. Dilution of neutrally-buoyant liquid wastes is achieved by an interaction between turbulent diffusion and differential convection; the overall process is referred to as dispersion. The primary objective of this research is to develop an efficient computational model for the prediction of time-dependent mass dispersion in natural streams; a secondary objective is experimentally to investigate the variation of transverse diffusivity in a triangular laboratory channel.

The basis of the computational model is a partial differential equation expressing conservation of pollutant mass in a control volume. Analytical solutions to this so-called dispersion equation are limited to idealized river geometries and simplified pollutant source configurations. The computational model developed in this study is based on a finite-difference solution to the depth-averaged dispersion equation; the model may be used to predict depth-averaged concentrations resulting from a pollutant source of arbitrary time and space configuration in a stream of arbitrary geometry and nonuniform but steady flow. Problems of numerical instability and damping in the convective stage of the computation are avoided through the use of a half-implicit and half-explicit second order differencing scheme for the space derivative; numerical dispersion cannot be eliminated, but may be minimized by judicious choice of time and distance steps. Transverse and longitudinal turbulent diffusion are computed by a second order space-centered implicit scheme. The overall result is a computational model which is unconditionally stable and whose accuracy is not critically dependent on the magnitudes of time and distance steps.

The computational model requires a priori knowledge of the river geometry, velocity distributions, and turbulent diffusivities. The river geometry is generally known, and velocities are either known or can be estimated. But at the present time there is little theoretical or experimental basis for the estimation of the magnitude and distribution of diffusivities in natural channels; yet knowledge of the transverse diffusivity in an essential requirement in predicting dispersion. The triangular-channel tests performed in this study indicate that the transverse diffusivity is constant within a cross section; this suggests an interaction between bed shear and transverse shear, the relative contributions of which cannot yet be determined.

The applicability of the computational model is demonstrated through simulation of dispersion experiments reported for the Missouri River and Clinch River. Model predictions are in good agreement with observed concentrations resulting from continuous point source and instantaneous plane source injections.

INTRODUCTION

Recent awareness of the environmental fragility of river systems has brought out the need to make detailed estimates of a river's waste assimilation capacity. Wildlife ecologists, utilizing specialized input from the fields of biology, botany, zoology, etc., can specify the maximum pollutant concentration levels and durations to which various aquatic organisms may be exposed. The engineer must then design waste treatment facilities, submerged outfalls, or other water purification systems which will achieve sufficient reduction of pollutant levels to meet the downstream water quality standards. Alternatively, the engineer may be required to show that, in the event of accidental spillage of toxic material into a river, sufficient dilution will occur to minimize damage to the aquatic environment, and pose no threat to downstream municipal users. These problems require an understanding of three general processes: initial dilution of an outfall jet, chemical and biological decay of nonconservative pollutants, and turbulent mixing. This work is concerned only with the third process, i.e., the turbulent mixing of a conservative pollutant in natural river flow. Furthermore, the study is limited to neutrally-buoyant pollutants, although the methods described could be extended to predict the mixing of sediments with finite fall velocity.

Mixing in rivers is described by the terms diffusion and dispersion, which are often used interchangeably although they connote distinctly different processes. In this study the two terms are used as suggested by Holley (1969); diffusion is the transport of mass by either molecular diffusion or by deviations of instantaneous turbulent velocity fluctuations from the local time average velocity. Dispersion, on the other hand, is the spreading out of a mass of pollutant caused by deviations of local time-averaged velocities from the depth-averaged or cross-sectional averaged velocity, i.e., due to differential convection. Dispersion is the more general of the two terms, as it is understood to include the effects of diffusion, which transfers mass between zones of varying velocity, and thus reduces differential convection.

Predictions of mixing in turbulent flow fields are based to a large extent on solutions to a partial differential equation which states mathematically that mass of pollutant, or tracer, must be preserved. Analytical solutions to the equation have been obtained for various injection configurations, but are generally limited to cases of pure diffusion, i.e., to flows having no gradients of longitudinal velocity. The few solutions for true dispersion are limited to special velocity gradients, unbounded fluids, and/or longitudinally uniform conditions. Predictions of mixing in streams of arbitrary geometry can be obtained only through numerical solutions of the mass conservation equation. Such solutions have been developed for time-dependent mixing in well-mixed estuaries, and for steady-state mixing in rivers. The primary purpose of this study is to develop a finite difference model of both time-dependent and steady-state mixing in rivers of arbitrary geometry.

Both numerical and analytical models of dispersion which are based on the mass conservation equation require prior knowledge of the turbulent diffusivities; yet the diffusivities have little basis in theory, and their spatial variation in natural channels is generally not known. Numerical models do not require that diffusivities be constant, thus opening up a need for improved information on not only the magnitude, but also the variation of diffusivity from point to point in a stream. A secondary purpose of this investigation is experimentally to determine the transverse variation of transverse diffusivity in a nonrectangular channel.

This paper consists of three major elements. Part I outlines some of the available methods for prediction of dispersion in streams and describes the development of the numerical model. Part II describes the theoretical basis of the transverse diffusivity, and presents the results and analysis of limited experiments conducted in a triangular laboratory channel. Part III consists of the application of the numerical model and experimental results to reproduce the data from field experiments in two rivers.

TWO DIMENSIONAL FINITE DIFFERENCE MODEL OF UNSTEADY, NEUTRALLY-BUOYANT MASS DISPERSION IN NONUNIFORM CHANNEL FLOW

Chapter I
PREDICTION OF MASS DISPERSION IN OPEN CHANNEL FLOW

1.1 Mass Conservation Equation

The prediction of mass dispersion in fluids is based on solutions to an equation which states mathematically that any imbalance between the transport of tracer mass into and out of a control volume of solute must result in an accumulation of tracer mass within that control volume. The tracer mass transport across the boundaries of the control volume can be either convective (related to the gross movement of the fluid, including turbulence), or diffusive (related to the exchange of tracer particles between adjacent layers of fluid at a molecular scale). Sayre (1968) has expressed the mass balance in a control volume in steady flow as

$$\frac{1}{\gamma} \frac{\partial W}{\partial t} = - \int_S C \underline{u} \cdot \underline{n} \, dS + \int_S \epsilon_m \nabla C \cdot \underline{n} \, dS \qquad (1.1)$$

where

- γ = weight of solute per unit volume,
- W = weight of tracer mass in the control volume,
- C = instantaneous concentration by weight of the tracer,
- $\underline{u}$ = instantaneous velocity vector,
- $\underline{n}$ = unit vector normal to the surface of the control volume,
- ϵ_m = molecular diffusivity,
- ∇ = gradient vector operator,
- S = surface of the control volume, and
- t = time.

Expressing $\frac{W}{\gamma}$ as $\int_V C dV$, where V is the control volume, and using the divergence theorem to express the surface integrals as volume integrals, Eq. 1.1 becomes

$$\int_V \frac{\partial C}{\partial t} \, dV = - \int_V \nabla \cdot (C\underline{u}) \, dV + \int_V \epsilon_m \nabla^2 C \, dV \qquad (1.2)$$

Now this expression must hold for any control volume, including one so small that the integrands may be considered to be constant; therefore the integrals may be dropped. Furthermore, from incompressible continuity, $\nabla \cdot \underline{u} = 0$. Thus Eq. 1.2 may be written

$$\frac{\partial C}{\partial t} + \underline{u} \cdot \nabla C = \epsilon_m \nabla^2 C \qquad (1.3)$$

or, in tensor notation,

$$\frac{\partial C}{\partial t} + u_i \frac{\partial C}{\partial x_i} = \epsilon_m \frac{\partial^2 C}{\partial x_i \partial x_i} \qquad (1.4)$$

Equation 1.4 is quite general. In laminar flow, where the instantaneous velocities u, v, and w might be known for all times and at all positions in the flow field, Eq. 1.4 could be solved analytically or numerically to yield a complete concentration distribution in space and time, given the appropriate initial and boundary conditions. But most flows are turbulent, and the variation of local velocities with space and time is exceedingly difficult to predict, even in simplified geometries. Thus Eq. 1.4 must be further modified for application to turbulent mixing problems.

As in the study of the dynamics of turbulent flow, the application of Reynolds' rules of averaging to the kinematic mixing process is useful. Considering the concentration and velocities to be composed of time-averaged and fluctuating components, $u_i = \bar{u}_i + u'_i$, etc., substituting these into Eq. 1.4, and averaging it over a time period which is long with respect to the turbulent fluctuations but short with respect to the gross phenomenon being studied, Eq. 1.4 becomes

$$\frac{\partial \bar{C}}{\partial t} + \bar{u}_i \frac{\partial \bar{C}}{\partial x_i} = \frac{\partial}{\partial x_i} \left(\epsilon_m \frac{\partial \bar{C}}{\partial x_i} - \overline{u'_i C'} \right) \qquad (1.5)$$

where the overbars denote time averages.

At this stage of the development two critical assumptions are made:

(a) The time-averaged mass transport in the ith direction due to turbulent convection, $\overline{u_i C_i}$, can be represented as the product of a turbulent diffusivity, and the concentration gradient in the ith direction. This is tantamount to assuming a direct analogy between molecular and turbulent diffusion.

(b) The mass transport due to molecular diffusion is much less than that due to turbulent fluctuations, and can be absorbed in the turbulent diffusivity.

Employing these assumptions, Eq. 1.5 may be written

$$\frac{\partial C}{\partial t} + u_i \frac{\partial C}{\partial x_i} = \frac{\partial}{\partial x_i} \left(\bar{\epsilon}_i \frac{\partial C}{\partial x_i} \right) \qquad (1.6)$$

where the overbars have been dropped and $\bar{\epsilon}_i$ is the turbulent diffusivity in the ith direction.[1]

Equation 1.6 is referred to as the turbulent conservation of mass, or dispersion, equation. It describes turbulent dispersion, i.e., the process by which a tracer mass is dispersed within a flow field by the interaction between turbulent diffusion, which tends to mix adjacent layers, and differential convection, which tends to move the layers one with respect to another. Solutions to Eq. 1.6, based on a known or assumed steady velocity field and known diffusivities $\bar{\epsilon}_i$, yield estimates of the complete concentration distribution at all times for specified initial and boundary conditions. It must be recognized, however, that concentration distributions predicted from solutions to Eq. 1.6 are valid only to the extent that the diffusivities are known and that assumptions (a) and (b) above are justified.

1.2 Solutions for Instantaneous Point Sources

The instantaneous point source is of only theoretical interest in a practical sense, as actual pollutant spills are never instantaneous, but are spread over some finite time interval. Nonetheless, analytical solutions to Eq. 1.6 for instantaneous sources can be superposed in space and/or time to model noninstantaneous sources of finite extent.

Csanady (1973) considered the turbulent diffusion of an instantaneous source of tracer solution of concentration C_o and volume V_o in an unbounded fluid having a constant velocity U in the x-direction, with $v = w = 0$. Through analogy with molecular diffusion, and assuming mutually independent diffusion in the x, y, and z-directions, he presented the following concentration distribution:

$$C(x,y,z,t) = \frac{C_o V_o}{(2\pi)^{3/2} \sigma_x \sigma_y \sigma_z}$$

$$\cdot \exp\{-\frac{(x-Ut)^2}{2\sigma_x^2} - \frac{y^2}{2\sigma_y^2} - \frac{z^2}{2\sigma_z^2}\} \quad (1.7)$$

Here σ_x^2, σ_y^2, and σ_z^2 are the variances of the concentration distribution in the x, y, and z-directions. The critical link between Eq. 1.7, which is a statement of analogy with molecular diffusion, and Eq. 1.6, which is a statement of conservation of mass of tracer, is developed by Csanady (1973) from the more general analysis by Batchelor (1949). By assuming the diffusivities to be constant in space (homogeneous turbulence), then taking the appropriate derivatives of Eq. 1.7 for substitution into Eq. 1.6, it may be shown that

$$\sigma_x^2 = 2\tilde{\varepsilon}_x t \quad (1.8a)$$

$$\sigma_y^2 = 2\tilde{\varepsilon}_y t \quad (1.8b)$$

$$\sigma_z^2 = 2\tilde{\varepsilon}_z t \quad (1.8c)$$

Taylor (1921) formulated a rigorous theory relating the variances of a diffusing cloud to the Lagrangian statistical properties of the turbulence. These properties are generally unknown and difficult to measure; but for diffusion times which are large compared to the time scale of the turbulent eddies, Taylor's results also reduce to Eq. 1.8, where the diffusivities are the product of the Lagrangian mean square velocity fluctuation and the Lagrangian integral time scale. Using these results, Eq. 1.7 becomes

$$C(x,y,z,t) = \frac{C_o V_o}{8(\pi t)^{3/2}(\tilde{\varepsilon}_x \tilde{\varepsilon}_y \tilde{\varepsilon}_z)^{1/2}}$$

$$\cdot \exp\{-\frac{(x-Ut)^2}{4\tilde{\varepsilon}_x t} - \frac{y^2}{4\tilde{\varepsilon}_y t} - \frac{z^2}{4\tilde{\varepsilon}_z t}\} \quad (1.9)$$

The concentration distribution is now expressed in terms of the turbulent diffusivities which appear in Eq. 1.6. In fact, Eq. 1.6 may be written for constant diffusivities and $v = w = 0$ as

$$\frac{\partial C}{\partial t} + U \frac{\partial C}{\partial x} = \tilde{\varepsilon}_x \frac{\partial^2 C}{\partial x^2} + \tilde{\varepsilon}_y \frac{\partial^2 C}{\partial y^2} + \tilde{\varepsilon}_z \frac{\partial^2 C}{\partial z^2} \quad (1.10)$$

Sayre (1973) has shown that Eq. 1.9 is also a solution to Eq. 1.10 for an instantaneous point source in an unbounded fluid.

For computational purposes, it is not necessary to relate the concentration distribution variances to the turbulent diffusivities; once the assumption of gradient-type turbulent mixing is made, Eq. 1.9 can be adopted as a satisfactory solution to Eq. 1.10 for the instantaneous point source. But the gradient-type turbulent mixing assumption is given a more formal basis by the analogy with molecular gradient diffusion, and by Taylor's fundamental relationship between the Lagrangian properties of the turbulence, the variances, and the turbulent diffusivities.

Equation 1.9 is applicable only to mixing in an unbounded fluid. This condition may be approximated by injection from an elevated point source in the atmosphere, (such as a smokestack), but is clearly inappropriate when applied to mixing in rivers. Most rivers are much wider than they are deep, and the proximity of the bed and/or water surface to a submerged source invalidates the unbounded fluid assumption. Cleary and Adrian (1973) have obtained a solution to Eq. 1.10 for boundary conditions of no tracer transport across the bed, banks, or water surface. The series solution is obtained by an integral transform method, and assumes uniform, unidirectional flow in a rectangular cross section with known and constant diffusivities. The resulting expression for $C(x,y,z,t)$, applicable to any point source location and given in terms of a convergent infinite series, is not presented here due to its complexity. The authors claim that their solution yields results identical to those obtained by Holley (1972) for a particular source location, but using virtual image sources to satisfy the zero-transport boundary conditions. Cleary and Adrian have also obtained a simpler two-dimensional solution, applicable to mixing from an instantaneous vertical line source in a rectangular, uniform channel.

The solutions just described require a constant downstream velocity U in the entire flow field. Carter and Okubo (1965) obtained a solution to Eq. 1.6 which allows the velocity u to vary within the cross section, although in a special way. In their so-called uniform shear flow, Eq. 1.6 is written

$$\frac{\partial C}{\partial t} + (U + \Gamma_y y + \Gamma_z z) \frac{\partial C}{\partial x}$$

$$= \tilde{\varepsilon}_x \frac{\partial^2 C}{\partial x^2} + \tilde{\varepsilon}_y \frac{\partial^2 C}{\partial y^2} + \tilde{\varepsilon}_z \frac{\partial^2 C}{\partial z^2} \quad (1.11)$$

where as before $v = w = 0$, the diffusivities are assumed not to vary within the cross section, and Γ_y and Γ_z are the vertical and transverse gradients of longitudinal velocity, respectively. For an instantaneous release of a tracer volume V_o and concentration C_o at the coordinate origin of an unbounded fluid, Carter and Okubo obtained the following solution to Eq. 1.11:

3

$$C(x,y,z,t) = \frac{C_o V_o}{8\pi^{3/2}(\bar{\varepsilon}_x \bar{\varepsilon}_y \bar{\varepsilon}_z)^{1/2} t^{3/2}(1+\phi^2 t^2)^{1/2}}$$

$$\cdot \exp - \left\{ \frac{[x-Ut-\frac{1}{2}(\Gamma_y y + \Gamma_z z)t]^2}{4\bar{\varepsilon}_x t(1+\phi^2 t^2)} + \frac{y^2}{4\bar{\varepsilon}_y t} + \frac{z^2}{4\bar{\varepsilon}_z t} \right\} \tag{1.12}$$

where $\phi^2 = \frac{1}{12}\left\{ \frac{\Gamma_y^2 \bar{\varepsilon}_y}{\bar{\varepsilon}_x} + \frac{\Gamma_z^2 \bar{\varepsilon}_z}{\bar{\varepsilon}_x} \right\}$

Note that when $u = U$, i.e., $\Gamma_y = \Gamma_z = 0$, Eq. 1.12 reduces to Eq. 1.9, as expected.

1.3 The Superposition Principle

The three-dimensional, instantaneous point source solutions are limited to idealized stream geometries, unidirectional flow, and constant diffusivities. Nonetheless, predictions can be brought one step closer to reality by use of the superposition principle, by which sources of arbitrary time and space extent can be modeled using the three-dimensional, instantaneous point source solution as a building block. The mathematical basis of superposition is the convolution integral, which expresses the desired concentration distribution as the sum of the distributions resulting from an infinite superposition of instantaneous point sources. For the most general case, Sayre (1973) has expressed the convolution as

$$C_1(x,y,z,t) = \int_0^t \int_{-\infty}^{\infty} \int_0^B \int_0^h f(x-x_o, y-y_o, z-z_o, t-t_o)$$

$$\cdot C(x_o, y_o, z_o, t_o)\, dy_o\, dz_o\, dx_o\, dt_o \tag{1.13}$$

where

C_1 = convoluted concentration distribution,
f = normalized instantaneous point source concentration distribution,
C = the source concentration distribution,
B = channel width, and
h = local channel depth.

The distribution f is normalized by $C_o V_o$. The closed-form integration of Eq. 1.13 is generally not possible, but numerical integration may be used to predict $C_1(x,y,z,t)$. The most serious deficiency of Eq. 1.13 as a predictive tool is its limitation to the idealized conditions demanded by the function f, usually an unbounded fluid, unidirectional velocity, and constant diffusivities.

Csanady (1973) describes the application of the superposition principle to model a continuous point source in an unbounded, three-dimensional flow field with constant unidirectional velocity U. Considering Eq. 1.13, f is given by

$$f = \frac{C(x,y,z,t)}{C_o V_o}$$

where $C(x,y,z,t)$ is given by Eq. 1.7. For constant injection of a tracer solution of concentration C_o

at a volumetric flow rate q_o at $x_o = y_o = z_o = 0$, Eq. 1.13 becomes

$$C(x,y,z) = \int_0^{\infty} \frac{C_o q_o}{(2\pi)^{3/2}\sigma_x \sigma_y \sigma_z}$$

$$\cdot \exp \left\{ \frac{-(x-Ut_o)^2}{2\sigma_x^2} - \frac{y^2}{2\sigma_y^2} - \frac{z^2}{2\sigma_z^2} \right\} dt_o \tag{1.14}$$

where the spatial integrations are not needed for a point source, the superposition being in time only. Frenkiel (1953) integrated Eq. 1.14 and obtained, after assuming that the longitudinal diffusion is much less important than the vertical or transverse diffusion,

$$C(x,y,z) = \frac{C_o q_o}{2\pi\sigma_y \sigma_z U} \cdot \exp \left\{ -\frac{y^2}{2\sigma_y^2} - \frac{z^2}{2\sigma_z^2} \right\} \tag{1.15}$$

Using the asymptotic results of Eq. 1.8, and instead of diffusion time using x/U,

$$C(x,y,z) = \frac{C_o q_o}{4\pi x(\bar{\varepsilon}_y \bar{\varepsilon}_x)^{1/2}} \cdot \exp \left\{ -\frac{y^2 U}{4\bar{\varepsilon}_y x} - \frac{z^2 U}{4\bar{\varepsilon}_z x} \right\} \tag{1.16}$$

Recapitulating, Eq. 1.16 is the concentration distribution resulting from continuous injection of tracer at the origin of coordinates in an unbounded fluid having constant unidirectional velocity U and negligible longitudinal diffusivity.

1.4 The Two-Dimensional, Depth-Averaged Mass Conservation Equation

For many problems of mixing in natural rivers the concentration field is adequately described by the depth-averaged values of concentration, rather than point values. In terms of analysis, this removes the vertical coordinate and the vertical diffusivity from the problem, consequently simplifying the governing equations. The two-dimensional mass conservation equation may be obtained by integrating the three-dimensional version, Eq. 1.6, over the depth of flow. It is convenient first to rewrite Eq. 1.6 without the simplifying application of incompressible continuity; since

$$\frac{\partial u_i}{\partial x_i} = 0,$$

it may be added to the left side of Eq. 1.6. Then, combining the space derivatives on the left side and writing the expression in Cartesian notation,

$$\frac{\partial C}{\partial t} + \frac{\partial}{\partial x}(uC) + \frac{\partial}{\partial y}(vC) + \frac{\partial}{\partial z}(wC)$$

$$= \frac{\partial}{\partial x}\left(\bar{\varepsilon}_x \frac{\partial C}{\partial x}\right) + \frac{\partial}{\partial y}\left(\bar{\varepsilon}_y \frac{\partial C}{\partial y}\right) + \frac{\partial}{\partial z}\left(\bar{\varepsilon}_z \frac{\partial C}{\partial z}\right). \tag{1.17}$$

Referring to the definition sketch, Fig. 1.1, integrate Eq. 1.17 with respect to y from a to b:

4

$$\int_a^b \frac{\partial C}{\partial t}\, dy + \int_a^b \frac{\partial}{\partial x}\,(uC)\, dy + \int_a^b \frac{\partial}{\partial y}\,(vC)\, dy + \int_a^b \frac{\partial}{\partial z}\,(wC)\, dy$$

$$= \int_a^b \frac{\partial}{\partial x}\left(\bar\varepsilon_x \frac{\partial C}{\partial x}\right) dy + \int_a^b \frac{\partial}{\partial y}\left(\bar\varepsilon_y \frac{\partial C}{\partial y}\right) dy + \int_a^b \frac{\partial}{\partial z}\left(\bar\varepsilon_z \frac{\partial C}{\partial z}\right) dy.$$

$$(1.18)$$

Apply Leibniz's Theorem for differentiation of an integral:

$$\int_a^b \frac{\partial C}{\partial t}\, dy + \frac{\partial}{\partial x}\int_a^b uC\, dy - (uC)\big|_b \frac{\partial b}{\partial x} + (uC)\big|_a \frac{\partial a}{\partial x}$$

$$+ (vC)\big|_b - (vC)\big|_a$$

$$+ \frac{\partial}{\partial z}\int_a^b wC\, dy - (wC)\big|_b \frac{\partial b}{\partial z} + (wC)\big|_a \frac{\partial a}{\partial z}$$

$$= \frac{\partial}{\partial x}\int_a^b \bar\varepsilon_x \frac{\partial C}{\partial x}\, dy - \left(\bar\varepsilon_x \frac{\partial C}{\partial x}\right)\big|_b \frac{\partial b}{\partial x} + \left(\bar\varepsilon_x \frac{\partial C}{\partial x}\right)\big|_a \frac{\partial a}{\partial x}$$

$$+ \left(\bar\varepsilon_y \frac{\partial C}{\partial y}\right)\big|_b - \left(\bar\varepsilon_y \frac{\partial C}{\partial y}\right)\big|_a$$

$$+ \frac{\partial}{\partial z}\int_a^b \bar\varepsilon_z \frac{\partial C}{\partial z}\, dy - \left(\bar\varepsilon_z \frac{\partial C}{\partial z}\right)\big|_b \frac{\partial b}{\partial z} + \left(\bar\varepsilon_z \frac{\partial C}{\partial z}\right)\big|_a \frac{\partial a}{\partial z}.$$

$$(1.19)$$

Recognizing that, for any integrand ϕ, $\int_a^b \phi\, dy = h\bar\phi$, where the overbar now denotes a depth average, Eq. 1.19 becomes after some rearrangement

$$h\frac{\overline{\partial C}}{\partial t} + \frac{\partial}{\partial x}\,(h\overline{uC}) + \frac{\partial}{\partial z}\,(h\overline{wC}) = \frac{\partial}{\partial x}\left(h\overline{\bar\varepsilon_x \frac{\partial C}{\partial x}}\right) + \frac{\partial}{\partial z}\left(h\overline{\bar\varepsilon_z \frac{\partial C}{\partial z}}\right)$$

$$+ C_b\left[u_b \frac{\partial b}{\partial x} + w_b \frac{\partial b}{\partial z} - v_b\right] + C_a\left[-u_a \frac{\partial a}{\partial x} - w_a \frac{\partial a}{\partial z} + v_a\right]$$

$$+ \left[-\left(\bar\varepsilon_x \frac{\partial C}{\partial x}\right)_b \frac{\partial b}{\partial x} - \left(\bar\varepsilon_z \frac{\partial C}{\partial z}\right)_b \frac{\partial b}{\partial z} + \left(\bar\varepsilon_y \frac{\partial C}{\partial y}\right)_b\right]$$

$$+ \left[\left(\bar\varepsilon_x \frac{\partial C}{\partial x}\right)_a \frac{\partial a}{\partial x} + \left(\bar\varepsilon_z \frac{\partial C}{\partial z}\right)_a \frac{\partial a}{\partial z} - \left(\bar\varepsilon_y \frac{\partial C}{\partial y}\right)_a\right] \quad (1.20)$$

The bracketed terms on the right side of Eq. 1.20 may be eliminated as follows: at any boundary, i.e., either the channel bed or the water surface, the water velocity and the diffusive tracer transport can only be parallel to the boundary. This implies that the component of either quantity projected normal to the surface must vanish. In vector terms,

$$\underline{U} \cdot \underline{n} = \underline{T} \cdot \underline{n} = 0 \qquad (1.21)$$

where

n = the normal vector to the bed or water surface, and
$\underline{T}$ = the diffusive tracer transport vector.

Noting that the normal vector to the water surface is $\underline{n} = \partial b/\partial x\,\underline{i} - \underline{j} + \partial b/\partial z\,\underline{k}$, (and similarly for the bed), recalling that

$$\underline{T} = \bar\varepsilon_x \frac{\partial C}{\partial x}\,\underline{i} + \bar\varepsilon_y \frac{\partial C}{\partial y}\,\underline{j} + \bar\varepsilon_z \frac{\partial C}{\partial z}\,\underline{k}$$

and $\underline{U} = u\underline{i} + v\underline{j} + w\underline{k}$, the bracketed terms of Eq. 1.20 are recognized as, respectively, $(\underline{U}\cdot\underline{n})_b$, $-(\underline{U}\cdot\underline{n})_a$, $(\underline{T}\cdot\underline{n})_b$, and $(\underline{T}\cdot\underline{n})_a$, each of which must vanish according to Eq. 1.21.

Equation 1.20 is still phrased in terms of the depth-average of products, such as $\overline{uC}$, $\overline{wC}$, etc; these must be simplified before solutions can be considered. First, express each quantity as the sum of a depth-averaged value and local deviation from it, such as

$$u = \bar u + u^y$$

where the superscript y denotes the local deviation. (It is important to note that these quantities are already time averages; depth-averaging alone is being performed here.) Then a quantity such as $\overline{uC}$ becomes, by Reynolds' Rules of Averaging,

$$\overline{(\bar u + u^y)(\bar C + C^y)} = \overline{\bar u\,\bar C} + \overline{u^y C^y} + \overline{u^y\,\bar C} + \overline{\bar u\, C^y}$$

$$= \bar u\,\bar C + \overline{u^y C^y} + \overline{u^y}\,\bar C + \bar u\,\overline{C^y}$$

$$= \bar u\,\bar C + \overline{u^y C^y}.$$

Applying similar reductions to the remaining terms, Eq. 1.20 may be written

$$h\frac{\partial \bar C}{\partial t} + \frac{\partial}{\partial x}\,(h\bar u\bar C) + \frac{\partial}{\partial z}\,(h\bar w\bar C) = \frac{\partial}{\partial x}\left(-h\overline{u^y C^y} + h\bar\varepsilon_x \frac{\partial C}{\partial x}\right)$$

$$+ \frac{\partial}{\partial z}\left(-h\overline{w^y C^y} + h\bar\varepsilon_z \frac{\partial C}{\partial z}\right). \qquad (1.22)$$

The final task is to express the transport terms on the right side of Eq. 1.22 as simple products of diffusivities and concentration gradients. The justification for so doing is discussed in detail by Holley (1971). The arguments are that (a) the convective transport due to the velocity-concentration differences over the depth can successfully be approximated as a gradient diffusion process (see, for example, Fischer, 1967), and (b) in natural channels mixing generally is complete over the depth, so that the C^y quantities are relatively small. Then the effects of $\overline{u^y C^y}$ and $\overline{w^y C^y}$ may be considered to be absorbed in gradient transport terms. Equation 1.22 finally becomes

$$h\frac{\partial C}{\partial t} + \frac{\partial}{\partial x}\,(huC) + \frac{\partial}{\partial z}\,(hwC) = \frac{\partial}{\partial x}\left(h\varepsilon_x \frac{\partial C}{\partial x}\right) + \frac{\partial}{\partial z}\left(h\varepsilon_z \frac{\partial C}{\partial z}\right)$$

$$(1.23)$$

where the depth-average overbars have been deleted, and ε_x and ε_y include transport due to both turbulent fluctuations and vertical variations of longitudinal and transverse velocity. The depth-averaged, two-dimensional mass conservation equation, Eq. 1.23, serves as the basis of a variety of analytical and numerical models of mixing in natural streams.

1.5 Two-Dimensional Mixing from an Instantaneous Vertical Line Source

For a fluid of constant unidirectional velocity U, constant diffusivities, and a constant depth H, Eq. 1.23 becomes

$$\frac{\partial C}{\partial t} + U \frac{\partial C}{\partial x} = \epsilon_x \frac{\partial^2 C}{\partial x^2} + \epsilon_z \frac{\partial^2 C}{\partial z^2} \qquad (1.24)$$

For instantaneous vertical line source injection of tracer, Sayre and Chang (1968) present the following solution to Eq. 1.24:

$$C(x,z,t) = \frac{C_o V_o}{4\pi H t (\epsilon_x \epsilon_z)^{1/2}} \cdot \exp\left\{ -\frac{(x-Ut)^2}{4\epsilon_x t} - \frac{z^2}{4\epsilon_z t}\right\}$$

$$(1.25)$$

where, as before, V_o is the total volume of solution of concentration C_o injected at the origin of coordinates, and the solution is applicable only to an unbounded fluid.

Monin and Yaglom (1971) obtained a similar solution, but in an unbounded so-called uniform shear flow, where the velocity u varies linearly with z. For this case Eq. 1.24 becomes

$$\frac{\partial C}{\partial t} + (U_o + \Gamma_z z)\frac{\partial C}{\partial x} = \epsilon_x \frac{\partial^2 C}{\partial x^2} + \epsilon_z \frac{\partial^2 C}{\partial z^2} \qquad (1.26)$$

where the uniform shear Γ_z is defined as before, and U_o is the velocity at $z = 0$. The solution is

$$C(x,z,t) = \frac{C_o V_o}{4\pi H t (1+\phi^2 t^2)^{1/2}(\epsilon_x \epsilon_z)^{1/2}}$$

$$\cdot \exp\left\{ -\frac{(x-U_o-\Gamma_z z t)^2}{4\epsilon_x t (1+\phi^2 t^2)} + \frac{z^2}{4\epsilon_z t}\right\} \qquad (1.27)$$

where $\phi^2 = (\Gamma_z/12)(\epsilon_x/\epsilon_z)$.

1.6 Two-Dimensional Mixing from a Continuous Line Source

As in the case of three-dimensional mixing, the superposition principle may be used to model continuous injection for two-dimensional line sources. Sayre and Chang (1968) integrated Eq. 1.25 over time to obtain

$$C(x,z) = \frac{q_o C_o}{2\pi H (\epsilon_x \epsilon_z)^{1/2}} \cdot \exp\left\{\frac{Ux}{2\epsilon_x}\right\} K_o[\frac{U}{2\epsilon_x}(x^2+\frac{\epsilon_x}{\epsilon_z}z^2)^{1/2}]$$

$$(1.28)$$

where the fluid is again assumed to be laterally unbounded, and $K_o[\ ]$ is a modified Bessel function at the second kind, order zero. When ϵ_x is relatively unimportant, as in the case in most natural rivers, Eq. 1.28 converges to

$$C(x,z) = \frac{q_o C_o}{2HU(\pi t \epsilon_z)^{1/2}} \cdot \exp\left\{-\frac{Uz^2}{4\epsilon_z x}\right\} \qquad (1.29)$$

A similar application of superposition can be used to model a continuous line source in a uniform shear velocity field, i.e., using an expression such as Eq. 1.27. But the resulting expression generally cannot be integrated in closed form, requiring the use of numerical integration techniques (Okubo and Karweit, 1969).

1.7 The Method of Images

With the exception of the recent solution published by Cleary and Adrian (1973), all of the mass conservation equation solutions discussed up to this point have assumed an unbounded fluid. Thus the solutions presented are valid only in the region down-stream from the injection point before any tracer contacts the bed or banks (or simply the banks in the depth-averaged, two-dimensional cases). This restriction is overcome by use of the method of images, through which artificial, or mirror image, sources are used to satisfy the required boundary conditions. For example, the boundary condition of no tracer transport through the bank can be constructed by adding a source of equal strength equidistant from the bank, but on the opposite, or dry side. Thus the concentrations immediately on either side of the bank are the same, and consequently there can be no diffusive tracer transport across the bank. This procedure can also be thought of as a reflection, whereby that portion of the computed tracer distribution which would fall outside the channel is assumed to be reflected back into the channel, and is added to the nonreflected concentration. Of course each such mirror image source requires another source reflected across the opposite bank so that in principle an infinite number of image sources are required. Sayre and Chang (1968) have generalized this requirement as follows: let the actual continuous source be located a distance $z = \zeta$ from the coordinate origin at the centerline of the channel. Then denoting the desired concentration distribution by C_1,

$$C_1(x,z) = C(x,z-\zeta) + \sum_{n=1}^{\infty} [C(x,nB-\zeta+(-1)^n z)$$

$$+ C(x,nB+\zeta-(-1)^n z)] \qquad (1.30)$$

where

B = channel width,
n = the number of the reflection cycle, and
$C(x,z)$ = the appropriate solution for uniform conditions in an unbounded fluid, (e.g., Eq. 1.29).

Sayre (1973) has indicated that the summation need only be carried out to $n = 4$ or $n = 5$.

An analytic solution to Eq. 1.23 which allows for the nonrectangular geometry of a natural channel has been developed by Yotsukura and Cobb (1972) using the method of images. For the case of continuous injection of tracer from a vertical line source into a stream where the depth, velocity, and diffusivities are allowed to vary with transverse position but not with longitudinal distance, Eq. 1.23 becomes

$$hu \frac{\partial C}{\partial x} = \frac{\partial}{\partial z} (h\epsilon_z \frac{\partial C}{\partial z}) \qquad (1.31)$$

where the longitudinal diffusivity has been assumed to be relatively unimportant, and deleted accordingly. As it stands, Eq. 1.31 is not in a form for which analytical solutions exist. Yotsukura and Cobb define a new independent variable q to replace z,

$$q = \int_0^z hu \, dz; \qquad (1.32)$$

q represents the cumulative partial discharge measured from the left bank. Introducing q in place of z in Eq. 1.31, they obtain

$$\frac{\partial C}{\partial x} = \frac{\partial}{\partial q} (\epsilon_z h^2 u \frac{\partial C}{\partial q}) \qquad (1.33)$$

which still cannot be solved analytically due to the q-dependence of the so-called diffusion factor, $\epsilon_z h^2 u$. Therefore Yotsukura and Cobb hypothesize that a solution to Eq. 1.33 can be approximated by a solution to

$$\frac{\partial C}{\partial x} = \frac{\partial}{\partial q} (\lambda \frac{\partial C}{\partial q}) \qquad (1.34)$$

where λ is the cross-sectional average value of the diffusion factor. They show empirically that for tracer injection near the centerline of the channel, the use of a constant diffusion factor should be acceptable.

A solution to Eq. 1.34 is

$$C(x,q) = \frac{q_o C_o}{2(\pi x \lambda)^{1/2}} \cdot \exp - \{\frac{(q + D)^2}{4x\lambda}\} \quad (1.35)$$

where D is a constant of integration. Yotsukura and Cobb use the method of images to satisfy the boundary condition of no tracer transport across the banks; superposition in space is then used to model a continuous vertical line source of finite width. The final general solution is

$$C'(\alpha,q') = \frac{1}{2(q'_{s2} - q'_{s1})} [\sum_{n=0}^{\infty} \{erf \frac{\alpha(q'_{s2} + 2n - q')}{\sqrt{2}}$$

$$- erf \frac{\alpha(q'_{s1} + 2n - q')}{\sqrt{2}} + erf \frac{\alpha(q'_{s2} + 2n + q')}{\sqrt{2}}$$

$$- erf \frac{\alpha(q'_{s1} + 2n + q')}{\sqrt{2}}\} + \sum_{n=1}^{\infty} \{erf \frac{\alpha(q'_{s2} - 2n - q')}{\sqrt{2}}$$

$$- erf \frac{\alpha(q'_{s1} - 2n - q')}{\sqrt{2}} + erf \frac{\alpha(q'_{s2} - 2n + q')}{\sqrt{2}}$$

$$- erf \frac{\alpha(q'_{s1} - 2n + q')}{\sqrt{2}}\}] \qquad (1.36)$$

where

$$\alpha^2 = Q^2/2x\lambda,$$
Q = the total discharge,
$q' = q/Q$
$C' = CQ/C_o q_o$

q'_{s1}, q'_{s2} = the left and right hand limits of the distributed line source, and
erf = the error function as tabulated in mathematical handbooks.

Recapitulating, Eq. 1.36 predicts the concentration distribution resulting from continuous injection of tracer as a distributed vertical line source into a longitudinally-uniform stream in which the velocity, depth, and diffusivity may vary transversely, although the product $\epsilon_z h^2 u$ is constant. This solution is more applicable to the computation of concentrations in natural rivers than any other two-dimensional analytic solution obtained to date (1975), though it is still limited to longitudinally-uniform conditions and continuous injection.

1.8 One-Dimensional Mixing from an Instantaneous Plane Source

Fundamental to the mathematical description of dispersion in channels is the assumption that tracer transport due not only to temporal, but also to spatial variations of velocity and concentration can be modeled as a gradient mixing process. This concept is employed in the derivation of Eq. 1.6, where the time-averaged turbulent transport $\overline{u'_i C'}$ is replaced by $\bar{\epsilon}_i \, \partial C/\partial x_i$, and again in the derivation of Eq. 1.23, where the depth-averaged transport $\overline{u_i^y C^y}$ and the turbulent diffusion $\bar{\epsilon}_i \, \partial C/\partial x_i$ are replaced by $\epsilon_i \, \partial C/\partial x_i$. The general approach was first employed in connection with the modeling of instantaneous plane source injection. Taylor (1954) hypothesized that, in turbulent flow through a pipe, the mixing of a tracer which has spread over the entire cross section can be described by a one-dimensional equivalent of Eq. 1.6,

$$\frac{\partial C_a}{\partial t} + U_a \frac{\partial C_a}{\partial x} = K_x \frac{\partial^2 C_a}{\partial x^2} \qquad (1.37)$$

where U_a and C_a are the cross-sectional average values of velocity and concentration, respectively, and K_x is the overall longitudinal dispersion coefficient, not to be confused with the turbulent diffusivity. A solution to Eq. 1.37 for the case of constant U_a is the normal or Gaussian distribution,

$$C_a(x,t) = \frac{C_o V_o}{2A(\pi K_x t)^{1/2}} \cdot \exp \{- \frac{(x - U_a t)^2}{4K_x t}\} \quad (1.38)$$

where V_o is the total volume of dispersant of concentration C_o distributed over the cross section of

area A. An important property of the one-dimensional, or Fickian, diffusion process is that the longitudinal variance of the cross-sectional average concentration, σ_a^2, must increase linearly at a rate of twice the dispersion coefficient, or

$$K_x = \frac{1}{2}\frac{2\sigma_a^2}{\partial t} \tag{1.39}$$

It is this property which makes it possible to evaluate K_x on the basis of plane-source injection experiments in natural streams. Attempts have been made, however, to evaluate K_x analytically. For turbulent flow in a pipe, Taylor (1954) obtained

$$K_x = 10.1\ a_o U_* \tag{1.40}$$

where

a_o = the radius of the pipe, and
U_* = the shear velocity.

Elder (1959) considered one-dimensional mixing in an infinitely-wide open channel, and obtained

$$K_x = 5.9\ H\ U_* \tag{1.41}$$

Elder's result considered only vertical variations in longitudinal velocity; Fischer (1966), recognizing that it is transverse variations in longitudinal velocity which contribute most significantly to longitudinal dispersion, obtained

$$K_x = -\frac{1}{A}\int_0^B u''(z)h(z)\int_0^z \frac{1}{\varepsilon_z h(z)}\int_0^z\int_0^{h(z)} u''(z)\ dy\ dz\ dz\ dz \tag{1.42}$$

where

$u''(z)$ = the local deviation of longitudinal velocity from the cross-sectional average, and
$h(z)$ = local depth.

Equation 1.38, along with Eq. 1.42, provides a useful method of computing concentration distributions resulting from an instantaneous plane source when the flow is longitudinally uniform and the transverse diffusivity is known. Fischer has also shown that Eq. 1.38 is applicable to the mixing resulting from an instantaneous source of any spatial configuration, but only downstream of the point where the tracer has spread over the entire cross section. In this case, the superposition principle may be used to route the observed distribution to successive downstream locations if K_x is known or computed.

A more rigorous treatment of the instantaneous plane source injection problem was introduced by Aris (1956) and further developed by Sayre (1968). The so-called moment technique involves the transformation of Eq. 1.6 into partial differential equations for the various longitudinal moments of the concentration distribution. Assuming that longitudinal diffusion is inconsequential, Sayre obtained numerical solutions for the first three moments, and by fitting statistical distributions to them was able to reconstruct the concentration distributions. Sayre's work was unique

in its applicability to the dispersion of sediment particles of specified fall velocity.

A recent thorough analysis of plane source injection data from natural streams performed by Nordin and Sabolt (1973) has shown that an assumption of one-dimensional mixing with a constant diffusivity is usually not justified. The general approach was originally suggested for use in natural rivers more on the basis of the convenience of a Gaussian solution than on the basis of any mixing theory. The present and future development of more rigorous numerical techniques for predicting dispersion with few restrictive assumptions precludes the need for much further use of the one-dimensional mixing concept.

1.9 Numerical Model of Two-Dimensional Mixing from a Continuous Line Source in a Natural Channel

All of the analytical solutions discussed thus far have been limited in their generality due to mathematical restrictions necessary for a solution. All require longitudinally uniform flow, and all but Eq. 1.36 require a uniform, unbounded fluid, a rectangular cross section, or plane source injection. Therefore a numerical solution, allowing for transverse and longitudinal variations of velocity, depth, and diffusivity, is worthy of consideration. Yotsukura et al. (1970) developed a numerical model for two-dimensional mixing, with specific application to the Missouri River between Sioux City, Iowa and Plattsmouth, Nebraska. Equation 1.23 was written for a continuous vertical line source injection as

$$\frac{\partial}{\partial x}(huC) = \frac{\partial}{\partial z}\left(h\varepsilon_z\frac{\partial C}{\partial z}\right) \tag{1.43}$$

where the transverse velocity, w, and the longitudinal diffusivity, ε_x, have been assumed to be zero. The stream is divided into stream tubes, each of which has variable width so as to maintain constant discharge in each, while reproducing the known depths and velocities at each cross section. Equation 1.43 is then written in discrete form; denoting longitudinal computational points by the subscript I, and stream tubes (i.e., transverse computational points) by J, Eq. 1.43 is written

$$B'_{I,J}\frac{[(huC)_{I+1,J}-(huC)_{I,J}]}{x_{I+1}-x_I} = (h\varepsilon_z)_{I;J,J+1}\left(\frac{C_{I,J+1}-C_{I,J}}{z_{I,J+1}-z_{I,J}}\right)$$
$$- (h\varepsilon_z)_{I;J,J-1}\left(\frac{C_{I,J}-C_{I,J-1}}{z_{I,J}-z_{I,J-1}}\right) \tag{1.44}$$

where

$x_{I,J}$ = the longitudinal coordinate of stream tube J at point I,
$z_{I,J}$ = the transverse coordinate of the center of stream tube J at point I,
$(h\varepsilon_z)_{I;J,J+1}$ = the depth-diffusivity product at the interface between tubes J and J+1, etc., and
$B'_{I,J}$ = the width of stream tube J at point I.

The solution to Eq. 1.44 proceeds as follows: at the upstream boundary the input concentration is known in each stream tube, $C_{1,J}$. The values of $C_{2,J}$ are then computed directly from Eq. 1.44, one tube at a time, with special consideration given to the tubes at

8

either bank, where there can be no mass transfer. The solution is direct, requiring only a single computation for each grid point, and allows the depth, velocity, and diffusivity to vary with transverse position. In their successful application of the model to the Missouri River, Yotsukura et al. assumed that the diffusivity ε_z was a constant within each cross section.

1.10 The Use of Physical Models for the Prediction of Dispersion in Natural Streams

Physical models of natural waterways are especially useful for the study of hydraulic phenomena when the irregular natural geometry precludes mathematical analysis. As shown in preceding sections, most closed-form mathematical analysis of dispersion is applicable only to uniform stream geometries and artificial velocity fields. Consequently it is tempting to consider the use of physical models for studying dispersion in natural streams, especially when neither the tracer injection nor the water flow can be considered steady state. But physical models usually are incapable of reproducing the prototype dispersion process faithfully.

There are two features of physical models which can effectively destroy their value in predicting dispersion. First, the use of artificial roughness elements (strips or cleats) to compensate for the relatively steep model slopes induces excessive turbulence within the flow. On the other hand, boundary-generated turbulence is primarily responsible for the diffusion in streams; the additional turbulence induced in a physical model accelerates the turbulent diffusion relative to the prototype. Second, restrictions of space and funds require that most physical models be distorted relative to the prototype; an exaggerated vertical dimension allows sufficient depth to reproduce the phenomenon being studied without requiring excessive stream widths and lengths. This distortion can be suitably accounted for in the study of flood stages, velocity fields, or other gross hydraulic features. But Fischer and Holley (1971) have shown that, considering one-dimensional, plane source dispersion in steady flow, a distorted model will produce longitudinal dispersion which is excessively dominated by vertical velocity gradients, and insufficiently responsive to transverse velocity gradients. Fischer (1966) has shown just the opposite tendencies to be characteristic of natural streams, where transverse velocity gradients dominate the mixing process. Holley and Karelse (1973) have presented a similar analysis for two-dimensional mixing from a continuous vertical line source, and concluded that, in a distorted model, the transverse diffusion is too great relative to the prototype. The analytical conclusion was further supported by direct comparisons of model and prototype mixing data.

The exact relationship between the concentration distributions resulting from mixing in model and prototype can be developed analytically only for idealized cases. This fact, added to the complexity of mixing within natural geometries, precludes the use of distorted physical models for studying dispersion phenomena in natural streams.

Chapter II
A FINITE DIFFERENCE SOLUTION TO THE COMPLETE
DEPTH-AVERAGED, TWO-DIMENSIONAL MASS CONSERVATION EQUATION

2.1 The Need for a Numerical Approach

The objective of this chapter is to develop a computational method for the prediction of depth-averaged concentration distributions resulting from the injection of a neutrally-buoyant, conservative tracer into steady river flow of arbitrary geometry. The method must allow for steady or unsteady tracer injection, and take into account the appropriate physical restrictions to mixing in a natural stream. The various analytical and numerical techniques discussed in Chapter 1 do not fulfill the above requirements for one reason or another. It is possible to model sources of arbitrary location in time and space by applying the superposition principle to the appropriate analytical solution; and the condition of zero tracer transport across the boundaries can be satisfied by using the method of images. But to do so in streams of nonrectangular cross section becomes exceedingly complex, if not impossible, and requires the assumptions of longitudinally uniform flow and constant, unidirectional velocity (or at best a uniform shear flow). The analytical solution of Yotsukura and Cobb (1972) requires longitudinally uniform flow, an assumption of a constant diffusion factor $\epsilon_z h^2 u$, and is applicable only to continuous, steady-state injection. The moment method of Sayre (1968) also requires uniform flow, and is applicable only to one-dimensional mixing from an instantaneous plane source, yielding no information on the spread of a point or line source.

The numerical method of Yotsukura et al. (1970) does allow for an arbitrary stream geometry and velocity distribution, but is limited to continuous injection of tracer; therefore the task at hand is the modification of a method such as this to allow for unsteady injection of tracer. But to do so is much more difficult than might be expected, because it involves a fundamental change in the nature of the equation to be solved. Equation 1.43, describing steady-state mixing from a continuous vertical line source, is classified as an elliptic partial differential equation (Carnahan, et al., 1969); the steady-state concentration distribution is dependent only on x and z, the longitudinal and transverse position, respectively. Once the transverse concentration distribution at the upstream boundary of the solution region is specified, and the boundary condition of no tracer transport across the banks is invoked, then in principle the complete concentration distribution can be obtained. In other words, at steady state, a single distribution $C(x,z)$ uniquely satisfies Eq. 1.43 at all points in the solution region. No iterative computation is required, and the accuracy of a numerical solution is governed primarily by the size of the computational grid.

The modification of Eq. 1.43 to allow for unsteady tracer injection is tantamount to reconsideration of the complete two-dimensional depth average dispersion equation, Eq. 1.23. Now there are three independent variables; the time t is added to the space coordinates x and z, and the equation is classified as a parabolic partial differential equation. In addition to the boundary conditions of no transport across the banks, the concentration distribution at the upstream boundary must be specified at all points in time and some constraint on mixing at the downstream boundary must be applied. Moreover, the convective portion of Eq. 1.23 can introduce an artificial or numerical diffusion which easily can dominate the physical diffusion and thus invalidate computational predictions. Thus the seemingly simple addition of the time-varying term to Eq. 1.43 not only requires that a concentration distribution be computed at each time increment, but also requires an additional boundary condition and, most importantly, introduces the possibility that the numerical solution may not even approximate the true solution. Section 2.2 demonstrates how this may occur, and Sect. 2.3 explores the numerical characteristics of a finite difference method for use in a two-dimensional mathematical model of dispersion.

2.2 The Occurrence of Artificial (Numerical) Diffusion

The purpose of this section is to demonstrate how the finite differencing of a linear convection equation can introduce artificial diffusion which has no physical basis, but is purely a consequence of the computation method. It is reasonable to ask why such behavior should be of concern, since real-life problems do involve physical diffusion. Consider depth-averaged diffusion in a rectangular channel having a transverse velocity distribution u(z). Further assuming that the diffusivities are constant and the transverse velocities are negligible, Eq. 1.23 can be written

$$\frac{\partial C}{\partial t} + u\frac{\partial C}{\partial x} = \epsilon_x \frac{\partial^2 C}{\partial x^2} + \epsilon_z \frac{\partial^2 C}{\partial z^2} \qquad (2.1)$$

One solution technique might be first to solve the convective portion of Eq. 2.1,

$$\frac{\partial C}{\partial t} + u\frac{\partial C}{\partial x} = 0 \qquad (2.2)$$

for each stream tube into which the channel is divided, convecting the tracer mass a certain distance downstream in each time step, depending on the local velocity assigned to that stream tube. Then the "new" convected concentrations could be diffused transversely and longitudinally by solving

$$\frac{\partial C}{\partial t} - \epsilon_x \frac{\partial^2 C}{\partial x^2} - \epsilon_z \frac{\partial^2 C}{\partial z^2} = 0 \qquad (2.3)$$

at each longitudinal computation point, and the entire process repeated for successive time increments. Since the solution would compute convection and diffusion separately, it would be desirable that the convection solution, Eq. 2.2, introduce no artificial diffusion; otherwise the total solution to Eq. 2.1 might appear physically reasonable, but in fact be dominated by artificial, as opposed to physical, diffusion. Therefore the convection solution must be analyzed in some detail.

Equation 2.2 represents a situation whereby, in a stream tube of longitudinal velocity u, any

either bank, where there can be no mass transfer. The solution is direct, requiring only a single computation for each grid point, and allows the depth, velocity, and diffusivity to vary with transverse position. In their successful application of the model to the Missouri River, Yotsukura et al. assumed that the diffusivity ε_z was a constant within each cross section.

1.10 The Use of Physical Models for the Prediction of Dispersion in Natural Streams

Physical models of natural waterways are especially useful for the study of hydraulic phenomena when the irregular natural geometry precludes mathematical analysis. As shown in preceding sections, most closed-form mathematical analysis of dispersion is applicable only to uniform stream geometries and artificial velocity fields. Consequently it is tempting to consider the use of physical models for studying dispersion in natural streams, especially when neither the tracer injection nor the water flow can be considered steady state. But physical models usually are incapable of reproducing the prototype dispersion process faithfully.

There are two features of physical models which can effectively destroy their value in predicting dispersion. First, the use of artificial roughness elements (strips or cleats) to compensate for the relatively steep model slopes induces excessive turbulence within the flow. On the other hand, boundary-generated turbulence is primarily responsible for the diffusion in streams; the additional turbulence induced in a physical model accelerates the turbulent diffusion relative to the prototype. Second, restrictions of space and funds require that most physical models be distorted relative to the prototype; an exaggerated vertical dimension allows sufficient depth to reproduce the phenomenon being studied without requiring excessive stream widths and lengths. This distortion can be suitably accounted for in the study of flood stages, velocity fields, or other gross hydraulic features. But Fischer and Holley (1971) have shown that, considering one-dimensional, plane source dispersion in steady flow, a distorted model will produce longitudinal dispersion which is excessively dominated by vertical velocity gradients, and insufficiently responsive to transverse velocity gradients. Fischer (1966) has shown just the opposite tendencies to be characteristic of natural streams, where transverse velocity gradients dominate the mixing process. Holley and Karelse (1973) have presented a similar analysis for two-dimensional mixing from a continuous vertical line source, and concluded that, in a distorted model, the transverse diffusion is too great relative to the prototype. The analytical conclusion was further supported by direct comparisons of model and prototype mixing data.

The exact relationship between the concentration distributions resulting from mixing in model and prototype can be developed analytically only for idealized cases. This fact, added to the complexity of mixing within natural geometries, precludes the use of distorted physical models for studying dispersion phenomena in natural streams.

Chapter II
A FINITE DIFFERENCE SOLUTION TO THE COMPLETE
DEPTH-AVERAGED, TWO-DIMENSIONAL MASS CONSERVATION EQUATION

2.1 The Need for a Numerical Approach

The objective of this chapter is to develop a computational method for the prediction of depth-averaged concentration distributions resulting from the injection of a neutrally-buoyant, conservative tracer into steady river flow of arbitrary geometry. The method must allow for steady or unsteady tracer injection, and take into account the appropriate physical restrictions to mixing in a natural stream. The various analytical and numerical techniques discussed in Chapter 1 do not fulfill the above requirements for one reason or another. It is possible to model sources of arbitrary location in time and space by applying the superposition principle to the appropriate analytical solution; and the condition of zero tracer transport across the boundaries can be satisfied by using the method of images. But to do so in streams of nonrectangular cross section becomes exceedingly complex, if not impossible, and requires the assumptions of longitudinally uniform flow and constant, unidirectional velocity (or at best a uniform shear flow). The analytical solution of Yotsukura and Cobb (1972) requires longitudinally uniform flow, an assumption of a constant diffusion factor $\epsilon_z h^2 u$, and is applicable only to continuous, steady-state injection. The moment method of Sayre (1968) also requires uniform flow, and is applicable only to one-dimensional mixing from an instantaneous plane source, yielding no information on the spread of a point or line source.

The numerical method of Yotsukura et al. (1970) does allow for an arbitrary stream geometry and velocity distribution, but is limited to continuous injection of tracer; therefore the task at hand is the modification of a method such as this to allow for unsteady injection of tracer. But to do so is much more difficult than might be expected, because it involves a fundamental change in the nature of the equation to be solved. Equation 1.43, describing steady-state mixing from a continuous vertical line source, is classified as an elliptic partial differential equation (Carnahan, et al., 1969); the steady-state concentration distribution is dependent only on x and z, the longitudinal and transverse position, respectively. Once the transverse concentration distribution at the upstream boundary of the solution region is specified, and the boundary condition of no tracer transport across the banks is invoked, then in principle the complete concentration distribution can be obtained. In other words, at steady state, a single distribution $C(x,z)$ uniquely satisfies Eq. 1.43 at all points in the solution region. No iterative computation is required, and the accuracy of a numerical solution is governed primarily by the size of the computational grid.

The modification of Eq. 1.43 to allow for unsteady tracer injection is tantamount to reconsideration of the complete two-dimensional depth average dispersion equation, Eq. 1.23. Now there are three independent variables; the time t is added to the space coordinates x and z, and the equation is classified as a parabolic partial differential equation. In addition to the boundary conditions of no transport across the banks, the concentration distribution at the upstream boundary must be specified at

all points in time and some constraint on mixing at the downstream boundary must be applied. Moreover, the convective portion of Eq. 1.23 can introduce an artificial or numerical diffusion which easily can dominate the physical diffusion and thus invalidate computational predictions. Thus the seemingly simple addition of the time-varying term to Eq. 1.43 not only requires that a concentration distribution be computed at each time increment, but also requires an additional boundary condition and, most importantly, introduces the possibility that the numerical solution may not even approximate the true solution. Section 2.2 demonstrates how this may occur, and Sect. 2.3 explores the numerical characteristics of a finite difference method for use in a two-dimensional mathematical model of dispersion.

2.2 The Occurrence of Artificial (Numerical) Diffusion

The purpose of this section is to demonstrate how the finite differencing of a linear convection equation can introduce artificial diffusion which has no physical basis, but is purely a consequence of the computation method. It is reasonable to ask why such behavior should be of concern, since real-life problems do involve physical diffusion. Consider depth-averaged diffusion in a rectangular channel having a transverse velocity distribution u(z). Further assuming that the diffusivities are constant and the transverse velocities are negligible, Eq. 1.23 can be written

$$\frac{\partial C}{\partial t} + u \frac{\partial C}{\partial x} = \epsilon_x \frac{\partial^2 C}{\partial x^2} + \epsilon_z \frac{\partial^2 C}{\partial z^2} \qquad (2.1)$$

One solution technique might be first to solve the convective portion of Eq. 2.1,

$$\frac{\partial C}{\partial t} + u \frac{\partial C}{\partial x} = 0 \qquad (2.2)$$

for each stream tube into which the channel is divided, convecting the tracer mass a certain distance downstream in each time step, depending on the local velocity assigned to that stream tube. Then the "new" convected concentrations could be diffused transversely and longitudinally by solving

$$\frac{\partial C}{\partial t} - \epsilon_x \frac{\partial^2 C}{\partial x^2} - \epsilon_z \frac{\partial^2 C}{\partial z^2} = 0 \qquad (2.3)$$

at each longitudinal computation point, and the entire process repeated for successive time increments. Since the solution would compute convection and diffusion separately, it would be desirable that the convection solution, Eq. 2.2, introduce no artificial diffusion; otherwise the total solution to Eq. 2.1 might appear physically reasonable, but in fact be dominated by artificial, as opposed to physical, diffusion. Therefore the convection solution must be analyzed in some detail.

Equation 2.2 represents a situation whereby, in a stream tube of longitudinal velocity u, any

specified concentration distribution at time t, $C(x,t)$, is moved a distance $u\Delta t$ without any change in shape during the time increment Δt, so that

$$C(\xi, t+\Delta t) = C(x,t) \qquad (2.4)$$

where

$$\xi = x + u\Delta t.$$

This is the exact solution to Eq. 2.2, obtained only if no artificial diffusion is present. But now consider a finite difference solution to Eq. 2.2; one simple scheme might be a one-sided explicit method, whereby Eq. 2.2 would be written

$$\frac{C_{I+1}^{n+1} - C_{I+1}^{n}}{\Delta t} = -\frac{u}{\Delta x}(C_{I+1}^{n} - C_{I}^{n}) \qquad (2.5)$$

where I and n are the longitudinal space and time subscripts and superscripts, respectively, and Δx and Δt are the space and time increments. Note that for $u\Delta t/\Delta x = 1$, Eq. 2.5 gives $C_{I+1}^{n+1} = C_{I}^{n}$, which is the exact solution corresponding to Eq. 2.4. For $u\Delta t/\Delta x > 1$, the solution Eq. 2.5 is unstable, and will not converge to the real solution (Roache, 1972); and for $u\Delta t/\Delta x < 1$, artificial diffusion is introduced. To show this, expand Eq. 2.5 in a Taylor Series about the point $I+1,n$:

$$C_{I+1}^{n} + \Delta t \frac{\partial C}{\partial t} + \frac{\Delta t^2}{2}\frac{\partial^2 C}{\partial t^2} + O(\Delta t^3) - C_{I+1}^{n} =$$

$$-\frac{u\Delta t}{\Delta x}(C_{I+1}^{n} - C_{I+1}^{n} + \Delta x\frac{\partial C}{\partial x} - \frac{\Delta x^2}{2}\frac{\partial^2 C}{\partial x^2} + O(\Delta x^3)$$

or

$$\frac{\partial C}{\partial z} = -\frac{\Delta t}{2}\frac{\partial^2 C}{\partial t^2} + \frac{u\Delta x}{2}\frac{\partial^2 C}{\partial x^2} - u\frac{\partial C}{\partial x} + O(\Delta t^2, \Delta x^2), \qquad (2.6)$$

the symbol O denoting the order of approximation. Now Eq. 2.2 may be differentiated to yield

$$\frac{\partial^2 C}{\partial t^2} = -u\frac{\partial}{\partial t}(\frac{\partial C}{\partial x}) = -u\frac{\partial}{\partial x}(\frac{\partial C}{\partial t}) = -u\frac{\partial}{\partial x}(-u\frac{\partial C}{\partial x})$$

or

$$\frac{\partial^2 C}{\partial t^2} = u^2\frac{\partial^2 C}{\partial x^2}. \qquad (2.7)$$

Substituting Eq. 2.7 into Eq. 2.6 and simplifying,

$$\frac{\partial C}{\partial t} + u\frac{\partial C}{\partial x} = \varepsilon_N\frac{\partial^2 C}{\partial x^2} + O(\Delta t^2, \Delta x^2) \qquad (2.8)$$

where

$$\varepsilon_N = \frac{u\Delta x}{2} - \frac{u^2\Delta t}{2}.$$

Now Eq. 2.8 is not the pure convection equation 2.2 at all, but a diffusion equation with a numerical diffusivity ε_N which vanishes only if $u\Delta t/\Delta x = 1$. Figure 2.1 demonstrates the effect of the numerical

diffusivity, which has no physical basis, but is a direct consequence of the discretization. In a flow situation for which the velocity is a constant U in each stream tube, the time and distance steps could be chosen so as to set $U\Delta t/\Delta x = 1$, and the numerical solution would be nondiffusive. But in a natural stream, where the velocity u changes from one stream tube to another, the condition $u\Delta t/\Delta x = 1$ could be maintained only for one stream tube; all others would exhibit artificial diffusion. Therefore Eq. 2.5 is an example of a finite-difference discretization which is unacceptable for the prediction of dispersion in streams.

Another difficulty in the numerical solution of Eq. 2.2 is the existence of artificial dispersion, or the spreading out of a convected distribution due to the variation in the celerity of the different Fourier components of which it is composed. Section 2.3 includes the analysis of both numerical diffusion and dispersion as applied to the choice of an acceptable finite difference scheme for solution of the convective portion of the depth-averaged mass conservation equation.

2.3 General Method of Analysis of Finite Difference Schemes for Convective Transport

It is, in general, not possible to analyze the numerical characteristics of finite-difference solutions to an equation such as Eq. 1.23. Nonetheless, useful comparisons may be made if the expression is simplified to some extent. With the goal in mind of analyzing a finite difference scheme for the convective portion of Eq. 1.23, the simplified form, Eq. 2.2, is used for analysis.

A general method for determining the stability and convergence characteristics of finite-difference schemes is the consideration of the Fourier components comprising the solution. Writing the solution to Eq. 2.2 as an infinite Fourier Series,

$$C(x,t) = \sum_{m=-\infty}^{m=+\infty} A_m \exp\{i(\sigma_m x - \beta_m t)\} \qquad (2.9)$$

where

A_m = the constant coefficient for the mth component of the series,

$i = \sqrt{-1}$

β_m = frequency of the mth component, $2\pi/T_m$,

σ_m = wave number of the mth component, $2\pi/L_m$,

T_m = the period of the mth component, and

L_m = the wavelength of the mth component.

Since Eq. 2.2 is linear, any component of Eq. 2.9 should be a solution and thus may be substituted into it; the objective here is to find the relationship between β_m and σ_m such that Eq. 2.9 is indeed a solution to Eq. 2.2. Performing the substitution,

$$-A_m(i\beta_m)\exp\{i(\sigma_m x - \beta_m t)\}$$

$$+ u A_m(i\sigma_m)\exp\{i(\sigma_m x - \beta_m t)\} = 0$$

or $\qquad -\beta_m + u\sigma_m = 0. \qquad (2.10)$

11

Therefore when $\beta_m = u\sigma_m$ for all components, Eq. 2.9 is the true solution to Eq. 2.2. The celerity of each series component is given by

$$c_m = \frac{L_m}{T_m} = \frac{\beta_m}{\sigma_m} = u. \qquad (2.11)$$

The constant celerity requires that all series components move downstream at the same rate, allowing no relative dispersion, or spreading, of the solution in space.

Now β_m may be complex, so that Eq. 2.9 may be written

$$C(x,t) = \sum_{m=-\infty}^{m=+\infty} A_m \exp\{Im\beta_m t\} \exp\{i(-Re\beta_m t + \sigma_m x)\}$$

where

$$\beta_m = Re\beta_m + i\, Im\beta_m.$$

Thus $\exp\{Im\beta_m t\}$ may be recognized as a time-dependent function which can amplify or damp the solution component m in time. But Eq. 2.10 requires that, since the wave number σ_m must be real, the frequency β_m must also be real. Consequently

$$Im\beta_m = 0,$$

and

$$\exp\{Im\beta_m t\} = 1, \qquad (2.12)$$

so that the solution is neither damped nor amplified in time. Equations 2.11 and 2.12 simply formalize the expected behavior of the solution to Eq. 2.2: any concentration distribution is displaced in a downstream direction with no change of shape due either to numerical diffusion (damping) or numerical dispersion (spreading out).

The above analysis describes the behavior of the components of the Fourier Series solution to the partial differential equation 2.2. The approach can also be applied to the components of solutions to finite difference approximations of Eq. 2.2, and the results compared to the desired behavior. Specifically, define a convergence coefficient R_1 as the ratio of the finite difference solution damping factor $\exp\{Im\beta\Delta t\}$ to the actual solution damping factor $\exp\{Im\beta t\} = 1.0$, so

$$R_1 = \exp\{Im\beta\Delta t\}. \qquad (2.13)$$

Define R_2 as

$$R_2 = \frac{c_m}{u} \qquad (2.14)$$

or the ratio of the finite difference solution component celerity c_m to the actual solution celerity u.

In Sect. 2.3.1 the coefficients R_1 and R_2 are developed in detail for the double-step implicit-explicit scheme which is applied to the depth-averaged mass conservation equation in Sect. 2.3. In

Appendix C seven other schemes which were also considered are described, and the R_1 and R_2 coefficients are presented and discussed, but without detailed derivation.

2.4 Double-Step Implicit-Explicit Scheme, Second Order

A finite difference method for convection, originally described by Peaceman and Rachford (1955), was applied to flow in estuaries by Leendertse (1970). The method can also be adapted to the present problem of convection in rivers. Each time increment Δt is broken into two halves of equal length; convection is computed implicitly over the first half step, and explicitly over the second. The discretization is shown schematically on Fig. 2.2, where the dashed lines indicate the finite difference approximations to the space and time derivatives. The first half step is called "implicit" because the space derivative at point I, $n+\frac{1}{2}$ must be written in terms of the unknown concentrations at I+1, $n+\frac{1}{2}$ and I-1, $n+\frac{1}{2}$, requiring an indirect solution. The second half step is called "explicit" because the corresponding space derivative is written in terms of known concentrations at I+1, $n+\frac{1}{2}$ and I-1, $n+\frac{1}{2}$, allowing a direct computation of C_I^{n+1}. Each step can be treated independently, and the results finally combined.

2.4.1 Implicit half step. The time derivative in the first half step is written as

$$\frac{\partial C}{\partial t} = \frac{C_I^{n+\frac{1}{2}} - C_I^n}{\Delta t/2}$$

and the space derivative as

$$\frac{\partial C}{\partial x} = \frac{C_{I+1}^{n+\frac{1}{2}} - C_{I-1}^{n+\frac{1}{2}}}{2\Delta x}$$

Equation 2.2 is then written

$$\frac{C_I^{n+\frac{1}{2}} - C_I^n}{\Delta t/2} + u \frac{(C_{I+1}^{n+\frac{1}{2}} - C_{I-1}^{n+\frac{1}{2}})}{2\Delta x} = 0 \qquad (2.15)$$

As before, consider the solution to be decomposed into a Fourier Series, but with time and distance written in discrete form:

$$C(I\Delta x, n\Delta t) = \sum_{m=-\infty}^{m=+\infty} A_m \exp\{i(\sigma_m I\Delta x - \beta_m n\Delta t)\} \qquad (2.16)$$

Substituting the mth component of Eq. 2.16 into Eq. 2.15 and dropping the subscript m yields, after some simplification,

$$\exp\{-i\frac{\beta\Delta t}{2}\}(1 + \frac{ir}{2}\sin\sigma\Delta x) = 1 \qquad (2.17)$$

where

$$r = \frac{u\Delta t}{\Delta x}.$$

In order to obtain R_1 and R_2, it is necessary ultimately to find the damping factor $\exp\{Im\beta\Delta t\}$ and the celerity $Re\beta/\sigma$. This can be done by first writing Eq. 2.17

$$\exp\{-i\,\beta\,\tfrac{\Delta t}{2}\} = \cfrac{1}{1 + \cfrac{ir}{2}\sin\sigma\Delta x}$$

or

$$\exp\{-i\,\beta\,\tfrac{\Delta t}{2}\} = \cfrac{1 - \cfrac{ir}{2}\sin\sigma\Delta x}{1 + \cfrac{r^2}{4}\sin^2\sigma\Delta x} \qquad (2.18)$$

In general, a complex exponential may be written

$$\exp\{i\theta\} = \exp\{iRe\theta - Im\theta\}$$

$$= \exp\{-Im\theta\}\exp\{iRe\theta\}$$

and by Euler's formula,

$$\exp\{i\theta\} = \exp\{-Im\theta\}(\cos Re\theta + i\sin Re\theta). \qquad (2.19)$$

Taking the modulus of Eq. 2.19,

$$|\exp\{i\theta\}| = \exp\{-Im\theta\}(\cos^2 Re\theta + \sin^2 Re\theta)^{1/2}$$

$$= \exp\{-Im\theta\}. \qquad (2.20)$$

Hence from Eq. 2.18,

$$\exp\{Im\beta\,\tfrac{\Delta t}{2}\} = |\exp\{-i\beta\,\tfrac{\Delta t}{2}\}| = \cfrac{(1 + \cfrac{r^2}{4}\sin^2\sigma\Delta x)^{1/2}}{1 + \cfrac{r^2}{4}\sin^2\sigma\Delta x}$$

$$= (1 + \tfrac{r^2}{4}\sin^2\sigma\Delta x)^{1/2}. \qquad (2.21)$$

To find $Re\beta$, first equate the real and imaginary parts on either side of Eq. 2.18:

$$\exp\{Im\beta\,\tfrac{\Delta t}{2}\}\cos(-Re\beta\,\tfrac{\Delta t}{2}) = \cfrac{1}{1 + \cfrac{r^2}{4}\sin^2\sigma\Delta x} \qquad (2.22)$$

and

$$\exp\{Im\beta\,\tfrac{\Delta t}{2}\}\sin(-Re\beta\,\tfrac{\Delta t}{2}) = \cfrac{-\cfrac{r}{2}\sin\sigma\Delta x}{1 + \cfrac{r^2}{4}\sin^2\sigma\Delta x}. \qquad (2.23)$$

Taking the ratio of Eq. 2.23 and Eq. 2.22,

$$\tan(Re\beta\,\tfrac{\Delta t}{2}) = \tfrac{r}{2}\sin\sigma\Delta x$$

or

$$Re\beta = \tfrac{2}{\Delta t}\arctan(\tfrac{r}{2}\sin\sigma\Delta x). \qquad (2.24)$$

2.4.2 Explicit half step. The time derivative in the second half step is written as

$$\frac{\partial C}{\partial t} + \frac{C_I^{n+1} - C_I^{n+\frac{1}{2}}}{\Delta t/2}$$

and the space derivative as

$$\frac{\partial C}{\partial x} = \frac{C_{I+1}^{n+\frac{1}{2}} - C_{I-1}^{n+\frac{1}{2}}}{2\Delta x}.$$

Equation 2.2 is written as

$$\frac{C_I^{n+1} - C_I^{n+\frac{1}{2}}}{\Delta t/2} + \frac{u\,(C_{I+1}^{n+\frac{1}{2}} - C_{I-1}^{n+\frac{1}{2}})}{2\Delta x} = 0. \qquad (2.25)$$

The Fourier Series solution to Eq. 2.25 is

$$C(I\Delta x, n\Delta t) = \sum_{m=-\infty}^{m=+\infty} A_m \exp\{i(\sigma_m I\Delta x - \beta_m n\Delta t)\}. \qquad (2.26)$$

Substituting the mth component of Eq. 2.26 into Eq. 2.25, dropping the subscripts, and simplifying yields

$$\exp\{-i\beta\,\tfrac{\Delta t}{2}\} + \tfrac{ir}{2}\sin(\sigma\Delta x) = 1$$

or

$$\exp\{-i\beta\,\tfrac{\Delta t}{2}\} = 1 - i\,\tfrac{r}{2}\sin(\sigma\Delta x). \qquad (2.27)$$

Applying Eq. 2.20

$$\exp\{Im\beta\,\tfrac{\Delta t}{2}\} = |\exp\{-i\beta\,\tfrac{\Delta t}{2}\}| = [1 + \tfrac{r^2}{4}\sin^2(\sigma\Delta x)]^{1/2}. \qquad (2.28)$$

To find $Re\beta$, equate the real and imaginary parts on either side of Eq. 2.27:

$$\exp\{Im\beta\,\tfrac{\Delta t}{2}\}\cos(-Re\beta\,\tfrac{\Delta t}{2}) = 1 \qquad (2.29)$$

$$\exp\{Im\beta\,\tfrac{\Delta t}{2}\}\sin(-Re\beta\,\tfrac{\Delta t}{2}) = \tfrac{r}{2}\sin(\sigma\Delta x) \qquad (2.30)$$

Taking the ratio of Eq. 2.30 and Eq. 2.29,

$$\tan(Re\beta\,\tfrac{\Delta t}{2}) = \tfrac{r}{2}\sin(\sigma\Delta x)$$

or

$$Re\beta = \tfrac{2}{\Delta t}\arctan(\tfrac{r}{2}\sin\sigma\Delta x). \qquad (2.31)$$

2.4.3 Full time step. The overall damping factor, $\exp\{Im\beta\Delta t\}$, is the product of the damping factors in each half step. Multiplying Eq. 2.21 by Eq. 2.28,

$$\exp\{Im\beta\Delta t\} = 1$$

and consequently

$$R_1 = 1. \qquad (2.32)$$

The component celerities over each half step must be averaged to obtain a representative value. Therefore adding Eq. 2.24 and Eq. 2.31, which are identical, and dividing by 2σ, the average celerity becomes

$$\frac{2}{\sigma\Delta t}\arctan(\tfrac{r}{2}\sin\sigma\Delta x)$$

and division by u gives

$$R_2 = \frac{2}{\sigma u \Delta t} \arctan \left(\frac{r}{2} \sin \sigma \Delta x\right). \qquad (2.33)$$

The result expressed in Eq. 2.32 is highly significant. It indicates that the double-step implicit-explicit finite difference scheme is not only stable for all values of $u\Delta t/\Delta x$, but also that it introduces no numerical damping. This feature is most attractive in view of the discussion in Sect. 2.2, as it eliminates the possibility of artificial diffusion in the purely convective stage. However Eq. 2.33 indicates that R_2 is always less than unity, and therefore all Fourier components will travel more slowly than the true solution, the numerical solution becoming spread out as it is transported downstream; this process may again look like physical diffusion. The key here is to keep $L/\Delta x$ as large as possible, as shown on Fig. 2.3, which is a plot of Eq. 2.33. If $u\Delta t/\Delta x$ is kept reasonably small, say 2.0 or less, then for $L/\Delta x$ greater than 10 the component celerities will be within 15 percent of the desired value. Physically, the most significant wavelength in the Fourier Series of an actual distribution is approximately the "wavelength" of the distribution itself. Therefore it is important that any input concentration distribution be spread over at least 10 computational points; this requirement is physically reasonable, as one would not expect two or three discrete values to describe adequately a concentration distribution.

A demonstration of the sensitivity of the double-step implicit-explicit scheme to values of $u\Delta t/\Delta x$ can be developed by applying Eq. 2.15 and Eq. 2.25 to a simple rectangular channel of width 30, length 10,000, depth 1.96, velocity 0.467, and distance step $\Delta x = 200$, all in arbitrary units.

The initial concentration distribution is a half-sine wave of amplitude 10 units centered at the eighth computational point, i.e.,

$$C(I\Delta x, 0) = 10 \sin[\pi(I-3)] \text{ for } 3 \leq I \leq 13,$$

$$= 0 \text{ otherwise.}$$

The distribution was routed downstream for 10,800 time units of $\Delta t = 98.5$, 398.3, and 1713.1 units, or $u\Delta t/\Delta x = 0.23$, 0.93, and 4.0. Figure 2.4 shows the results of the computation, demonstrating that although for $u\Delta t/\Delta x = 0.23$ and $u\Delta t/\Delta x = 0.93$ some numerical dispersion is present, the primary distribution gives a satisfactory reproduction of the ideal solution. But for $u\Delta t/\Delta x = 4.0$, the computed distribution gives a poor estimate of the desired curve. Oscillations behind the primary distribution are caused by low-amplitude Fourier solution components moving much more slowly. Concentrations from the leading edge of the distribution to its peak, where most practical interest is generally focused, are relatively unaffected by the oscillations.

The double-step implicit-explicit scheme is of second order accuracy. That is, a Taylor Series expansion of the finite difference solution is identical to the exact solution if terms the order of Δx^2, Δt^2 are dropped. In Appendix C seven additional schemes of first, second, and fourth order are discussed. The derivations of R_1 and R_2 are not shown, but follow the general pattern used in this section.

2.5 Comparison of Finite Difference Schemes for Convective Transport

In general it is not possible to choose one of the schemes analyzed in Sect. 2.4 and Appendix C as superior to the others. Each scheme has its own set of advantages and disadvantages over some range of conditions, and any one of them might be the best choice for the computation of pure convection in a specified flow situation. But an important consideration in selecting a scheme for general use is its flexibility in demonstrating favorable characteristics over a broad range of flow conditions. Therefore it is instructive to compare some general characteristics of the eight schemes.

Fully explicit methods, such as schemes A, D, and E, are generally easy to program for the computer and use relatively little computer time. But they are unstable, i.e., yield no solution, when the Courant number, $u\Delta t/\Delta x$, exceeds unity. Moreover, scheme A introduces numerical damping whenever $u\Delta t/\Delta x$ is less than unity.

The fully implicit methods, on the other hand, are unconditionally stable for all values of the Courant number. But schemes B and C do introduce numerical damping for all values of the Courant number, and moreover require significantly greater programming complexity and computer time.

There are two fundamental questions to be considered in choosing between fully explicit and fully implicit schemes:

a) Is natural damping, or diffusion a significant factor in the physical phenomenon being modeled?

b) Does the longitudinal velocity vary significantly from one point in the stream to another?

For dispersion in streams the answer to a) is obviously "yes"; and the chosen scheme must minimize numerical diffusion. For the prediction of dispersion in man-made channels such as canals or floodways, the answer to b) may be "no", and a simple explicit method may be used with Δx and Δt chosen so as to keep $u\Delta t/\Delta x$ as close to unity as possible throughout. Then the solution will be stable and artificial damping will be at a minimum. But in a natural stream, where the transverse gradient of longitudinal velocity can be significant, it is impossible to have $u\Delta t/\Delta x = 1$ everywhere, and an implicit method might be more useful. Then the time and distance steps can be chosen so that the average value of $u\Delta t/\Delta x$ is near unity; the solution will always be stable, but artificial damping will be introduced over most of the cross section. In order to minimize the damping over the entire section, and at the same time allow some flexibility in time and distance steps so that the solution may be obtained with the desired detail, it is necessary to adopt a composite scheme such as F, G, or the implicit-explicit scheme described in Sect. 2.4.

Among the composite methods, the second order implicit-explicit scheme is clearly the most attractive, as it is unconditionally stable and nondamping. The fourth-order version offers little improvement for the increased programming complexity, and the predictor-corrector method, (scheme G), while unconditionally stable, still introduces numerical damping always.

The second order double-step implicit-explicit scheme, described in Sect. 2.4, offers the best convergence characteristics among the eight methods studied insofar as solutions to Eq. 2.2 are concerned. For the more general convection equation, i.e., the left-hand side of Eq. 1.23, convergence coefficients simply cannot be derived, and thus there is no basis for the direct choice of an optimum scheme. Therefore it is simply assumed that the relative desirability of the scheme in Sect. 2.4, as shown for the solution of Eq. 2.2, extends also to the solution of Eq. 1.23.

2.6 Application of the Second Order Double-Step Implicit-Explicit Scheme to Solution of the Depth-Averaged Dispersion Equation

The depth-averaged mass conservation equation, Eq. 1.23, describes the mixing process within an infinitesimally narrow control volume, i.e., at a point. It is important to ensure that, in solving Eq. 1.23 numerically on a discrete grid of computational points, the principle of conservation of mass is not violated. For this reason the river is conceptualized as a group of stream tubes each of which extends from the bed to the water surface, and is bounded laterally by streamlines, as shown in Fig. 2.5. Thus the tube widths, depths, and longitudinal velocities vary longitudinally so as to keep the discharge constant in each, and the tube centerlines may shift back and forth in the channel as the transverse distribution of discharge changes. The centerline of each stream tube is a computational point J, located at longitudinal computational points I.

Equation 1.23, written in terms of depth-averaged variables, must be rewritten in terms of stream-tube averages. This may be done by integrating over the width of a stream tube whose left and right hand transverse coordinates are $z = a'$ and $z = b'$, respectively:

$$\int_{a'}^{b'} h \frac{\partial C}{\partial t} dz + \int_{a'}^{b'} \frac{\partial}{\partial x} (huC) dz + \int_{a'}^{b'} \frac{\partial}{\partial z} (hwC) dz$$

$$= \int_{a'}^{b'} \frac{\partial}{\partial x} (h\varepsilon_x \frac{\partial C}{\partial x}) dz + \int_{a'}^{b'} \frac{\partial}{\partial z} (h\varepsilon_z \frac{\partial C}{\partial z}) dz. \quad (2.34)$$

Applying Leibniz's theorem for differentiation of an integral, and noting that, by definition, the depth-averaged transverse velocity w must vanish at the stream tube boundaries, Eq. 2.34 may be written as

$$\frac{\partial}{\partial t} \int_{a'}^{b'} hC \, dz + \frac{\partial}{\partial x} \int_{a'}^{b'} (huC) \, dz = \frac{\partial}{\partial x} \int_{a'}^{b'} (h\varepsilon_x \frac{\partial C}{\partial x}) \, dz$$

$$+ \frac{\partial}{\partial z} \int_{a'}^{b'} (h\varepsilon_z \frac{\partial C}{\partial z}) \, dz + (huC)|_{b'} \frac{\partial b'}{\partial x} - (huC)|_{a'} \frac{\partial a'}{\partial x}$$

$$- (h\varepsilon_x \frac{\partial C}{\partial x})|_{b'} \frac{\partial b'}{\partial x} + (h\varepsilon_x \frac{\partial C}{\partial x})|_{a'} \frac{\partial a'}{\partial x}. \quad (2.35)$$

Denoting the stream tube width by B', lumping the last four terms into a single term R, and using an overbar to denote a stream tube average, Eq. 2.34 may be written

$$\frac{\partial}{\partial t} (B'\overline{hC}) + \frac{\partial}{\partial x} (B'\overline{huC}) = \frac{\partial}{\partial x} (B'\overline{h\varepsilon_x \frac{\partial C}{\partial x}})$$

$$+ (h\varepsilon_z \frac{\partial C}{\partial z})|_{b'} - (h\varepsilon_z \frac{\partial C}{\partial z})|_{a'} + R. \quad (2.36)$$

In a prismatic channel, the stream tube boundaries are parallel to the x-axis, and $R = 0$. In a nonprismatic channel, the boundaries are parallel neither to the x-axis nor to each other; therefore the longitudinal convection and diffusion, assumed to be parallel to the x-axis in Eq. 2.36, are actually not parallel to the stream tube boundaries. The terms in R account for the mass transport across nonparallel tube boundaries due to longitudinal diffusion and convection. As long as enough stream tubes are used to keep $\partial a'/\partial x$, $\partial b'/\partial x$, and the variation of hu across the tube relatively small, the effect of neglecting R will be negligible. Finally, noting that the product $B'\overline{h}$ is the cross-sectional area of the stream tube, A, and dropping the overbars, Eq. 2.36 may be written

$$A \frac{\partial C}{\partial t} + \frac{\partial}{\partial x} (AuC) = \frac{\partial}{\partial x} (A\varepsilon_x \frac{\partial C}{\partial x})$$

$$+ (h\varepsilon_z \frac{\partial C}{\partial z})|_{b'} - (h\varepsilon_z \frac{\partial C}{\partial z})|_{a'}. \quad (2.37)$$

It is important to recognize that Eq. 2.37, which is the basis of the numerical model, does not require that secondary transverse velocities be zero. The longitudinal variation of stream tube widths, required to satisfy continuity, results in a longitudinal variation of the transverse coordinates of stream tube centroids. An observer moving with the flow in a particular stream tube would see this as a gradual movement across the channel, i.e., as the effect of depth-averaged transverse velocity. The stream tube averaging process has removed the depth-averaged transverse velocity w as an explicit parameter, but w implicitly governs the dimensioning of stream tubes to satisfy continuity. Moreover, additional transverse mixing caused by secondary velocities, i.e., the mixing associated with deviations of concentration and transverse velocity from their respective depth averages, has been absorbed in the transverse diffusivity, ε_z. Therefore Eq. 2.37 is, of itself, applicable to flow around alternate bars and in bends; any limitation is in the degree to which the secondary mixing contribution to ε_z can be quantified.

Fischer (1969) and Chang (1971) have attempted theoretical and experimental quantifications of the secondary mixing in bends, based on the secondary flow theories of Rozovskii (1957). Neither investigator was able to obtain definitive results, due primarily to the weakness of existing secondary flow theory, and due to the difficulty of obtaining secondary velocity measurements.

The general strategy for the numerical solution of Eq. 2.37 is as follows: in each time step, first route the concentration distribution in each stream tube downstream by solving for pure convection using the second order double-step implicit-explicit scheme. Second, solve for transverse diffusion by applying a fully implicit scheme to the convected concentrations. Finally, diffuse the concentration distributions longitudinally with another fully implicit scheme. The details of the computation are outlined in the following three subsections.

15

2.6.1 <u>Longitudinal convection</u>. The finite difference method of Sect. 2.4 is used to solve the convective portion of Eq. 2.37,

$$A \frac{\partial C}{\partial t} + \frac{\partial}{\partial x}(AuC) = 0, \qquad (2.38)$$

separately in each stream tube J. Assume that the entire concentration field is known at time n. Equation 2.38 is written for the implicit half step as

$$A_{I,J} \frac{(C_{I,J}^{n+\frac{1}{2}} - C_{I,J}^n)}{\Delta t/2}$$

$$+ \frac{(Au)_{I+1,J} C_{I+1,J}^{n+\frac{1}{2}} - (Au)_{I-1,J} C_{I-1,J}^{n+\frac{1}{2}}}{x_{I+1} - x_{I-1}} = 0$$

which may be rewritten

$$C_{I,J}^{n+\frac{1}{2}} = C_{I,J}^n + R_{I,J} C_{I-1,J}^{n+\frac{1}{2}} - S_{I,J} C_{I+1,J}^{n+\frac{1}{2}} \qquad (2.39)$$

where

$$R_{I,J} = \frac{\Delta t \ (Au)_{I-1,J}}{2A_{I,J}(x_{I+1} - x_{I-1})} \qquad (2.40a)$$

and

$$S_{I,J} = \frac{\Delta t \ (Au)_{I+1,J}}{2A_{I,J}(x_{I+1} - x_{I-1})}. \qquad (2.40b)$$

Note that the coefficients R and S are known at all times, but Eq. 2.39 contains three unknown concentrations. The writing of Eq. 2.39 for each of N-2 computational points will generate a system of N-2 linear equations in N unknowns, where N is the total number of computational points. Therefore two boundary conditions must be supplied before a solution is possible.

The appearance of only three adjacent unknowns in each of the N equations makes the linear system diagonally dominant, or banded (Carnahan et al., 1969). This is noteworthy as it obviates the need for a time consuming, complex matrix inversion. Instead, a tridiagonal matrix method, also known as the double-sweep method, may be used to solve the linear system. First, express the concentration at I-1 as a linear function of the concentration at I:

$$C_{I-1,J}^{n+\frac{1}{2}} = E_{I-1,J} C_{I,J}^{n+\frac{1}{2}} + F_{I-1,J} \qquad (2.41)$$

where E and F are constants yet to be determined. Substituting Eq. 2.41 into Eq. 2.39,

$$C_{I,J}^{n+\frac{1}{2}} = C_{I,J}^n + R_{I,J} E_{I-1,J} C_{I,J}^{n+\frac{1}{2}}$$

$$+ R_{I,J} F_{I-1,J} - S_{I,J} C_{I+1,J}^{n+\frac{1}{2}}$$

or

$$C_{I,J}^{n+\frac{1}{2}} = \frac{-S_{I,J}}{1-R_{I,J} E_{I-1,J}} C_{I+1,J}^{n+\frac{1}{2}} + \frac{C_{I,J}^n + R_{I,J} F_{I-1,J}}{1-R_{I,J} E_{I-1,J}}. \ (2.42)$$

Comparing Eqs. 2.41 and 2.42, it may be seen that

$$E_{I,J} = \frac{-S_{I,J}}{1-R_{I,J} E_{I-1,J}} \qquad (2.43a)$$

and

$$F_{I,J} = \frac{C_{I,J}^n + R_{I,J} F_{I-1,J}}{1-R_{I,J} E_{I-1,J}}. \qquad (2.43b)$$

The significance of Eqs. 2.41 and 2.43 is that after appropriate application of the upstream boundary condition, $E_{1,J}$ and $F_{1,J}$ are known, and by recurrence all the remaining E and F values may be computed from Eq. 2.43. Then the downstream boundary condition fixes $C_{N,J}^{n+\frac{1}{2}}$, and by recurrence the remaining values of C may be computed from Eq. 2.41. By this means the double-sweep technique allows a complete solution in each time step through a direct computation.

The boundary conditions are applied as follows: at the upstream boundary of each stream tube, the concentration input is known at all times. Denoting this value at time $n+\frac{1}{2}$ as $C_{1,J}^{n+\frac{1}{2}}$, Eq. 2.41 may be written

$$C_{1,J}^{n+\frac{1}{2}} = E_{1,J} C_{2,J}^{n+\frac{1}{2}} + F_{1,J}$$

which will satisfy the boundary condition if

$$E_{1,J} = 0 \quad \text{and} \quad F_{1,J} = C_{1,J}^{n+\frac{1}{2}}.$$

Then the remaining values of E and F may be computed and stored for each stream tube.

At the downstream boundary there is no specified condition. Thus it is necessary to create one by assuming the existence of a fictitious point whose x-coordinate differs from one tube to another and is computed as

$$x_{N+1,J} = x_N + u_{N,J} \frac{\Delta t}{2}.$$

Now assume that between these last two points there is no change in shape of the concentration distribution in the half step, so that

$$C_{N+1,J}^{n+\frac{1}{2}} = C_{N,J}^n.$$

Then

$$C_{N,J}^{n+\frac{1}{2}} = E_{N,J} C_{N+1,J}^{n+\frac{1}{2}} + F_{N,J}$$

or

$$C_{N,J}^{n+\frac{1}{2}} = E_{N,J} C_{N,J}^n + F_{N,J}$$

and by recurrence using Eq. 2.41 the remaining concentrations may be computed using the previously-stored E and F values. This procedure is carried out for each tube J, completing the implicit half step of the convective stage.

The explicit half step computes the convected concentrations at time n+1 given the values at time $n+\frac{1}{2}$ as computed in the implicit half step.

Equation 2.38 is written explicitly as

$$A_{I,J} \frac{(C_{I,J}^{n+1} - C_{I,J}^{n+\frac{1}{2}})}{\Delta t/2}$$

$$+ \frac{(Au)_{I+1,J} C_{I+1,J}^{n+\frac{1}{2}} - (Au)_{I-1,J} C_{I-1,J}^{n+\frac{1}{2}}}{x_{I+1} - x_{I-1}} = 0$$

which may be rewritten

$$C_{I,J}^{n+1} = C_{I,J}^{n+\frac{1}{2}} + R_{I,J} C_{I-1,J}^{n+\frac{1}{2}} - S_{I,J} C_{I+1,J}^{n+\frac{1}{2}} \qquad (2.44)$$

where R and S are as defined previously in Eq. 2.40. Equation 2.44 contains only one unknown concentration. The upstream boundary condition is sufficient to start the calculation; $C_{1,J}^{n+1}$ is known, and the remaining concentrations may be computed directly in each stream tube using Eq. 2.44.

At this stage in the computation, the known concentration distribution in each stream tube has been routed downstream for one time step without any numerical diffusion, but possibly with some numerical dispersion. The routed distributions are now to be diffused transversely and longitudinally.

2.6.2 Transverse diffusion. To this point nothing has been said regarding the finite difference scheme to be used for transverse and longitudinal diffusion. Consider a fully implicit scheme applied to a simplified one-dimensional diffusion equation,

$$\frac{\partial C}{\partial t} = \varepsilon_\eta \frac{\partial^2 C}{\partial \eta^2} \qquad (2.45)$$

where η represents either the x or z direction and ε_η is a constant. Applying a symmetrical implicit scheme to Eq. 2.45,

$$\frac{C_J^{n+1} - C_J^n}{\Delta t} = \varepsilon_\eta \frac{(C_{J+1}^{n+1} - 2C_J^{n+1} + C_{J-1}^{n+1})}{\Delta \eta} \qquad (2.46)$$

where the J index refers to the η-direction computational point. A Taylor Series expansion of Eq. 2.46 about the point (n,J) yields, after some simplification,

$$\frac{\partial C}{\partial t} = \varepsilon_\eta \frac{\partial^2 C}{\partial \eta^2} - \frac{\Delta t}{2} \frac{\partial^2 C}{\partial t^2} + O(\Delta t^2, \Delta \eta^2). \qquad (2.47)$$

Thus the finite difference approximation (Eq. 2.46) converges to the partial differential equation (Eq. 2.45) as the time step Δt and distance step $\Delta \eta$ approach zero. Moreover, Eq. 2.46 is unconditionally stable; the method is used herein for both transverse and longitudinal diffusion.

The transverse diffusion portion of Eq. 2.37,

$$A \frac{\partial C}{\partial t} = (h\varepsilon_z \frac{\partial C}{\partial z})\Big|_{b'} - (h\varepsilon_z \frac{\partial C}{\partial z})\Big|_{a'} \qquad (2.48)$$

is written in implicit form as

$$A_{I,J} \frac{(C_{I,J}^{n+1} - C_{I,J}^n)}{\Delta t} = (h\varepsilon_z)_{I;J,J+1} \frac{(C_{I,J+1}^{n+1} - C_{I,J}^{n+1})}{z_{I,J+1} - z_{I,J}}$$

$$- (h\varepsilon_z)_{I;J,J-1} \frac{(C_{I,J}^{n+1} - C_{I,J-1}^{n+1})}{z_{I,J} - z_{I,J-1}} \qquad (2.48a)$$

where the concentrations have already been convected for the time step, $z_{I,J}$ denotes the centroid of the Jth stream tube at the Ith computational point, and $(h\varepsilon_z)_{I;J,J+1}$ is the product of the average diffusivity in tubes J and $J+1$, and the smaller of the two tube depths. Noting that

$$z_{I,J+1} - z_{I,J} = \frac{(B'_{I,J+1} + B'_{I,J})}{2}$$

Equation 2.48a may be rewritten

$$D1\, C_{I,J-1}^{n+1} + D2\, C_{I,J}^{n+1} + D3\, C_{I,J+1}^{n+1} = C_{I,J}^n \qquad (2.49)$$

where

$$D1 = \frac{-2\Delta t}{A_{I,J}} \frac{(h\varepsilon_z)_{I;J,J-1}}{B_{I,J} + B_{I,J-1}} \qquad (2.50a)$$

$$D2 = 1 + \frac{2\Delta t\,(h\varepsilon_z)_{I;J,J+1}}{A_{I,J}(B_{I,J+1} + B_{I,J})} + \frac{2\Delta t\,(h\varepsilon_z)_{I;J,J-1}}{A_{I,J}(B'_{I,J} + B'_{I,J-1})} \qquad (2.50b)$$

$$D3 = \frac{-2\Delta t}{A_{I,J}} \frac{(h\varepsilon_z)_{I;J,J+1}}{B_{I,J+1} + B_{I,J}} \qquad (2.50c)$$

Once again the system of $M-2$ linear equations in M unknowns (where M is the number of stream tubes) must be solved simultaneously with the addition of boundary conditions at both banks. To develop the double-sweep method, first express the concentration in the tube $J-1$ as a linear function of the concentration in tube J:

$$C_{I,J-1}^{n+1} = E_{I,J-1} C_{I,J}^{n+1} + F_{I,J-1}. \qquad (2.51)$$

Substituting Eq. 2.51 into Eq. 2.49,

$$D1(E_{I,J-1} C_{I,J}^{n+1} + F_{I,J-1}) + D2\, C_{I,J}^{n+1} + D3\, C_{I,J+1}^{n+1} = C_{I,J}^n$$

or

$$C_{I,J}^{n+1} = \left(\frac{-D3}{D1\, E_{I,J-1} + D2}\right) C_{I,J+1}^{n+1} + \frac{C_{I,J}^n - D1\, F_{I,J-1}}{D1\, E_{I,J-1} + D2}. \qquad (2.52)$$

Comparing Eqs. 2.51 and 2.52, it may be seen that

$$E_{I,J} = \frac{-D3}{D1\, E_{I,J-1} + D2} \qquad (2.53a)$$

and

17

$$F_{I,J} = \frac{C_{I,J}^n - D1\ F_{I,J-1}}{D1\ E_{I,J-1} + D2}. \qquad (2.53b)$$

Equations 2.51 and 2.53 represent concentration and sweep coefficient recurrence relations, which may be used when the boundary conditions are employed.

At the left boundary there can be no transverse diffusion. Thus $D1 = 0$, and $D2$ is written for this special case as

$$D2^{*} = 1 + \frac{2\Delta t}{A_{I,1}} \frac{(h\varepsilon_z)_{I;1,2}}{(B_{I,2} + B_{I,1})}$$

and Eq. 2.49 is written

$$D2^{*}\ C_{I,1}^{n+1} + D3\ C_{I,2}^{n+1} = C_{I,1}^n.$$

By comparison with Eq. 2.51,

$$E_{I,1} = -\frac{D3}{D2^{*}}$$

and

$$F_{I,1} = \frac{C_{I,1}^n}{D2^{*}}.$$

Thus the remaining values of E and F may be computed through tube $M-1$ and stored for each computational point I.

At the right boundary, the same condition of no transverse diffusion applies, so that $D3 = 0$ and $D2$ is written for this second special case as

$$D2^{**} = 1 + \frac{2\Delta t\ (h\varepsilon_z)_{I;M-1,M}}{A_{I,M}(B_{I,M} + B_{I,M-1})}$$

and Eq. 2.49 is written

$$D1\ C_{I,M-1}^{n+1} + D2^{**}\ C_{I,M}^{n+1} = C_{I,M}^n.$$

Using Eq. 2.72, this may be rewritten

$$D1(E_{I,M-1}\ C_{I,M}^{n+1} + F_{I,M-1}) + D2^{**}\ C_{I,M}^{n+1} = C_{I,M}^n$$

or

$$C_{I,M}^{n+1} = \frac{C_{I,M}^n - D1\ F_{I,M-1}}{D1\ E_{I,M-1} + D2^{**}} \qquad (2.54)$$

Note that the coefficients E and F are not needed for tube M, and once $C_{I,M}^{n+1}$ is found from Eq. 2.54, the remaining concentrations in each tube are computed using the stored E and F values, and the recurrence relation Eq. 2.51. The entire process is repeated at each computational point, the end result being a concentration field which has been convected and diffused transversely in the time step. All that remains is the computation of longitudinal diffusion.

2.6.3 Longitudinal diffusion. The implicit longitudinal diffusion computation is nearly identical to the transverse diffusion, but uses the same boundary conditions as the longitudinal convection routine. The longitudinal diffusion portion of Eq. 2.37,

$$A\ \frac{\partial C}{\partial t} = \frac{\partial}{\partial x}\ \left(A\varepsilon_x\ \frac{\partial C}{\partial x}\right) \qquad (2.55)$$

is written in implicit form as

$$A_{I,J}\ \frac{(C_{I,J}^{n+1} - C_{I,J}^n)}{\Delta t} = \frac{1}{x_{I+\frac{1}{2}} - x_{I-\frac{1}{2}}}$$

$$[(A\varepsilon_x)_{I,I+1;J}\ \frac{(C_{I+1,J}^{n+1} - C_{I,J}^{n+1})}{x_{I+1} - x_I}$$

$$-\ (A\varepsilon_x)_{I-1,I;J}\ \frac{(C_{I,J}^{n+1} - C_{I-1,J}^{n+1})}{x_I - x_{I-1}}] \qquad (2.55a)$$

where the concentrations have already been convected and diffused transversely, $x_{I+\frac{1}{2}} = (X_{I+1} + X_I)/2$, and $(A\varepsilon_x)_{I,I-1;J}$ is the product of the average cross-sectional areas and diffusivities in tube J at adjacent computational points.

Equation 2.55a may be rewritten

$$G1\ C_{I-1,J}^{n+1} + G2\ C_{I,J}^{n+1} + G3\ C_{I+1,J}^{n+1} = C_{I,J}^n \qquad (2.56)$$

where

$$G1 = \frac{-2\Delta t}{A_{I,J}}\ \frac{(A\varepsilon_x)_{I-1,I;J}}{(x_{I+1} - x_{I-1})(x_I - x_{I-1})} \qquad (2.57a)$$

$$G2 = 1 + \frac{2\Delta t}{A_{I,J}}\ \frac{(A\varepsilon_x)_{I,I-1;J}}{(x_{I+1} - x_{I-1})(x_I - x_{I-1})}$$

$$+\ \frac{2\Delta t}{A_{I,J}}\ \frac{(A\varepsilon_x)_{I,I+1;J}}{(x_{I+1} - x_{I-1})(x_{I+1} - x_I)} \qquad (2.57b)$$

$$G3 = -\ \frac{2\Delta t}{A_{I,J}}\ \frac{(A\varepsilon_x)_{I,I+1;J}}{(x_{I+1} - x_{I-1})(x_{I+1} - x_I)}. \qquad (2.57c)$$

To solve the system of $N-2$ equations in N unknowns again apply the two boundary conditions and use the double-sweep method. First, write

$$C_{I-1,J}^{n+1} = E_{I-1,J}\ C_{I,J}^{n+1} + F_{I-1,J}. \qquad (2.58)$$

Substitute Eq. 2.58 into Eq. 2.56:

$$G1(E_{I-1,J}\ C_{I,J}^{n+1} + F_{I-1,J}) + G2\ C_{I,J}^{n+1} + G3\ C_{I+1,J}^{n+1} = C_{I,J}^n$$

or

$$C_{I,J}^{n+1} = \left(\frac{-G3}{G1\ E_{I-1,J} + G2}\right) C_{I+1,J}^{n+1} + \frac{C_{I,J}^n - G1\ F_{I-1,J}}{G1\ E_{I-1,J} + G2}.$$

Comparing Eqs. 2.58 and 2.59,

$$E_{I,J} = \frac{-G3}{G1 \, E_{I-1,J} + G2} \qquad (2.60a)$$

and

$$F_{I,J} = \frac{C_{I,J}^n - G1 \, F_{I-1,J}}{G1 \, E_{I-1,J} + G2} \qquad (2.60b)$$

At the upstream boundary the concentration $C_{1,J}^{n+1}$ is known, so by setting $E_{1,J} = 0$ and $F_{1,J} = C_{1,J}^{n+1}$ the boundary condition is satisfied and the remaining E and F values may be computed. At the downstream boundary assume that there is no longitudinal diffusion, so that

$$C_{N,J}^{n+1} = C_{N,J}^n.$$

Then by Eq. 2.58 the remaining values of concentration are computed, and the process repeated for each stream tube.

This completes the numerical solution of Eq. 2.37 in one time step. The total solution may proceed for as long a time as desired, and the time step Δt may be changed whenever necessary. The input concentration at the upstream boundary of each stream tube must be specified, and any initial concentration field may also be established on the computational grid before the computation begins. Appendix D contains a listing of the complete computer program. Appendix E describes the recommended procedure for establishing stream tube dimensions.

2.7 Practical Considerations in the Selection of a Computational Grid

The selection of computational grid dimensions is governed by the convergence requirements of the numerical method, and by the computer time and storage available. While it is always true that the smaller the time and distance steps, the more reliable the solution, it is seldom feasible to obtain the time and space resolution which is desired. It is the purpose of this section to outline the minimum requirements of the numerical method.

2.7.1 *Transverse computational points*. At the furthest upstream reference section, the stream tube centerline locations (i.e., the transverse computational points) are fixed arbitrarily by the user's specification of tube widths and/or discharges. But at downstream sections the tube centerlines must shift back and forth across the stream as the bulk of the river flow shifts; thus the user has little control over the location of the transverse computational points over most of the river reach. Nonetheless, the expected pattern of mixing can be taken into account in assigning stream tube dimensions at the upstream reference section; the tubes should be narrowest (the computational points closest together) in the region where most of the tracer is expected to be located. For injection at the right bank, for example, it is desirable to have most of the computational points near the bank throughout the reach. Equation 2.47 shows that, in a rectangular channel, the numerical solution becomes more convergent as the spacing of transverse computational points decreases; moreover, the assumption that the terms labeled R in Eq. 2.36 approach zero improves as the number of stream tubes

increases. Therefore it is always desirable to use as many stream tubes as possible.

The recent use of remote sensing techniques in river mechanics has brought about an increased awareness of weak secondary cells in straight reaches of large rivers. These cells, as indicated by the collection of drift and foam along well-defined lines at the surface, appear to be quite stable, effectively partitioning the reach into parallel longitudinal elements. Although little is known about the detailed structure of these weak cells, it is evident that they could serve as barriers to the gradient-type mixing assumed in Eq. 2.37. Whenever possible, evidence of these cells should be used to position stream tubes so as to enclose the drift lines, and thus minimize the potential disruption of gradient mixing at the boundaries between stream tubes.

2.7.2 *Longitudinal computational points*. The spacing of longitudinal computational points is governed by the convective, rather than diffusive, portion of the solution to the mass conservation equation, and depends to some extent on whether a steady-state or unsteady mixing process is being simulated. The steady-state concentration distribution resulting from continuous injection of tracer is independent of numerical dispersion considerations, as long as the simulation is run long enough for a true steady state to be obtained. Therefore the longitudinal computational points must simply be spaced closely enough to reproduce the stream geometry in adequate detail, and positioned so as to provide transverse concentration distributions at points of significant interest.

Simulations of unsteady dispersion require that more consideration be given to the spacing of longitudinal computational points. It is pointed out in Sect. 2.4 that, for a fixed value of $u\Delta t/\Delta x$, the convergence coefficient R_2 approaches unity as $L/\Delta x$ increases, where L is the wavelength of one component of the Fourier Series solution to a simplified form of the convection equation. As a general guideline the longitudinal concentration distribution in any stream tube should be described by at least 10 computational points; this demands that the longitudinal computational points be spaced more closely together near the source than further downstream. Furthermore, rapidly varying sources require a much closer spacing than unsteady but slowly varying sources.

2.7.3 *Time increments*. The type of tracer injection also influences the choice of the time step Δt. For continuous injection, anomalous concentrations due to numerical dispersion are dissipated as the solution approaches a steady state, yet the time step must be small to obtain good convergence as demonstrated by Eq. 2.47. For unsteady injection, it is desirable to keep the parameter $u\Delta t/\Delta x$ less than about 2.0. The distance step Δx, although not necessarily constant, is fixed by the considerations of Sect. 2.7.2, and the velocity u is known at all locations. A satisfactory choice of Δt is made by considering the largest value of $\Delta x/u$ to be encountered in the zone where significant mixing is expected to occur; Δt should be smaller than twice $\Delta x/u$. The time step need not be constant, and may be increased as the tracer moves downstream into regions of larger Δx.

It is often advisable to check the choice of time and distance steps by first running the simulation for reasonable choices of Δt, Δx, and stream tube widths, then rerunning the simulation after decreasing each parameter individually. A satisfactory computational

model has been specified when the predicted concentration distribution is relatively insensitive to a further refinement of the grid and/or time step.

2.8 Comparison of Numerical Predictions and Two Analytical Solutions

The numerical dispersion model described in Sect. 2.6 is capable of producing approximate solutions to Eq. 1.23 in situations where no analytical solution is available. But quantitative tests of the model's efficacy must necessarily be made in relatively simple flow fields, where idealized stream geometry allows analytical solutions to be obtained. Comparisons are made for the cases of (a) continuous injection in a rectangular channel, and (b) instantaneous injection in a uniform shear flow. These comparisons should not be viewed as a verification of the model; it is known from the outset that the finite difference solution to a partial differential equation may represent a solution to an entirely different equation, as shown in Sect. 2.2 and Sect. 2.6.2. The comparisons are made so that the degree of approximation of the correct concentration distributions can be viewed for the entire solution, and so that the sensitivity of the approximations to the computational grid dimensions can be tested.

2.8.1 Continuous injection in a rectangular channel. One of the simplest dispersion situations is continuous vertical line source injection at the centerline of a rectangular channel with constant longitudinal velocity U at all transverse and longitudinal locations. Equation 1.29 is a solution to Eq. 1.23 for these conditions, provided that the method of images described in Sect. 1.7 is used to reproduce the proper boundary conditions, and longitudinal diffusion is neglected. Using five reflection cycles as suggested by Sayre (1973), Eq. 1.29 may be written for this problem as

$$C(x,z) = \frac{q_o C_o U^{-\frac{1}{2}}}{2H(\pi \epsilon_z x)^{\frac{1}{2}}} [\exp\{\frac{-U z^2}{4\epsilon_z x}\}$$

$$+ \sum_{n=1}^{5} (\exp\{\frac{-U(nB+(-1)^n z)^2}{4\epsilon_z x}\}$$

$$+ \exp\{\frac{-U(nB(-1)^n z)^2}{4\epsilon_z x}\})] \qquad (2.61)$$

The channel geometry and hydraulic parameters were taken from Test 2 reported by Miller (1971);

$$B = 2.0 \text{ ft,}$$
$$h = 0.415 \text{ ft,}$$
$$U = 1.75 \text{ ft/sec,}$$
$$\epsilon_z = 0.01039 \text{ ft}^2/\text{sec.}$$

A 50-foot length of channel was divided into computational points one foot apart; a tracer flowrate of 0.145 ppb-cfs (parts per billion-cubic feet per second) was introduced at the upstream boundary. For the first simulation 11 stream tubes were used, and for the second, 21 tubes; the two computational grids are sketched in Fig. 2.6, and the stream tube dimensions are presented in Table 2.1. Steady state concentration distributions were obtained by allowing the upstream concentration in the centerline tube to rise from zero to its steady state value in three time steps; approximately 50 more time steps, representing

about ten times the time required for the tracer to be convected through the channel, were run, until the concentrations at the downstream boundary were no longer changing from one time step to the next.

The analytical solution (Eq. 2.61) and the numerical simulation results are compared on Fig. 2.7. Both the longitudinal centerline distribution and the transverse distribution at $x = 25$ feet indicate two significant things: first, the number of stream tubes did not significantly affect the simulation predictions, nor did the relatively wider stream tubes near the banks weaken the predictions there. Second, the predicted concentrations at the centerline are consistently too high by about 12 percent, as if the simulation used a diffusivity which was too low and/or had an injection concentration which was too high. The error can be explained only by recalling that, as discussed in Sect. 2.6.2, the transverse diffusion discretization introduces an error which is the order of Δt and Δz^2, and is a consequence of the numerical differencing technique. The error should be put into proper perspective by noting that the model predicts the concentration distributions within roughly 10 percent as the peak concentration decays from as high as 40 ppb down to 0.1 ppb, or two orders of magnitude.

2.8.2 Instantaneous injection in uniform shear flow. The analytic solution most nearly approximating a field situation for unsteady injection is the jointly Gaussian distribution presented by Monin and Yaglom (1971) for instantaneous vertical line source injection in an unbounded fluid of constant depth and having a constant transverse gradient of longitudinal velocity, Eq. 1.27. The situation is difficult to model numerically, for two reasons; first, the simulation can model only a finite, bounded fluid; second it can only accept injections of finite amplitude and duration. The first difficulty may partially be overcome by restricting comparisons to short dispersion times, before significant amounts of tracer reach the model limits, and by using extremely broad stream tubes adjacent to the banks. The second difficulty can be minimized by using a source of high concentration at one computational point for one time step.

The hydraulic conditions for the comparison were as follows:

$$H = 1.0 \text{ ft,}$$
$$U = 1.0 \text{ ft/sec,}$$
$$\Gamma_z = 2.857/\text{sec,}$$
$$\epsilon_x = 0.038 \text{ ft}^2/\text{sec,}$$
$$\epsilon_z = 0.13051 \text{ ft}^2\text{sec.}$$

The computational grid is sketched on Fig. 2.8, and the stream tube dimensions and velocities are summarized in Table 2.2. The centerline tube is made narrow to allow for an approximate "point" source, and the bank tubes are of exaggerated width to approximate an unbounded fluid. The injection consisted of 1000 ppb concentration at $x = .05$ feet, tube 6, during the first time step, for an injection strength of 0.10 ppb-ft^3. Figure 2.19 compares the numerical predictions 0.07 seconds after the injection with the jointly Gaussian solution, Eq. 1.27. The three time steps used represent centerline Courant numbers $u\Delta t/\Delta x$ of 0.5, 1.0, and 1.75; over this range the numerical solution is relatively insensitive to the time step. The numerical solution is in excellent agreement with the jointly Gaussian distribution at

x = .08 feet from the injection, though the model consistently underestimates the centerline concentrations plotted longitudinally. The underestimation is due in large part to the noninfinite instantaneous point source concentration used in the model; secondary sources of error are the limit to upstream diffusion at x = -.05 feet, and the second order approximation of the finite-difference solution. But again, the predictions should be viewed in perspective; the model predicts peak concentrations within 20 percent over three orders of magnitude reduction in concentration.

EXPERIMENTAL INVESTIGATION OF THE VARIATION
OF TRANSVERSE DIFFUSIVITY IN A NONRECTANGULAR CHANNEL

Chapter III
THEORETICAL AND EXPERIMENTAL BASIS FOR EVALUATION OF
THE TRANSVERSE DIFFUSIVITY

The analytical and numerical techniques for solution of the dispersion equation, described in Chapters 1 and 2, all are based on an assumption that turbulent mixing can be described as a gradient process through direct analogy with molecular diffusion. Moreover, the turbulent diffusion coefficients must be known before any of the solutions may be applied to a laboratory or field mixing situation. While there is a theoretical basis for estimation of the vertical turbulent diffusivity $\bar{\varepsilon}_y$, estimation of the comparable transverse and longitudinal diffusivities, and especially the depth-averaged diffusivities ε_x and ε_z, must be based primarily on experimental studies.

It is the purpose of this chapter to review the theoretical and experimental basis of the transverse diffusivity. Specific attention is devoted to the possibility that the diffusivity may not be constant within a cross section; Chapter 4 describes some limited experimental results which bear on this question.

The longitudinal diffusivity is largely ignored in this and following discussions, as it has been shown to have little effect on steady-state mixing from a continuous source, though it may be important in unsteady mixing (Holley, 1971). Transverse diffusion, rather than longitudinal, is the critical process influencing dispersion in rivers.

3.1 Theoretical Basis of Turbulent Diffusivity

The turbulent diffusivities appearing in Eq. 1.23 absorb mixing due to molecular diffusion, turbulent velocity fluctuations, and depth-averaged differential convection. Recalling the assumptions leading to Eqs. 1.6 and 1.23, the depth-averaged transverse diffusivity ε_z may be written

$$\varepsilon_z = \frac{\varepsilon_m \frac{\partial \overline{C}}{\partial z} - \overline{w}^y \overline{C}^y - \overline{w'c'}}{\partial \overline{C}/\partial z} \tag{3.1}$$

where the straight overbar denotes a local time average and all terms are depth-averaged. The three terms appearing in the right hand side numerator of Eq. 3.1 represent, respectively, the molecular, convective, and turbulent contributions to depth-averaged transverse mixing. Absorption of all three mechanisms into a single apparent diffusivity has little theoretical basis, but is commonly justified by the computational convenience of the resulting gradient-law description of the depth-averaged mixing process.

For flows in a prismatic channel, secondary circulation is generated only by differential resistance related to the channel shape, and may be considered negligible insofar as transverse mixing is concerned (Holley, 1971). Thus $\overline{w}^y = 0$, and the differential convection term $\overline{w}^y \overline{C}^y$ in Eq. 3.1 disappears. Furthermore, the molecular diffusivity ε_m is several orders of magnitude less than turbulent

diffusivity, (Sayre and Chang, 1968), so that Eq. 3.1 may be written for prismatic channels as

$$\varepsilon_z = - \frac{\overline{w'C'}}{\partial \overline{C}/\partial z} . \tag{3.2}$$

Equation 3.2 has an indirect theoretical basis through the Reynolds analogy between vertical transport of mass and momentum in a turbulent boundary layer. Since the vertical transport of momentum per unit mass, $-\overline{u'v'}$, can be described as a gradient mixing process such that

$$-\overline{u'v'} = \varepsilon_t \frac{\partial \overline{u}}{\partial y} , \tag{3.3}$$

where ε_t is the eddy viscosity, Reynolds hypothesized that

$$-\overline{v'C'} = \bar{\varepsilon}_y \frac{\partial \overline{C}}{\partial y} ; \tag{3.4}$$

the analogy has been well established for vertical mixing in wide open channels.

The Reynolds analogy is especially attractive because it allows the direct estimation of the vertical diffusivity $\bar{\varepsilon}_y$. Noting that $\rho \overline{u'v'}$ is the turbulent shear stress, which varies linearly with distance above the bed, and assuming that $\varepsilon_t = \bar{\varepsilon}_y$, Elder (1959) obtained

$$\bar{\varepsilon}_y = \frac{(1 - \frac{y}{H}) U_*^2}{\partial \overline{u}/\partial y} \tag{3.5}$$

where

U_* = shear velocity, $(\tau_o/\rho)^{1/2}$,

τ_o = bed shear stress, $\rho g R_h S$,

ρ = fluid density, and

R_h = hydraulic radius, cross-sectional area divided by wetted perimeter.

Assuming a logarithmic velocity distribution, Elder integrated Eq. 3.5 over the depth of flow to obtain

$$\varepsilon_y = \frac{\kappa}{6} U_* H \tag{3.6}$$

where κ is von Karman's constant, approximately equal to 0.4.

The development leading up to Eq. 3.6 is made possible by the requirement that the shear stress must vary linearly from a maximum at the bed to zero at the water surface. No analogous constraint can be placed on the transverse shear, i.e., $\rho \overline{u'w'}$, to achieve a comparable result for transverse eddy viscosity and/or diffusivity.

Recognizing that a transverse equivalent to Eq. 3.6 could not be developed from theoretical considerations, Elder simply postulated that the transverse diffusivity can be written similarly as

$$\epsilon_z = KU_*H \qquad (3.7)$$

where K is a constant requiring experimental determination. The analogy may be justified qualitatively on the basis of the strong correlation between vertical and transverse turbulent velocity fluctuations. It is important to note that Eq. 3.7, which is widely assumed to represent correctly the transverse diffusivity, suggests that transverse diffusion is attributable entirely to bed-generated turbulence. Experimental results described in Chapter 4 suggest that this may be an incomplete description of transverse mixing.

3.2 Experimental Determination of Transverse Diffusivity

With few exceptions experimental determinations of ϵ_z have been conducted in rectangular channels, often with large width-to-depth ratios, and have utilized continuous tracer injection into a steady, longitudinally-uniform flow of constant velocity U. For these conditions the Gaussian concentration distribution, Eq. 1.29, is expected, (for ϵ_x vanishingly small), the variance of which is given by

$$\sigma_z^2 = 2\epsilon_z t$$

or, noting that ϵ_z is a constant and the diffusion time $t = x/U$,

$$\epsilon_z = \frac{U}{2}\frac{d\sigma_z^2}{dx} \qquad (3.8)$$

Thus to determine ϵ_z one need only compute the transverse variance of steady-state distributions at successive downstream locations, (before significant amounts of tracer reach the banks), and find the slope of a straight line fit to the plot of σ_z^2 versus x. Equation 3.8 may also be obtained by taking the second z-moment of the appropriate simplified version of Eq. 1.23. The method has been applied to mixing in nonrectangular channels and nonuniform flows such as the Columbia River (Glover, 1964) and the Missouri River (Yotsukura et al., 1967), using for U the discharge velocity Q/A. The resulting values of K have been summarized by Okoye (1970) and Prych (1970); K ranges from as low as about 0.1 in a straight laboratory channel, to about 0.7 in large natural rivers, with Elder's value of 0.23 widely adopted for use in rectangular flumes and small canals. Fischer (1970) reported values of K as high as 2.5 in a curved laboratory flume, where the mixing due to $\overline{w}^y \overline{C}^y$ was significant.

Implicit in all the early analyses was the assumption that ϵ_z is constant within a cross section; this appeared reasonable, since tracer was injected at the centerline of the channels, where there was little transverse variation of depth or velocity, or at the bank of a nearly rectangular channel (Fischer, 1970). The only mixing experiments conducted in a zone of transverse variation of velocity or depth are those reported by Holley (1971), in which the effect of groin-generated turbulence on transverse mixing was investigated using bank injection; these experiments and their analysis are discussed in Sect. 3.3.

The study of transverse mixing in zones of roughly constant depth and velocity has provided useful general information on the mixing process in rivers; moreover, this type of mixing is amenable to analysis using Eq. 3.8. Yet many pollutant spills occur at or near the bankline, where concentrations can be relatively high due to the limited depths available for dilution, and where transverse variations of depth and velocity might influence the mixing. The transverse diffusivity in such a region has even less theoretical basis than in a region of constant depth and velocity; therefore recourse must again be made to experiments for information on the magnitude and variation of the transverse diffusivity.

3.3 The Generalized Change of Moments Method

3.3.1 Mathematical basis. The magnitude and distribution of the transverse diffusivity in a non-uniform flow in a channel of arbitrary shape can be determined by using the Generalized Change of Moments (GCM) method developed by Holley (1971). The method effectively extends Eq. 3.8 to allow for transverse and longitudinal variation of depth, velocity, and transverse diffusivity, and allows for depth-averaged transverse velocities. Equation 1.23, written for steady-state mixing in a flow with negligible longitudinal diffusivity, becomes

$$\frac{\partial}{\partial x}(huC) + \frac{\partial}{\partial z}(hwC) = \frac{\partial}{\partial z}\left(h\epsilon_z\frac{\partial C}{\partial z}\right). \qquad (3.9)$$

After assuming that ϵ_z could be written

$$\epsilon_z = K\phi(x,z), \qquad (3.10)$$

where $\phi(x,z) =$ some function of x and z, Holley took the second moment of Eq. 3.9 with respect to z_0, a reference transverse coordinate, and integrated the result longitudinally to obtain

$$\frac{d(\sigma_{huC}^2 - G)}{dF} = 2K \qquad (3.11)$$

where

$$\sigma_{huC}^2 = \frac{\displaystyle\int_{z_L}^{z_R} huC\, z_1^2\, dz}{\displaystyle\int_{z_L}^{z_R} huC\, dz}, \qquad (3.12)$$

$$F = -\int_0^x \left[\frac{\displaystyle\int_{z_L}^{z_R} h\phi\frac{\partial C}{\partial z}z_1\, dz}{\displaystyle\int_{z_L}^{z_R} huC\, dz}\right] dx',$$

$$G = \frac{2 \int_{z_L}^{z_R} hwC\, z_1\, dz}{\int_{z_L}^{z_R} huC\, dz}.$$

$$z_1 = z - z_o, \text{ and}$$

z_L, z_R = left and right channel boundary z-coordinates.

The quantity σ^2_{huC} is the transverse variance of the tracer mass flux; the parameter F may be thought of as a modified length variable, (dimensions of length squared) which is always positive, since $\partial C / \partial z$ and z_1 generally have opposite signs when z_o is taken as the transverse location of the peak concentration. G represents mixing due to net transverse velocities. Equation 3.11 is valid throughout the mixing zone, whether or not the tracer has reached the banks. For idealized conditions of $u = U = $ constant, $w = 0$, and an infinitely wide channel, Eq. 3.11 reduces to Eq. 3.8.

The GCM method is quite a powerful tool for the estimation of transverse diffusivities using observed concentration distributions from continuous injection in a natural channel. The proper choice of the diffusivity function $\phi(z)$ should result in a linear plot of $(\sigma^2_{huC} - G)$ versus F, the slope of which is $2K$. The generality of the GCM method is obtained at the expense of increased data requirements and computations, including the need to estimate $\partial C / \partial z$ from scattered data points, and to estimate w by integrating the two-dimensional continuity equation as described by Holley (1971). For most applications the computation may be considerably simplified by assuming w to be negligible; the validity of the assumption may be checked by using the GCM-determined diffusivity in a numerical simulation of the experiment.

3.3.2 Application to Delft experiments. The GCM method was used to analyze groin-influenced mixing in laboratory and natural channels by Holley (1971) who proposed the following four possible diffusivity functions:

$$\epsilon_z = K_1' U_* H = K_1 H^{3/2} \qquad (3.12a)$$

$$\epsilon_z = K_2' \frac{U_*}{U_a} uh = K_2 uh \qquad (3.12b)$$

$$\epsilon_z = K_3' u_* h = K_3 h^{3/2} \qquad (3.12c)$$

$$\epsilon_z = K_4' u_a h = K_4 h \qquad (3.12d)$$

where K_1', K_2', K_3', and K_4' are dimensionless constants, and K_1, K_2, K_3, and K_4 are dimensioned constants for a particular cross section,

$$K_1 = K_1' (gS)^{1/2} \qquad (3.13a)$$

$$K_2 = K_2' (gHS)^{1/2}/U_a \qquad (3.13b)$$

$$K_3 = K_3' (gS)^{1/2} \qquad (3.13c)$$

$$K_4 = K_4' U_a \qquad (3.13d)$$

Equation 3.12a is the traditional constant-diffusivity assumption, equivalent to Eq. 3.7. The remaining functions have no theoretical basis, according to Holley, but simply introduce transverse variation of ϵ_z through local analogy with cross-sectional average parameters. Holley demonstrated that, particularly for side injection into a trapezoidal channel, peak concentrations near the source are particularly sensitive to the choice of the diffusivity function.

The difficulty of obtaining true time-average concentrations in an experimental dispersion study within reasonable constraints of time and effort precluded the drawing of firm conclusions from Holley's experiments, which were conducted at Delft Hydraulics Laboratory, the Netherlands. Indications were, however, that the functions which allowed transverse variation of diffusivity, i.e., Eqs. 3.12b - 3.12d, were more appropriate than the constant diffusivity, Eq. 3.12a, in the laboratory channels with and without groins. In these channels the cross sections were approximately rectangular, the presence of groins accounting for most of the transverse velocity gradient.

3.3.3 Computational application. The GCM method is applied to the experiments reported in Chapter 4. As suggested by Holley (1971), the reference coordinate z_o is taken as the centroid of the tracer flux distribution for injections at the centerline of a channel, or as the coordinate of the bank for bank injections. For injections at other locations, Holley gives no guidance as to the best choice of z_o; but the GCM derivation requires that z_o not be a function of x, even though the centroid of a concentration distributin shifts toward the center of the channel as the tracer becomes completely mixed. Therefore the centroid of the distribution at the injection point is used in this case.

The various terms in Eq. 3.11 are evaluated numerically using normalized concentration distributions (described in Chapter 4) and the stream-tube discretization of the test channel, as described in Appendix E. Velocities, depths, and incremental widths are assigned to each measured concentration at a cross section by linear interpolation between depths and velocities previously assigned to stream tube centroids; velocities are assumed to be zero at the banks. The integrations of Eq. 3.11 are then approximated by simple summations.

The scatter in measured concentration distributions requires that special consideration be given to the evaluation of the concentration gradient, $\partial C / \partial z$, appearing in F. If the functional form of the distribution is known a priori, it is possible to fit the function to the data using a least squares technique; for example, considering centerline injection in a wide, rectangular channel, a Gaussian distribution can be fit to the data, and the gradient computed analytically. But in general the functional form is not known, especially in a natural channel. If the data define a smooth curve, a polynomial of appropriate order can be fit to sets of data points, and the gradient again computed analytically. The technique breaks down, unfortunately, when a particular data

point does not follow the general trend of the distribution.

These difficulties were obviated by using a linearization technique to compute the concentration gradients from data described in Chapter 4. The technique averages the slopes of least squares lines fit to successive groups of data. Figure 3.1a illustrates the method applied to five data points, fit three at a time. Define the line by

$$C = a_1 z + a_2$$

where a_1 and a_2 are the slope and intercept of the line, computed by standard formulas (see Carnahan et al., 1970). The slope a_1 is computed for points 1, 2, and 3, then for 2, 3, and 4, and finally for 3, 4, and 5, as shown on the figure. The appropriate slope at each data point is taken as the average of the slopes of the lines computed using that point. Thus

$$(\frac{\partial C}{\partial z})_1 = a_1(1,2,3)$$

$$(\frac{\partial C}{\partial z})_2 = \frac{a_1(1,2,3) + a_1(2,3,4)}{2}$$

$$(\frac{\partial C}{\partial z})_3 = \frac{a_1(1,2,3) + a_1(2,3,4) + a_1(3,4,5)}{3}$$

etc.

The gradient thus assigned to each data point describes the general trend of the distribution without giving undue weight to an isolated bad point. The procedure is illustrated for three-point computations, yet an arbitrary number of points may be used. The tradeoff is between the need to use enough points to smooth the curve, without losing local gradient trends by using too many points. In practice, three-point fits were found to reproduce the general data trend most faithfully. Figure 3.1b shows the gradients thus computed for a typical set of concentration data from the Missouri River (Yotsukura et al., 1967); noting that the method is used only to estimate the gradients of the distribution at measured data points, the results are satisfactory.

Limited dispersion experiments were conducted in a laboratory flume of triangular cross section at Colorado State University from August through December, 1974. The purpose of these experiments was partially to verify the numerical model of Chapter 2 in a nonrectangular channel, but primarily to test the hypotheses of Holley (1971), Eq. 3.12, in a channel having transverse variations of depth and longitudinal velocity.

4.1 Goal and Strategy of Experiments

The choice of a channel shape for the experiments was governed by the need to maximize the effects of depth and velocity variations on the mixing process, while not violating the assumptions made in deriving Eq. 1.23, the depth-averaged mass conservation equation. Specifically, this required that transverse variations of depth not be so severe as to induce strong secondary flow cells which might dominate the transverse mixing. Moreover, it was considered important approximately to reproduce prototype values of the Froude number and width-to-depth ratio. The triangular cross section shown in Fig. 4.1a was adopted as a reasonable compromise among several alternatives which included trapezoidal sections and a composite section of discrete rectangular elements; the Froude number was about 0.3 (based on average velocity) and the width-to-depth ratio was about 10, a minimum value for small streams and artificial canals. The Reynolds number, based on depth-averaged velocity and flow depth, ranged from about 5,000 near the flume wall to about 90,000 at the centerline; by comparison, Elder's (1959) experiments used a Reynolds number range of 2,300 to 4,500.

Once the cross-sectional shape had been selected, it was necessary to determine what types of water flow and tracer injection would most effectively amplify the effects of transverse variations of diffusivity. Steady water flow is required by the numerical model, and no particular advantage in using nonuniform flow was apparent. Therefore steady, longitudinally-uniform flow was adopted for all dispersion tests.

An important question to be answered before the experimental program could be designed was whether continuous or instantaneous tracer injection would respond most clearly to the transverse variation of transverse diffusivity. The question had been studied using a mathematical model of the symmetrical composite channel sketched in Fig. 4.2; longitudinal velocities were computed by the backwater routine described in Appendix E. Tracer was injected at the upstream boundary centerline of the model by means of either continuous injection or as a short-period sine wave. Comparisons between the two injection methods were made by considering the effect of two diffusivity assumptions on the peak centerline concentrations resulting from each injection. Let $\psi(x)$ denote the ratio of centerline concentration computed using $\epsilon_z = .23U_*H$ to the centerline concentration computed using $\epsilon_z = .23U_*/U_a$ uh; for the unsteady injection ψ is evaluated using the peak concentration occurring at x during the passage of the tracer cloud. Figure 4.3a demonstrates that for both types of injection, ψ differs from unity at most downstream locations; this simply verifies that the centerline concentrations are indeed sensitive to the transverse

variation of diffusivity. But ψ differs more greatly from unity for the unsteady injection, and this is significant, as it suggests that unsteady injection may be a better experimental technique for the detection of the proper distribution of transverse diffusivity when a transverse velocity gradient exists. However Fig. 4.3b indicates that, when the longitudinal velocity is forced to be a constant in the entire flow field, the variation of ψ with x is relatively insensitive to the mode of tracer injection.

In spite of the apparent advantages of instantaneous injection for detection of the proper transverse diffusivity function, there are three practical reasons why continuous injection is more attractive.

(a) The diffusion of a single cloud of tracer represents a particular realization of the turbulent flow field; another cloud may diffuse quite differently. Therefore the results of many instantaneous releases would have to be averaged to obtain a concentration distribution which is representative of the time-averaged properties of the turbulent flow field. But for continuous injection, (an infinite superposition of instantaneous puffs) time averaged concentrations at fixed points are sufficient to describe the average turbulent mixing process.

(b) Measurement of the diffusion of instantaneous injection clouds requires that multiple fixed probes or samples record the time history of concentration as the cloud passes. Continuous injection mixing requires only that finite-volume samples be collected for later analysis using a single probe or instrument.

(c) The powerful Generalized Change of Moments method is applicable only to steady-state mixing resulting from continuous injection.

For the above reasons, continuous tracer injection was adopted as the more practical technique for use in these limited tests. But the potential advantages of instantaneous injection must not be overlooked in future studies, especially if available resources permit the use of more extensive instrumentation.

4.2 Experimental Equipment and Data Collection System

4.2.1 Flume and water circulation system. The experiments were performed in the 60-foot long, four-foot wide tilting flume belonging to the Agricultural Research Service, United States Department of Agriculture, and operated at Colorado State University's Engineering Research Center. The facility recirculates water through a 1000-cubic-foot sump, a 12-inch return line, and a 0.45-foot orifice plate which is calibrated to measure discharge from 0.25 to 2.5 cubic feet per second.

The flume bottom, and consequently the invert of the triangular section built upon it, deviated considerably from a plane surface. Using a surveying level, the bottom contour was established as shown on Fig. 4.4; piezometer tubes mounted at either end of the flume and connected by a one-inch pipe indicated the net slope of the bottom, i.e., the slope of the dashed line on the figure.

The exact dimensions of the triangular section, shown on Fig. 4.1, were fixed by the standard dimensions of lumber used to frame the false bottom as sketched on Fig. 4.5a. Artificial roughness was added using expanded metal lath placed over the entire bottom and dimensioned as shown on Fig. 4.5b. The metal lath was chosen over discrete blocks or strips because it generates turbulence uniformly, avoiding any local zones of accelerated mixing. Vent holes were provided through end and intermediate wedge supports to allow the underside of the false bottom to fill completely and thus avoid the possibility of the entire structure popping up should any unwanted leakage occur.

4.2.2 *Velocity measuring system.* Time-averaged point velocities were measured with a 1/8-inch diameter Dwyer Pitot Tube; differential pressures were measured using a Validyne transducer with a 0.1 psi diaphragm installed, connected to a Pace Model CD 10 Carrier Demodulator. Differential pressure measurements of from one to two minutes were recorded on a Mosley Strip Chart Recorder, connected in parallel with a large capacitor to damp the turbulent fluctuations. The voltage trace on the strip chart was averaged by eye, and then the linear calibration between output voltage and velocity was applied to obtain a time-averaged, point velocity. The transducer calibration was obtained using a two-chamber head tank with micrometer point gauges, and a pitot-tube coefficient of unity was used as suggested by the manufacturer. The transducer calibration was found to be quite stable, as long as no air was allowed to accumulate in the pressure lines.

4.2.3 *Dye injection system.* The choice of a tracer injection system was governed by the need to inject over the full depth at a constant rate and with minimum disruption of the flow field. These objectives were met by injecting through a vertical 5/32-inch O.D. brass tube, plugged at the lower end, with 1/16-inch holes drilled at 1/4-inch centers over the full injection depth. Tracer was supplied by a five-gallon constant-head Muerriat vessel; the tracer flowrate was controlled by a Poly-Flo needle valve downstream from a Fischer and Porter Company Precision Bore Flowrator, which accurately measures flows from 1 to 200 ml/min (milliliters per minute).

Rhodamine WT was chosen as the tracer material, of its availability and favorable characteristics as described by Wilson (1968). Test injection solutions were made up by diluting from four to six milliliters of 12 percent (by weight) WT solution in five gallons of flume water. Tracer solution was injected at 140 ml/min, allowing as much as 135 minutes for a test run.

4.2.4 *Tracer sampling system.* A siphon system was used to withdraw discrete water samples from the flume. The samplers were 18-inch-long, 1/16-inch I.D. brass tubes bent 90 degrees at the bottom so that the tube openings faced into the flow direction. Once the siphons were primed, 1/8-inch I.D. Tygon tubes carried the samples over the flume walls and down to pint sample bottles.

It was important to ensure that the sampling tube withdrawal velocity was about the same as the flume flow velocity at the sampling point, so that the sampling process would not affect the flow immediately upstream. The required siphon heights can be determined by an application of the Bernoulli equation and a quick experiment. Let Δh denote the vertical distance from the water surface down to the open end of the siphon tube. Application of the Bernoulli

equation between the two ends of the siphon tube, assuming a constant diameter, constant friction factor, and laminar flow, yields

$$\Delta h = cu_e \qquad (4.5)$$

where u_e is the siphon tube entrance velocity and c is a constant related to the tube dimensions and friction factor. The constant could be computed, but a more reliable value was obtained experimentally using the actual siphon system. Tests in still water showed that Eq. 4.5 is indeed linear, and that for this particular system $c = 1.435$ sec. The value was checked in an actual sampling configuration and found to be satisfactory.

For any sampling location the local velocity u was known. Setting $u = u_e$, Δh was computed, and the siphon tube opening was clamped at that distance below the water surface. Four samples were collected at a time, over a period of from one to three minutes; individual sample volumes ranged from a quarter to a half pint.

4.2.5 *Concentration measuring system.* Samples collected from the flume were analyzed using a Turner Model 111 Fluorometer. The instrument was recalibrated using standard solutions before each test; sample temperatures were recorded frequently, and all fluorometric dial readings were adjusted to the calibration temperature, following the procedure suggested by Wilson (1968). The fluorometer calibrations were found to be quite stable, and linear. Samples taken near the tracer injection often read off-scale, and had to be diluted using flume water before the concentration could be determined.

4.3 Test Procedure

Before any dispersion tests were conducted, the hydraulic characteristics of the flume flow were measured in detail. This process included a trial-and-error establishment of approximately uniform flow, and the detailed measurement of velocities and water surface elevations throughout the flume.

Each dispersion test began with the mixing of an injection solution in the Muerriat vessel, the concentration of which was made strong enough to ensure good resolution of concentrations at the downstream end of the flume. Once the flume flow had reached steady state at the desired discharge, the injection was turned on and allowed to stabilize. Sampling was begun at the downstream end of the flume, and moved progressively upstream through a total of seven cross sections. Sufficient time was allowed to ensure that the siphon lines were fully purged between samples. The entire process occupied about two hours for one test.

The limited sump capacity of the Agricultural Research Service flume made it especially important to monitor the buildup of background concentration as the test progressed. A grab sample was taken in the headbox upstream of the injection point as each set of four samples was being siphoned downstream. Then the fluorometer dial reading of the background sample was subtracted from the reading for each test sample before concentrations were computed, effectively giving the concentration with respect to the background level. While this procedure correctly adjusted the observed concentrations, it did not account for the steady decrease of effective tracer injection strength

as the test progressed. That the decrease in strength was occurring can be seen by imagining an unlimited supply of tracer solution of fixed concentration C_o, injected continuously into a recirculating flume water supply until the flume concentration, C_f, approached C_o; the injection strength, given by $q_o(C_o - C_f)$, would approach zero.

The decrease in effective injection strength was not of sufficient magnitude to cause any concern in the tests reported herein. For all tests C_o was about 10^4 ppb, while the background concentration C_f rose from 0 ppb to about 30 ppb during a typical test. The maximum change in source strength was thus less than one-half of one percent during a test.

4.4 Analysis of Test Data

4.4.1 Hydraulic conditions. Two flume roughness configurations were used, and approximate uniform flow was established for each. For dispersion tests A, B, and C, the expanded metal lath covered the entire flume bottom; the center half of the metal lath was removed for tests D, E, and F. Table 4.1 lists the overall hydraulic characteristics of each flow. The energy slope S was estimated by adding observed water surface elevations to the known flume invert elevations with respect to a horizontal datum, thus taking into account the waviness of the invert; the velocity head was approximately constant at all longitudinal locations, as the flow was essentially uniform. Note that the discharge cross-sectional area, and average velocity for each flow were approximately equal, though the slopes were different to compensate for the different roughnesses.

It was recognized during the planning of the experimental program that to have a high relative roughness in the shallow areas near the flume walls could induce sufficient secondary flow to dominate the turbulent mixing process. For this reason a low-roughness, flat-slope flow was considered best, even though it might mean that the energy slope could be difficult to measure. The flow cross-sectional area, the mean velocity, and thus the discharge were chosen to produce the desired water surface elevation and Froude number; then the bed slope and the flume tail-gate were adjusted until the centerline depth was approximately constant throughout the flume. The expanded-metal-lath roughness, while achieving the goal of a uniform roughness without inducing significant secondary flow, was still relatively smooth, as reflected in the energy slope and Manning roughness coefficient in Table 4.1. The drop in water surface elevation from one end of the flume to the other was less than the deviations of the wavy bottom from a plane surface, and the water surface, or energy, slope could not be measured with any precision over such a short distance. Moreover, the full-roughness flow was so smooth that removal of the center half of the metal-lath mesh had only a small effect on the depth-averaged velocity distributions, to be discussed shortly. The secondary flow strength was qualitatively estimated by observing the transverse movement of surface floats and/or instantaneous point source dye clouds as they moved downstream from various transverse injection points. No net transverse movement could be observed over a 40-foot length, suggesting that the turbulent mixing process would not be too strongly influenced by secondary flow.

In summary, the need to minimize secondary flow effects demanded that the energy slope be so flat that it could only roughly be estimated. The slopes in Table 4.1 were obtained using a least-squares fit to the water surface elevations above a horizontal datum; but note that the total drop in water surface elevation was less than 0.3 feet over a length of 50 feet.

Complete time-averaged velocity measurements were made at five longitudinal locations for tests A, B, and C, and at three locations for D, E, and F. From these measurements it was evident that the flow became fully developed in the first twenty feet downstream from the headbox. Figure 4.6 shows the time-averaged velocity contours at $x = 40$ feet for the full roughness flow, and at $x = 30.6$ feet for the half-roughness. From the contours it is evident that the flow was essentially symmetrical about the centerline, and that the centerline velocities were actually lower for the half-roughness flow. The smoother center section of the half-roughness flows causes a thinner turbulent boundary layer, allowing the depth-averaged velocity to be closer to the bed, thus reducing the velocities at the surface. Figure 4.7, a plot of depth-averaged velocities for both flows, shows also that the depth-averaged centerline velocity is depressed relative to the full roughness flow, although continuity is preserved by higher velocities in the region half-way to the flume wall. This behavior cannot directly be explained without more extensive velocity measurements; it most likely represents the effect of weak secondary velocity cells on either side of the centerline, generated by the roughness discontinuities at $z = 0.92$ feet and $z = 3.08$ feet.

4.4.2 Dispersion test data. Since the mathematical model and the GCM analysis both deal with depth-averaged concentrations, it was necessary to obtain depth-averaged values in the laboratory experiments. The experimental effort could be greatly simplified by taking concentration samples only at mid-depth, as a satisfactory approximation to an actual depth-averaging process. Two tests were conducted to test the efficacy of this approximation, using test B and F conditions. Figure 4.8 shows the observed vertical concentration distributions at two transverse positions at each of two longitudinal positions, for injection at the centerline and at $z = 3.0$ feet. From these data it is apparent that mid-depth sampling should provide a reasonable estimate of the depth-averaged concentration.

Three continuous-injection dispersion tests were performed in each of the two roughness configurations, half and full. The primary variable among these tests was the injection location, which is listed with the source solution strengths in Table 4.2. For each test the injection was at $x = 18$ feet; mid-depth samples were taken at seven cross sections from $x = 20$ feet to $x = 50$ feet. Transverse sample locations were chosen so as to describe the transverse concentration distribution in sufficient detail; for tests C and F, which used centerline injection, most samples were taken on only one side of the centerline, with a few on the other side to check the symmetry of the distribution. The measured distributions from all tests are presented after the following discussion of concentration normalization and adjustment.

At steady state, the measured tracer flowrate should be the same as the injection tracer flowrate for a conservative tracer. Nonetheless, factors

such as experimental error in measuring concentrations, loss of dye through seepage in a river or leakage in a flume, and chemical decay of the tracer can cause the observed tracer flowrate to deviate above or below the injection strength. Figure 4.9 is a plot of the recovery ratio, RR, versus x for all six tests, where RR is defined as

$$RR = \frac{\int_0^4 huCdz}{C_o q_o} \qquad (4.5)$$

The recovery ratio for tests B and E is greater than unity at $x = 20$ feet, just downstream of the source, and remains above unity for most of the mixing region. This strongly suggests that the measured injection vessel concentrations were inaccurate, which is quite possible due to the need for a large dilution of the injection solution sample before it could be analyzed on the Fluorometer. Since the injection concentrations were subject to error, it is more instructive to consider the trend of values on Fig. 4.9 than the numerical value of the recovery ratio. Ideally, for a particular test RR would not deviate from its value at $x = 20$ feet. That it deviates a fair amount for most tests suggests that samples of larger volume and longer duration should have been taken to obtain more representative time averages at a point. Other sources of error undoubtedly include the mid-depth sampling, Fluorometer errors, and some loss of dye due to leakage.

Whatever the cause of recovery ratio deviations from unity, it is necessary to adjust measured concentrations so that continuity of tracer is preserved. This was done at each cross section by dividing each concentration by the recovery ratio, thus uniformly increasing or decreasing the concentration magnitudes. The adjustment may be combined with a normalization technique whereby the concentration magnitudes reflect the relative strength of the injection source. Specifically, each adjusted concentration C_a is divided by the concentration which would result if the injected solution were fully mixed over the cross section, $C_o q_o/Q$, to yield a normalized concentration C_n. Thus, writing both the adjustment and the normalization together,

$$C_n = \frac{C_a Q}{q_o C_o} = \frac{C Q}{q_o C_o RR} = \frac{C Q}{\int_0^4 huCdz} . \qquad (4.6)$$

Thus recovery-ratio adjustment and source-strength normalization may be accomplished in a single step.

The normalized concentrations for all six tests are shown on Figs. 4.10 to 4.15. Note that for the centerline injection, tests C and F, some of the data points for $z < 2.0$ feet are not actual measurements, but are mirror images of measured concentrations on the opposite side of the centerline.

4.4.3 Analysis of dispersion test results. The measured concentration distributions were used to detect the proper assumption for transverse diffusivity through a two-stage process. First, the normalized distributions for each test were analyzed using the Generalized Change of Moments method for each of the first three suggested diffusivity assumptions, Eq. 3.12a-c. Although the fourth assumption,

Eq. 3.12d, appeared to be most appropriate for groin-influenced mixing in Holley's (1971) experiments, it was not suggested by Holley as a potential general diffusivity function, but rather as a specialized function for mixing in groined channels. Therefore the applicability of Eq. 3.12d was not investigated in this study.

Application of the GCM method to the test data is summarized in Figs. 4.16 through 4.21, which show the resulting plots of σ_{huC}^2 versus F. It is immediately evident from these plots that the scatter of data points is sufficiently great to preclude using the apparent linearity of a σ_{huC}^2 versus F plot to detect the proper diffusivity assumption. But the slope $d\sigma_{huC}^2/dF$ of each line may be determined using a least squares fit, and the proper coefficient K thus established for each possible assumption as if it were the proper one, using Eq. 3.11. The variances at $x = 50$ feet for tests A, E, and F departed significantly from the general data trends, and thus were not used in the least squares computations. Since concentration sampling began at $x = 50$ feet for all tests, the anomalous variances are probably a consequence of allowing insufficient time for the steady state distribution to develop before sampling was begun.

The resulting least-squares K values are listed in Table 4.3, along with the mean coefficient values for each flume roughness configuration, half and full. If one of the three diffusivity functions analyzed is the correct description of the mixing process, then the coefficient K for that function should be a constant property of the flow conditions. Thus the averaging of K values for each flow condition, i.e., half and full roughness, should provide an estimate of the proper K for each function in that flow, regardless of the injection location. Note, however, that the K values for test A were quite high compared to tests B and C. This fact, coupled with the obviously severe GCM data scatter for test A as seen on Fig. 4.16, lends suspicion to the validity of the test A GCM results. Therefore the full roughness K values were obtained by averaging only test B and C results.

In the second stage of the analysis, the complete diffusivity functions for each assumption were used in a numerical simulation of the experiments, thus providing a direct means of detecting the proper assumption through comparison of observed and simulated distributions. The hydraulic characteristics of the model were established using the velocity distributions shown on Fig. 4.7; Table 4.4 lists the parameters of the 21-tube models developed for the full and half roughness flows; the stream tube arrangements are sketched in Fig. 4.16. Input concentration distributions were taken as the observed normalized distributions at $x = 20$ feet, reproduced within the constraint of fixed stream tube transverse positions. The models were run for at least five times the slowest transit time through the mixing region, to ensure that steady-state predictions were obtained.

The numerical model predictions, using the mean diffusivity values for each roughness as in Table 4.3, are plotted with the normalized test data on Figs. 4.10 through 4.15. The "predictions" at $x = 20$ feet for each test are actually the stream-tube equivalents of the observed distributions; the

apparent low simulation values are a result of the need to spread the contribution of high point values of concentration over stream tubes of finite width. As expected, the predicted concentrations distributions resulting from injection at the centerline and at $z = 3.0$ feet (tests B, C, E, and F) are fairly insensitive to the assumed diffusivity function; but the side-injection simulations, tests A and D, clearly show that a constant diffusivity, Eq. 3.12a, best reproduces the peak concentrations at the bank. Note also that, considering tests B and E, the constant-diffusivity simulations predict a more rapid movement of the peak concentration to the bank than the other two diffusivity assumptions, and in so doing better predict the observed data at the bank.

The concentration distributions could be better reproduced by the numerical simulations if the exact K values for each test were used in the simulation. The use of the averaged values in Table 4.3 is more consistent with the assumption that, if the proper diffusivity function is used, K should be a constant for the flow conditions.

4.5 Discussion of Test Results and Data Analysis

Much of the data scatter in the recovery ratio plots, the measured concentration distributions, and the GCM analysis is due to the limited nature of the experimental program. A more extensive program would have taken longer samples, probably of at least five minutes duration, and would have obtained depth-averaged concentrations by averaging samples taken at multiple locations along a vertical line, rather than relying on mid-depth concentrations as an approximation to depth averages. Also, a more complete program would include multiple tests of the same flow and injection conditions, to check the reproducibility of the data.

The major conclusion of the experimental program is that the assumption of a constant transverse diffusivity is more appropriate than the two other assumptions suggested by Holley (1971), at least for the particular triangular section tested. The conclusion is based essentially on the results of the side-injection tests A and E, for both of which the constant-diffusivity assumption reproduces the peak concentrations and the general shape of the distributions quite well. Since the conclusion is based on the numerical simulation rather than the GCM analysis, it is important to be sure that the results do not depend on the particular stream tube arrangement used in the model. Table 4.5 lists the specifications of an alternate 21-tube model. Stream tubes have now been concentrated on the right side of the flume, where most of the mixing takes place in a side-injection test; Fig. 4.1c is a sketch of this alternate configuration. Test D was resimulated using the alternate model and the same K values used previously for the half roughness flow. Figure 4.22 shows the results of the simulation, and clearly demonstrates that the changed stream tube discretization had no effect on the conclusion that the constant diffusivity best reproduces the test data. The consistent underestimation of peak concentrations is due to the fact that the simulation uses the average K_1 for tests D, E, and F, which is higher than the value for test D alone as shown in Table 4.3.

There is little theoretical basis for a rational explanation of the apparent constancy of the transverse diffusivity in the triangular channel. Chapter 3 points out that the functional form of

transverse diffusivity in a rectangular channel, which is supposed to describe mixing due to transverse velocity fluctuations, is assumed by analogy with vertical diffusivity, which describes mixing due to vertical velocity fluctuations. Evidently the analogy is acceptable in channels of roughly constant depth, but in a channel with transverse variations of depth and velocity, a transverse shear must contribute to transverse mixing of mass; yet the analogy with vertical diffusivity takes no account explicitly of transverse shear. In the shallow flow near the flume wall, the proximity of the free surface to the bottom limits the scale and intensity of vertical turbulent fluctuations, and, due to a strong correlation, transverse fluctuations. Yet the transverse shear, as reflected in the transverse velocity gradient, is greatest near the wall. At the centerline, on the other hand, vertical turbulent fluctuations can be of larger scale while the transverse shear is negligible. The net effect of the two contributions to transverse mixing, one bed-generated and the other transverse-shear-generated, might be a roughly constant transverse diffusivity across the entire section.

The values of K_1' for the test data, which can be obtained from the K_1 values in Table 4.3 using the depth and estimated slope, are from two to three times larger than those reported in the literature for rectangular channels. But as discussed earlier, the energy slope could not be measured with any precision for these tests, and this undoubtedly accounts for some error in the apparent K_1' values. However, it is also quite possible that the transverse shear in the triangular channel is reflected in a K_1' value which is higher than the values found in rectangular channels where bed-generated turbulence governs the mixing process. The higher K_1' values reported by Okoye (1970) were from natural, nonrectangular channels where transverse shear could well have dominated the mixing.

The above arguments are heuristic at best. But they serve to illustrate the fact that past analogies between bed-generated turbulence and transverse diffusivity are incapable of describing the effects of transverse shear. There is a great need for a detailed analysis of the interaction between vertical and transverse shear in producing apparent transverse diffusivity; experimental studies must include measurements of the transverse velocity-concentration covariances, as reported for vertical mixing by Keefer (1971).

The problem of assigning diffusivities to the overbank flow area when a river is at flood stage is not addressed by the single-channel experiments discussed here. It is possible to have distinct changes in depth, roughness, and velocity at the bankline in such a case, suggesting that the overbank flow be treated as a separate channel insofar as mixing problems are concerned. Thus a constant transverse diffusivity should be assigned to each of the quasi-separate channels, using the functional form of Eq. 3.12a, and using Okoye's (1970) review for guidance as to the proper value of K_1'.

A secondary conclusion to be drawn from the experimental program is that the numerical model described in Chapter 2 provides an effective and versatile means of estimating steady-state transverse mixing in a nonrectangular channel, once the diffusivities are known.

Chapter V

TRANSVERSE MIXING IN THE MISSOURI RIVER

It is the purpose of this chapter to illustrate the application of the numerical dispersion model to steady-state mixing in a natural river. A six-mile reach of the Missouri River was chosen for the application, since its hydraulic and mixing properties were reported in detail by Yotsukura et al. (1967).

5.1 Description of Field Experiments

The study reach, immediately downstream from Blair Highway Bridge in Iowa, was selected by Yotsukura et al. because of fairly gentle meandering over a six-mile reach, the availability of a bridge from which to inject the tracer, and minimum river traffic. Figure 5.1 shows the general alignment of the reach, in which the average width and depth were about 600 feet and nine feet, respectively, for the test discharge of 34,100 cfs. A Rhodamine BA solution was injected at a constant rate for four hours near the center of the river at the Blair Highway Bridge. Steady-state concentration distributions were measured at ten cross sections downstream from grab samples taken from a boat. These distributions, combined with detailed depth and velocity measurements taken at two cross sections in the reach, are the basis of comparisons with the numerical model.

5.2 Adaptation of Hydraulic and Geometric Data to Numerical Model

The availability of velocity and depth data at only two cross sections required that data be assumed for the rest of the reach. The measured sections were just above the injection site, at mile 648.5, and midway through the reach, at mile 645.0; these velocity distributions were distributed over the reach as suggested by Yotsukura et al. At the injection point and at station 5, the mile 648.5 distribution was assumed to apply. At mile 645 the measured distribution was used, and its mirror image was used at the midpoint between stations 8 and 9. The mirror image of mile 648.5 was used at station 10. At each of these five reference sections the cross-sectional area was assumed to be the same as the source section; depths were thus uniformly adjusted as the widths were increased or decreased to correspond to known channel widths. Table 5.1 summarizes the reference section locations and adjustment factors.

Eleven stream tubes of equal discharge were assigned to each of the two source sections by the procedure described in Sect. 2.6.2; Fig. 5.2 shows the resulting stream tube configurations and velocity distributions. Table 5.2 summarizes the stream tube dimensions and velocities at each reference section after width and depth adjustment; a constant energy slope of 0.0002 for the entire reach was suggested by Yotsukura et al. Longitudinal computational points were established at approximately 600-foot intervals; ten of the 54 total points were at the dye sampling stations shown on Fig. 5.1.

5.3 Generalized Change of Moments Analysis

Concentration distributions as reported by Yotsukura et al. were normalized as described in Sect. 4.4.2, then analyzed using the Generalized Change of Moments method (assuming $w = 0$). In view of the apparent invariance of the transverse diffusivity as discussed in Sect. 4.4.3, and the general insensitivity of centerline injection mixing to the diffusivity function, only Eq. 3.12a was tested. Figure 5.3 presents the curve of σ^2_{huC} versus F; the relationship is linear within the limits of data scatter, and indicates an apparent K'_1 value of 0.63.

This is in good agreement with the value of 0.60 determined by Yotsukura et al. through a trial-and-error application of the steady-state numerical model described in Sect. 1.9. It should be noted that Yotsukura et al. attempted to apply Eq. 3.8 to this nonuniform flow, and obtained $K'_1 = 0.71$ using concentration variances from the injection location downstream to station 7, where significant amounts of tracer began to reach the banks. The GCM method, on the other hand, utilized all ten distributions and took account of transverse variations of depth and velocity.

5.4 Simulation of Field Experiments

The GCM-determined value of K'_1 was used with the observed concentration distribution at station 1 to simulate the field mixing experiment. Steady-state distributions were obtained by running 37 time steps of 12 minutes each for a total time of 7.4 hours, compared with a transit time through the reach of about 1.5 hours. Figure 5.4 shows the predicted and measured normalized concentrations at seven of the sampling stations; the station 1 "predictions" are simply stream-tube equivalents of the observed tracer flowrate. Peak concentrations are generally estimated well, as are the shapes of the distributions. Apparent transverse shifts of the predicted distributions as compared to measured ones are no doubt a consequence of the rather gross use of only two measured cross sections to describe the entire reach.

The prediction described above is not unique but corroborates the results obtained by Yotsukura et al. using the steady-state model described in Sect. 1.9 with 20 stream tubes and a slightly different assumed stream geometry. The comparison was made further to verify the numerical computational method, to demonstrate its utility, and to confirm the rather large value of K'_1 previously reported. Results indicate that this large value is indeed appropriate, thus supporting the demonstrated need for further analytical and experimental studies of the magnitude and variation of transverse diffusivity in natural channels.

The strength of the numerical model described in Chapter 2 is its capability of predicting unsteady mixing in nonuniform flow, to include cyclical injection from a submerged outfall, or sudden injection from, say, a barge collision anywhere in a river. Yet experimental data for these types of unsteady mixing simply are not available. Unsteady mixing experiments have been performed only for the special case of instantaneous plane source injection, to test the one-dimensional mixing assumption of Sect. 1.8, and to evaluate the overall longitudinal mixing coefficient K_x. It is the purpose of this chapter to verify the numerical model to the extent possible for instantaneous plane source injection, and then to demonstrate the utility of the model by simulating unsteady bank injection into nonuniform flow.

6.1 Description of Field Experiments

Godfrey and Frederick (1970) reported eleven tests conducted in natural rivers to test the one-dimensional dispersion assumption. Their test 10, performed on a straight, four-mile reach of the Clinch River, near Speers Ferry, Virginia was selected for the model application. In that test, detailed velocity and topographical data were first obtained at six cross sections. Then radioactive tracer was injected at the upstream limit of the reach; it took about one minute to distribute the tracer over the entire cross section. Concentrations of the passing cloud were determined at five downstream stations, at each of which radiation detection equipment recorded the time history of centerline concentrations at an unspecified distance below the water surface. Table 6.1 summarizes the hydraulic and geometric properties of the six reference sections.

6.2 Adaptation of Hydraulic and Geometrical Data to Numerical Model

Eleven stream tubes of equal discharge were assigned to each of the six reference sections as described in Appendix E; Fig. 6.1 shows the resulting stream tube configurations, the dimensions and velocities of which are tabulated in Table 6.2. The first 50 feet from the left bank at section 1 had no flow, and thus was ignored in the stream tube discretization.

6.3 Simulation of Field Experiment

Since neither the rate of tracer injection nor the injection concentration were known precisely, the simulation used for the measured concentration distribution at section 1, x = 2,260 feet, as upstream input. Although only centerline concentrations were measured, it was necessary to assume the same concentration-time curve for each stream tube at section 1, as if the dispersion upstream of x = 2,260 feet was due entirely to turbulent diffusion, with no spreading due to differential convection.

Time and distance steps were chosen so as to minimize numerical dispersion without requiring excessive computer memory and/or computation time. The input distribution, shown on Fig. 6.2, was spread over about 18 minutes, or, using an average velocity of about 2.5 ft/sec, 2,700 feet. In order that the distribution be described by at least 10 computational

points, it was necessary to use Δx = 250 feet near the source. Knowing u and Δx, it was important to use Δt less than 100 seconds to keep $u\Delta t/\Delta x$ approximately equal to or less than unity. Computer program output constraints made it more convenient to use an initial time step of only 30 seconds. The simulation could have been run using these time and distance steps throughout, but some economy could be achieved by increasing them as the distribution spread out in time and space. Based on the observed distributions reported by Godfrey and Frederick (1970), the distance step Δx was gradually increased so as to describe the distribution by at least 10 points everywhere. The maximum allowable time step was correspondingly increased gradually to keep $u\Delta t/\Delta x$ approximately equal to unity. Table 6.3 summarizes the time and distance steps finally used in the simulation.

A more typical field application would not have the benefit of concentration distributions known a priori, obviously. For such a case it is best first to compute Δx and Δt using the assumed concentration input, and to run the full simulation using these conservatively small values. Once the approximate dispersion pattern is known from the simulation, Δx and Δt may be increased as above to minimize computational cost on repetitive trials.

Transverse and longitudinal diffusivities were chosen as if no special information was available. The diffusivities were assumed to be constant within a cross section, as traditionally assumed and supported by the results described in Chapter 4. Elder's (1959) coefficients, also commonly accepted, were adopted, so that

$$\epsilon_x = 5.93 \, U_*H \qquad (6.1a)$$

and

$$\epsilon_z = 0.23 \, U_*H \qquad (6.1b)$$

Note that Eq. 6.1a represents longitudinal diffusion due both to turbulent fluctuations and to differential convection related to the vertical gradient of velocity. The simulation was run for two hours, i.e., long enough for most of the tracer to be convected out of the reach; this required 80 seconds of computation time on the CDC 6400 digital computer at Colorado State University.

Direct comparison could not be made between the measured concentration-time curves (at specific locations) and the computed concentration-distance curves (at specific times). Nonetheless, a rough comparison can be made by converting a computed concentration-distance curve to an equivalent concentration-time curve using the convective velocity of the tracer cloud, and assuming no change in the shape of the distribution as it passes the station in question. The computed curve at t = 0.61 hours, which peaked at x_o = 8,970 feet, was transformed to a concentration-time curve peaking at t_o = 0.62 hours (to correspond to the measured section 3 distribution) by the relation

$$t = t_o - \frac{x - x_o}{U_c} \qquad (6.2)$$

where

t = equivalent time corresponding to x,

t_o = time of peak concentration passage at measured section,

x = longitudinal coordinate of simulated concentration value,

x_o = location of peak concentration for simulation, and

U_c = convective velocity of tracer cloud.

The convective velocity U_c, taken from Fig. 6.4 (to be discussed further) was about 3 ft/sec. Figure 6.2 shows the measured and computed curves; units of concentration are microcuries per cubic feet. The trailing edge oscillations in the computed curve are an inevitable consequence of the finite-difference computation, and are caused by the differential celerities of Fourier Series solution components as predicted by Eq. 2.33; the sample computation for pure convection shown in Fig. 2.4 displays the same oscillations. Fortunately, however, the oscillatory behavior always occurs on the trailing edge of a distribution, whereas the leading edge and the peak concentrations are generally of most practical importance in pollution problems.

The computed concentrations appear to begin rising sooner at $x = 8,170$ feet than the measured ones; the error is due in part to the effects of numerical dispersion, and the transformation of the concentration-distance curve to a concentration-time curve. But it also suggests that Elder's coefficient of 5.93 may overestimate the longitudinal diffusion, at least upstream of this particular location. Note also that the simulation underestimates the peak concentration by 17 percent; but Fig. 6.3, which compares peak concentrations over the entire reach, indicates that at most locations the simulation predicts peak concentrations quite well. Figure 6.4 shows also that the celerity of the peak centerline concentration was accurately predicted by the simulation. It is important to recognize that the celerity is determined by the interaction between differential convection and transverse diffusion; the apparent value of about 3 ft/sec from Fig. 6.4 falls between the mean stream velocity of approximately 2.6 ft/sec and the centerline velocity of approximately 3.3 ft/sec. Moreover, the good general agreement of the simulation predictions with experimental results reinforces recent criticism of the one-dimensional mixing concept (Section 1.8) in natural rivers; Nordin and Sabolt (1974) showed that the Clinch River experiments could not be modeled as a one-dimensional Fickian process.

The simulation's accurate prediction of the Clinch River experimental results provides a strong argument for its efficacy and utility. Neither calibration nor coefficient adjustment were required;

topographic information, water surface elevations, and velocity measurements were input along with traditionally assumed diffusivities to provide mixing information essentially as good as that obtained by a costly field experiment.

6.4 Simulation of Hypothetical Unsteady Bank Injection

A final demonstration of the numerical model's utility is its application to the prediction of mixing resulting from the injection of a slug of pollutant near the bank of a river. Such a situation might result from a temporary breakdown of mechanical equipment in a sewage treatment plant or chemical facility, such that untreated waste is discharged through a submerged outfall for a short period of time. Outfalls are designed to provide as much initial dilution as possible, so that complete mixing over the depth is an acceptable first assumption.

The Clinch River was again chosen for the simulation; the computational grid and time steps were left unchanged from the instantaneous plane source simulation described earlier. A full sine wave concentration curve of period 15 minutes and peak concentration 100 ppb was input into tube 2 at $x = 2,260$ feet:

$$C(t) = 50[1 - \sin\pi(\frac{2t}{900} + \frac{1}{2})] \qquad (6.3)$$

where t is in seconds. The simulation was run for two hours, long enough to convect the cloud through most of the reach, and for three diffusivity combinations, as follows:

(a) $\varepsilon_x = 5.93\ U_*H$, $\varepsilon_z = 0.23\ U_*H$

(b) $\varepsilon_x = 0$, $\varepsilon_z = 0.23\ U_*H$

(c) $\varepsilon_x = 0$, $\varepsilon_z = 0.23\ U_*/U\ uh$

Run (a) represents conditions normally assumed; (b) tests the influence of the longitudinal diffusivity; and (c) tests the influence of nonconstant transverse diffusivity (Eq. 3.12b) in this channel. Figure 6.5 shows the results of the simulation at two times, one only 16 minutes after the start of the injection, the other after 71 minutes. At each time the transverse concentration distribution is shown at three arbitrary x-locations, showing the three-dimensional shape of the tracer cloud. Two conclusions are immediately evident: first, the mixing is quite insensitive to the magnitude of the longitudinal diffusivity ε_x,

as has been suggested in the literature (Sayre and Chang, 1968; Holley, 1971). Second, in this channel the distribution of transverse diffusivity has only a minimum influence on the mixing process.

CONCLUSIONS

The primary objective of this study was to develop and apply a numerical model for the prediction of time-dependent mass dispersion in natural streams. Numerical diffusion in the computation of streamwise convection is eliminated by using the double-step implicit-explicit second order method described by Peaceman and Rachford (1955); numerical dispersion can be minimized by judicious choice of time and distance steps. Computation time and computer storage requirements are kept reasonably conservative by the use of a tri-diagonal matrix solution technique for the implicit computations. The overall result is an easily-applied model for the computation of both steady-state and time-dependent depth-averaged mixing of a conservative, neutrally-buoyant pollutant in steady but non-uniform channel flow of arbitrary cross section. Both longitudinal and transverse diffusion are computed; depth-averaged transverse velocities are taken into account, and mixing due to transverse secondary circulation can be absorbed in the transverse diffusivity, which need not be constant within a cross section.

The numerical model was verified against analytical solutions for simplified flow fields. Comparison with solutions for a continuous vertical line source in a rectangular channel of constant velocity, and for an instantaneous vertical line source in an unbounded fluid having a constant transverse gradient of longitudinal velocity, indicated that model provides satisfactory prediction of the analytical concentration distributions. Model predictions are relatively insensitive to the magnitude of time and distance steps used in the numerical computation.

The secondary goal of this investigation was an experimental determination of the variation of transverse diffusivity in a triangular laboratory channel. The capability of numerical models to allow the transverse diffusivity to vary within a cross section exposes a need for information on not only the magnitude, but also the distribution of the diffusivity within a cross section. The experiments were designed specifically to test the diffusivity functions proposed by Holley (1971). Analysis of steady-state concentration distributions resulting from continuous injection at the bank and at two other transverse positions indicates that the traditional constant diffusivity assumption best reproduces the observed distributions. The apparent invariance of the transverse diffusivity represents an interaction between bed shear and transverse shear, the relative contributions of which cannot yet be determined.

Application of the numerical model to two field experiments confirms its utility. The previously reported constant transverse diffusivity in a reach of the Missouri River was verified using Holley's (1971) Generalized Change of Moments method, and a numerical simulation of the continuous-injection experiment using minimal hydraulic and geometric data successfully reproduced the measured concentration distributions. The model's capability for predicting time-dependent mixing was demonstrated through comparison with an instantaneous plane source injection experiment performed on the Clinch River. The decay and convective velocity of the peak centerline concentration, as well as the general shape of the longitudinal centerline concentration distributions, were predicted quite well by the numerical model. The predictions used commonly accepted values for longitudinal and transverse diffusivity, requiring no adjustment or calibration to reproduce the observed behavior.

Application of the model to predict time-dependent mixing from a hypothetical vertical line source near one bank of the Clinch River confirmed the insignificance of longitudinal turbulent diffusion for most situations. Moreover, these simulations demonstrate that, in an approximately rectangular channel, predicted concentration distributions are insensitive to the assumed variation of transverse diffusivity. The applicability of the numerical model should further be tested through comparison with mixing experiments in natural rivers using vertical line sources of finite duration.

This study has demonstrated that a relatively simple finite difference model can successfully predict time-dependent concentration distributions in a river. But the predictions are no more accurate than the transverse diffusivity assigned by the user. The diffusivity is assumed to describe mixing due to molecular diffusion, turbulent velocity fluctuations, and differential convection; yet existing theory and experimental investigation have been focused solely on the relationship of diffusivity to bed shear. There is a need for a better theoretical and experimental understanding of the individual contributions of several components comprising transverse diffusivity. Specific effort should be devoted to the mixing contribution of transverse gradients of longitudinal velocity and secondary circulation in bends.

REFERENCES

1. Aris, R., (1956), "On the Dispersion of a Solute in a Fluid Flowing Through a Tube," Proceedings Royal Society of London, Vol. 235 A, pp. 67-77.

2. Barnes, H.H., (1967), "Roughness Characteristics of Natural Channels," U.S. Geological Survey Water Supply Paper 1849.

3. Batchelor, G.K., (1949), "Diffusion in a Field of Homogeneous Turbulence," Australian Journal of Scientific Research, Vol. 2, pp. 437-450.

4. Carnahan, B., H.A. Luther, and J.O. Wilkes, (1969), Applied Numerical Methods, John Wiley and Sons, Inc., New York.

5. Carter, H.H., and A. Okubo, (1965), "A Study of the Physical Processes of Movement and Dispersion in the Cape Kennedy Area," Final Report, U.S. Atomic Energy Commission Contract No. AT(30-1)-2973.

6. Chang, Y., (1971), "Lateral Mixing in Meandering Channels," Dissertation submitted in partial fulfillment of the requirements for the degree of Doctor of Philosophy, The University of Iowa.

7. Cleary, R.W., and D.D. Adrian, (1973), "New Analytical Solutions for Dye Diffusion Equations," Journal of the Environmental Engineering Division, ASCE, Vol. 99, No. EE3, June, pp. 213-227.

8. Csanday, G.T., (1973), Turbulent Diffusion in the Environment, D. Reidel Publishing Company, Boston.

9. Elder, J.W., (1959), "The Dispersion of Marked Fluid in Turbulent Shear Flow," Journal of Fluid Mechanics, Vol. 5, No. 4, pp. 544-560.

10. Fischer, H.B., (1966), "Longitudinal Dispersion in Laboratory and Natural Streams," Report No. KH-R-12, W.M. Keck Laboratory of Hydraulics and Water Resources, California Institute of Technology, Pasadena.

11. Fischer, H.B., (1967), "The Mechanics of Dispersion in Natural Streams," Proc ASCE, Vol. 93, No. HY6, pp. 187-216.

12. Fischer, H.B., (1969), "The Effect of Bends on Dispersion in Streams," Water Resources Research, Vol. 5, No. 2, April, pp. 496-506.

13. Fischer, H.B., (1970), "Transverse Mixing in a Sand Bed Channel," U.S. Geological Survey Professional Paper 575-D, pp. D267-D272.

14. Fischer, H.B., and E.R. Holley, (1971), "Analysis of the Use of Distorted Hydraulic Models for Dispersion Studies," Water Resources Research, Vol. 7, No. 1, pp. 46-51.

15. Frenkiel, F.N., (1953), "Turbulent Diffusion," Advanced Applied Mechanics, 3, 61, pp. 61-107.

16. Glover, R.E., (1964), "Dispersion of Dissolved or Suspended Materials in Flowing Streams," U.S. Geological Survey Professional Paper 433-B.

17. Godfrey, R.C., and B.J. Frederick, (1970), "Stream Dispersion at Selected Sites," U.S. Geological Survey Professional Paper 433-K.

18. Holley, E.R., (1971), "Transverse Mixing in Rivers," Report No. S 132, Delft Hydraulics Laboratory, Delft, The Netherlands.

19. Holley, E.R., (1972), discussion of "Dispersion in Natural Streams," by M.K. Bansal, Journal of the Hydraulics Division, ASCE, Vol. 98, No. HY6, June, pp. 1089-1091.

20. Holley, E.R., and M. Karelse, (1969), "Model-Prototype Comparisons for Transverse Mixing in Rivers," Proc XVth Congress of the IAHR, Istanbul, pp. 311-318.

21. Keefer, T.N., (1971), "The Relation of Turbulence to Diffusion in Open-Channel Flows," Dissertation submitted in partial fulfillment of the requirements for the degree of Doctor of Philosophy, Colorado State University, Fort Collins.

22. Lauwerier, H.A., (1954), "Diffusion from a Source in a Skew Velocity Field," Applied Science Research, 4A, pp. 153-156.

23. Leendertse, J.J., (1970), "A Water-Quality Simulation Model for Well-Mixed Estuaries and Coastal Seas: Volume I, Principles of Computation," Rand Corporation Memorandum, RM-6230-RC, February.

24. Miller, A.C., (1971), "Turbulent Diffusion and Longitudinal Dispersion Measurements in a Hydrodynamically Rough Open Channel Flow," Dissertation submitted in partial fulfillment of the requirements for the degree of Doctor of Philosophy, Colorado State University, Fort Collins.

25. Monin, A.S., and A.M. Yaglom, (1971), Statistical Fluid Mechanics, Massachusetts Institute of Technology Press, Cambridge.

26. Nordin, C.F., and G.V. Sabol, (1974), "Empirical Data on Longitudinal Dispersion in Rivers," U.S. Geological Survey Water Resource Investigation 20-74, August.

27. Okoye, J.K., (1970), "Characteristics of Transverse Mixing in Open-Channel Flows," Report No. KH-R-23, W.M. Keck Laboratory of Hydraulics and Water Resources, California Institute of Technology, Pasadena.

28. Okubo, A., and M.J. Karweit, (1969), "Diffusion from a Continuous Source in a Uniform Shear Flow," Limnology and Oceanography, Vol. 14, pp. 514-520.

29. Peaceman, D.W., and H.H. Rachford, (1955), "The Numerical Solution of Parabolic and Elliptic Differential Equation," Journal Society of Industrial Applied Mathematics, Vol. 3, No. 1, March, pp. 28-45.

30. Prych, E.A., (1970), "Effects of Density Differences on Lateral Mixing in Open Channel Flows," Report No. KH-R-21, W.M. Keck Laboratory of Hydraulics and Water Resources, California Institute of Technology, Pasadena.

31. Roache, P.J., (1972), "On Artificial Viscosity," Journal of Computational Physics, Vol. 10, No. 2, October, pp. 169-184.

32. Rozovskii, I.L., (1970), Flow of Water in Bends of Open Channels, Academy of Sciences of the Ukrainian SSR, Translation No. OTS60-51133, Office of Technical Services, U.S. Department of Commerce, Washington, D.C.

33. Sayre, W.W., (1968), "Dispersion of Mass in Open Channel Flow, " Hydraulics Papers, Colorado State University, Fort Collins, Colorado, No. 3, February.

34. Sayre, W.W., (1973), "Natural Mixing Processes in Rivers," Chapter 6 of Environmental Impact on Rivers, Edited by H.W. Shen, Department of Civil Engineering, Colorado State University, Fort Collins, Colorado.

35. Sayre, W.W., and F.M. Chang, (1968), "A Laboratory Investigation of Open-Channel Dispersion Processes for Dissolved, Suspended, and Floating Dispersants," U.S. Geological Survey Professional Paper 433-E.

36. Taylor, G.I., (1921), "Diffusion by Continuous Movements," Proc London Mathematical Society, A20, pp. 196-211.

37. Taylor, G.I., (1954), "The Dispersion of Matter in Turbulent Flow Through a Pipe," Proceedings Royal Society of London, Vol. 233A, pp. 446-468.

38. Wilson, J.F., (1968), "Flurometric Procedures for Dye Tracing," Chapter A12, Techniques of Water Resources Investigations of the United States Geological Survey, U.S. Department of the Interior.

39. Yotsukura, N., and E.D. Cobb, (1972), "Transverse Diffusion of Solutes in Natural Streams," U.S. Geological Survey Professional Paper 582-C.

40. Yotsukura, N., H.B. Fischer, and W.W. Sayre, (1970), "Measurement of Mixing Characteristics of the Missouri River Between Sioux City, Iowa and Plattsmouth, Nebraska," U.S. Geological Survey Water Supply Paper 1899-G.

APPENDIX A

TABLES

Table 2.1. Stream Tube Dimensions and Injection Concentrations, Rectangular Channel

	11-Tube Model			21-Tube Model	
Tube	Width B' (ft)	Injection Concentration (ppb)	Tube	Width B' (ft)	Injection Concentration (ppb)
1,11	0.55	0	1,21	0.55	0
2,10	0.20	0	2,20	0.10	0
3,9	0.10	0	3,19	0.10	0
4,8	0.10	0	4,18	0.05	0
5,7	0.04	0	5,17	0.05	0
6	0.02	10	6,16	0.05	0
			7,15	0.05	0
			8,14	0.02	0
			9,13	0.02	0
			10,12	0.0075	0
			11	0.005	40

Table 2.2. Stream Tube Dimensions and Velocities, Uniform Shear Flow

Tube	Width B' (ft)	Velocity u (ft/sec)
1	10.000	0.000
2	0.100	0.000
3	0.100	0.286
4	0.100	0.571
5	0.095	0.850
6	0.010	1.000
7	0.095	1.150
8	0.100	1.430
9	0.100	1.710
10	0.100	2.000
11	10.000	2.000

Table 4.1. Hydraulic Test Data

	Tests A,B,C	Tests D,E,F
Q(cfs)	1.69	1.69
A(ft^2)	1.53	1.56
$\bar{U}$(ft/sec)	1.11	1.08
R(ft)	0.37	0.37
S(ft/ft)	0.00052	0.00025
n(sec/ft$^{1/3}$)	0.0158	0.0112
U_*(ft/sec)	0.079	0.055
Froude No.	0.32	0.31

Table 4.2. Dispersion Test Injection Data

Test	Roughness	Injection Location, z_o (ft)	Injection Concentration C_o (ppb)	Injection Rate q_o (ml/min)	Injection Strength $q_o C_o$ (ppb-cfs)
A	Full	4.0	3.5×10^4	140	2.884
B	Full	3.0	4.9×10^4	140	4.038
C	Full	2.0	5.4×10^4	140	4.450
D	Half	4.0	4.3×10^4	140	3.543
E	Half	3.0	4.8×10^4	140	3.955
F	Half	2.0	6.2×10^4	140	5.109

Table 4.3. Results of Generalized Change of Moments Analysis for Test Data

Test	Least-Squares K' for Indicated Diffusivity Function		
	K_1' U*H	K_2' $\frac{U_*}{U_a}$ uh	K_3' u_*h
A	0.45[1]	0.50[1]	0.48[1]
B	0.30	0.20	0.18
C	0.34	0.27	0.25
Average of Tests A,B,C	0.32[2]	0.24[2]	0.22[2]
D	0.55	0.48	0.45
E	0.67[1]	0.39[1]	0.35[1]
F	0.63[1]	0.50[1]	0.48[1]
Average of Tests D,E,F	0.62	0.46	0.43

(1) Excludes variance at x=50 ft.

(2) Full-roughness averages formed using test B and C results only.

Table 4.4. Stream Tube Parameters for Numerical Model of Triangular Channel

Tube	Full - Roughness Flow			Half - Roughness Flow		
	B' (ft)	h (ft)	u (ft/sec)	B' (ft)	h (ft)	u (ft/sec)
1	0.1	0.0996	0.4925	0.1	0.1098	0.2350
2	0.2	0.1435	0.7486	0.2	0.1540	0.5800
3	0.2	0.2020	0.8274	0.2	0.2130	0.7200
4	0.2	0.2605	0.8865	0.2	0.2720	0.8500
5	0.2	0.3190	0.9456	0.2	0.3310	0.9950
6	0.2	0.3775	1.0047	0.2	0.3900	1.1000
7	0.2	0.4360	1.0737	0.2	0.4490	1.1550
8	0.2	0.4945	1.1426	0.2	0.5080	1.1950
9	0.2	0.5530	1.2116	0.2	0.5670	1.2050
10	0.2	0.6115	1.2608	0.2	0.6260	1.1950
11	0.2	0.6700	1.3002	0.2	0.6850	1.1830
12	0.2	0.6115	1.2903	0.2	0.6260	1.2000
13	0.2	0.5530	1.2707	0.2	0.5670	1.2200
14	0.2	0.4945	1.2214	0.2	0.5080	1.2150
15	0.2	0.4360	1.1525	0.2	0.4490	1.1750
16	0.2	0.3775	1.0934	0.2	0.3900	1.1160
17	0.2	0.3190	1.0145	0.2	0.3310	1.0000
18	0.2	0.2605	0.9357	0.2	0.2720	0.8500
19	0.2	0.2020	0.8471	0.2	0.2130	0.6650
20	0.2	0.1435	0.7584	0.2	0.1540	0.5350
21	0.1	0.0996	0.3940	0.1	0.1098	0.2250

Table 4.5. Stream Tube Parameters for Alternate Numerical Simulation, Test D

Tube	B' (ft)	h (ft)	u (ft/sec)
1	1.0	0.2425	0.7708
2	1.0	0.5375	1.2090
3	0.5	0.6113	1.2141
4	0.4	0.4785	1.2090
5	0.3	0.3753	1.0881
6	0.2	0.3015	0.9420
7	0.1	0.2573	0.8060
8	0.09	0.2292	0.7254
9	0.08	0.2042	0.6650
10	0.07	0.1820	0.6096
11	0.06	0.1629	0.5743
12	0.05	0.1466	0.5239
13	0.04	0.1333	0.4165
14	0.03	0.1230	0.3044
15	0.02	0.1157	0.2243
16	0.01	0.1112	0.1762
17	0.01	0.1083	0.1442
18	0.01	0.1053	0.1121
19	0.01	0.1024	0.0801
20	0.01	0.0994	0.0481
21	0.01	0.0965	0.0160

Table 5.1. Missouri River Source Reference Sections

x (ft)	Source Section (mile)	Width (ft)	Width adjustment factor	Depth adjustment factor
0	648.5	601	1.0	1.0
11,850	648.5	627	1.043	0.958
17,105	645	738	1.0	1.0
25,050	645*	631	0.855	1.170
32,970	648.5*	509	0.847	1.181

* denotes mirror image

39

Table 5.2. Missouri River Reference Section Stream Tube Parameters

Section	1			2			3			4			5		
	x = 0 ft			x = 11,850 ft			x = 17,105 ft			x = 25,050 ft			x = 32,970 ft		
Tube	B' (ft)	h (ft)	u (ft/sec)	B' (ft)	h (ft)	u (ft/sec)	B' (ft)	h (ft)	u (ft/sec)	B' (ft)	h (ft)	u (ft/sec)	B' (ft)	h (ft)	u (ft/sec)
1	213	6.3	2.3	223	6.0	2.3	191	5.6	2.9	67	10.4	4.5	42	15.5	4.8
2	90	8.3	4.2	94	8.0	4.2	81	7.1	5.4	37	12.0	7.0	26	16.9	7.0
3	49	10.4	6.1	51	10.0	6.1	58	9.2	5.8	40	12.0	6.5	19	19.3	8.5
4	38	11.7	7.0	40	11.2	7.0	67	9.4	4.9	28	12.0	9.3	17	19.1	9.6
5	32	13.0	7.5	33	12.5	7.5	48	10.0	6.5	38	11.5	7.2	24	18.3	7.1
6	28	14.1	7.9	29	13.5	7.9	48	9.4	6.9	41	11.0	6.9	24	16.6	7.9
7	28	15.5	7.2	29	14.8	7.2	44	9.8	7.2	41	11.7	6.5	27	15.3	7.5
8	20	16.2	9.6	21	15.5	9.6	33	10.3	9.1	57	11.0	5.0	32	13.8	7.0
9	22	16.3	8.7	23	15.6	8.7	47	10.3	6.4	50	10.8	5.8	42	12.3	6.1
10	31	14.3	7.0	32	13.7	7.0	43	10.3	7.0	69	8.3	5.4	76	9.8	4.2
11	50	13.1	4.8	52	12.6	4.8	78	8.9	4.5	163	6.6	2.9	180	7.4	2.3

Table 6.1. Clinch River Channel Geometry and Flow Data

Section	1	2	3	4	5	6
x(ft)	2,260	5,170	8,170	11,800	15,300	19,300
B(ft)	200	165	160	183	175	166
H(ft)	5.70	5.31	6.50	7.43	7.37	8.92
S(ft/ft)	.0012	.00078	.00058	.00044	.00044	.00040
Q(cfs)	3,030	2,820	3,150	3,070	2,960	3,010
$\overline{U}$(ft/sec)	2.66	3.22	3.03	2.26	2.29	2.03

Table 6.2. Clinch River Reference Section Stream Tube Parameters

Section	1 x = 2,260 ft			2 x = 5,170 ft			3 x = 8,170 ft			4 x = 11,800 ft			5 x = 15,300 ft			6 x = 19,300 ft		
Tube	B' (ft)	h (ft)	u (ft/sec)	B' (ft)	h (ft)	u (ft/sec)	B' (ft)	h (ft)	u (ft/sec)	B' (ft)	h (ft)	u (ft/sec)	B' (ft)	h (ft)	u (ft/sec)	B' (ft)	h (ft)	u (ft/sec)
1	27	6.2	1.6	32	4.1	2.1	33	4.5	1.8	40	6.0	1.1	33	6.0	1.4	31	5.0	1.8
2	10	6.4	3.6	13	6.1	3.5	13	7.6	2.8	14	9.3	2.1	13	7.9	2.7	17	10.2	1.6
3	11	6.3	4.0	12	6.4	3.6	12	8.0	2.9	12	8.8	2.6	12	7.9	2.9	10	11.8	2.3
4	8	8.6	4.0	13	5.9	3.6	12	7.5	3.0	11	8.6	2.9	11	8.5	2.9	8	11.9	2.9
5	9	8.0	3.8	14	5.3	3.7	10	8.0	3.4	11	8.3	3.0	13	8.2	2.6	7	11.4	3.4
6	12	5.5	4.2	11	6.6	3.8	9	8.9	3.4	11	8.0	3.1	11	8.6	2.9	10	11.2	2.4
7	6	6.2	7.3	11	6.4	3.9	8	9.4	3.6	11	8.0	3.1	13	7.3	2.9	9	11.1	2.7
8	7	7.5	5.2	8	6.2	5.5	10	7.8	3.5	10	7.5	3.6	12	7.4	3.1	10	10.9	2.5
9	9	8.0	3.8	10	6.9	4.0	9	8.9	3.4	12	7.3	3.1	11	8.6	2.9	13	10.7	2.0
10	12	8.1	2.8	12	6.4	3.6	11	7.9	3.6	13	7.3	2.6	13	9.3	2.3	14	9.3	2.1
11	35	6.7	1.2	27	4.2	2.4	31	4.5	2.0	36	5.5	1.4	32	5.5	1.6	33	5.9	1.4

Table 6.3. Clinch River Simulation Time and Distance Steps

Distance Range (ft)	Δx (ft)	Time Range (hours)	Δt (sec)
2,260 - 3,715	100	0.0 - 0.067	30
3,715 - 9,985	200	0.067 - 0.683	60
9,985 - 13,550	275	0.683 - 1.383	120
13,550 - 17,300	300	1.383 - end	180
17,300 - 19,300	350		
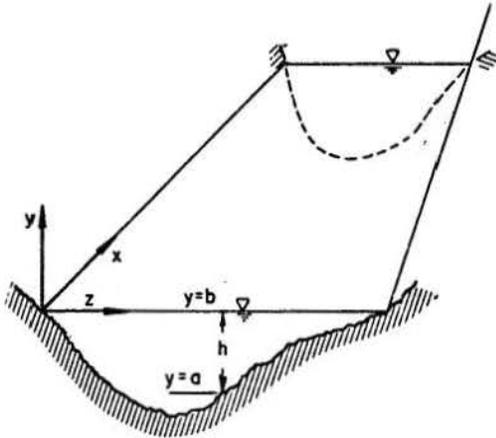
Fig. 1.1. Definition sketch for depth-integration of mass conservation equation
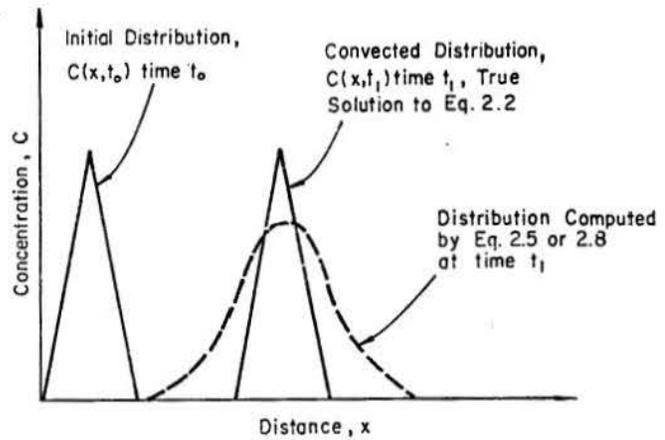
Fig. 2.1. Schematic representation of numerical diffusion
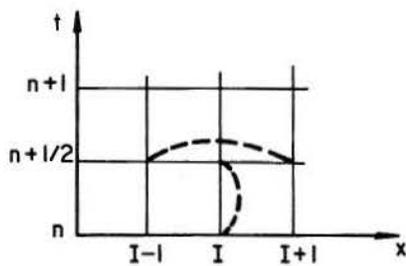
Implicit Half-step
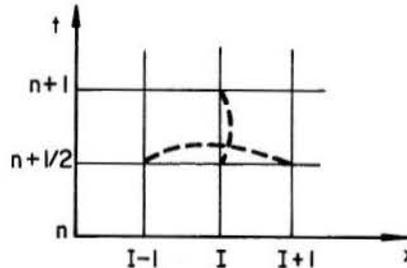
Explicit Half-step

Fig. 2.2. Finite difference discretization, double-step implicit-explicit second order scheme
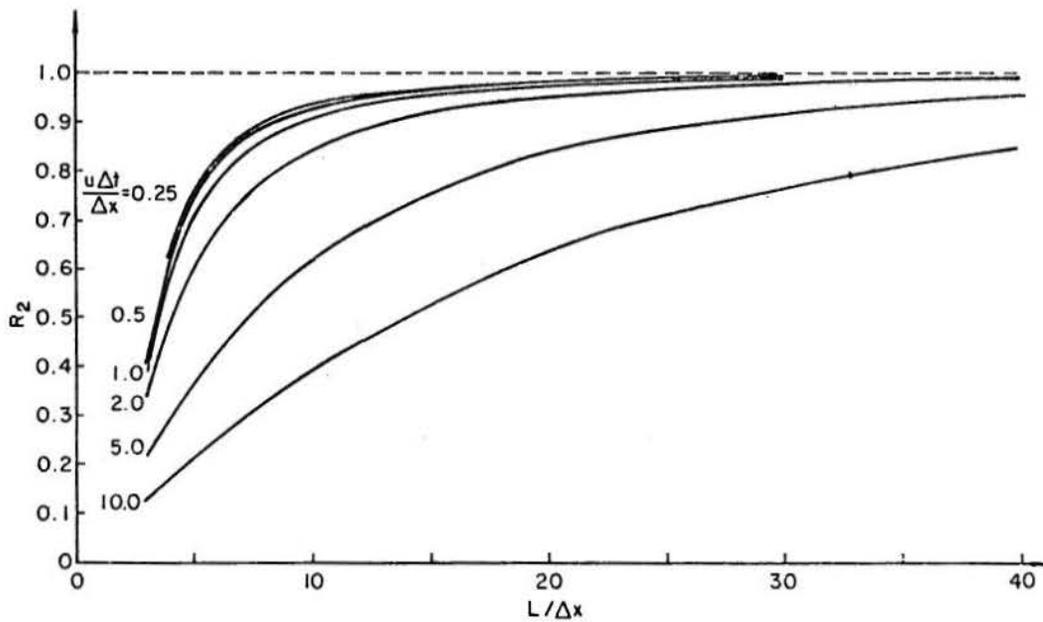
Fig. 2.3. Numerical dispersion characteristics of the double-step, implicit-explicit second order scheme
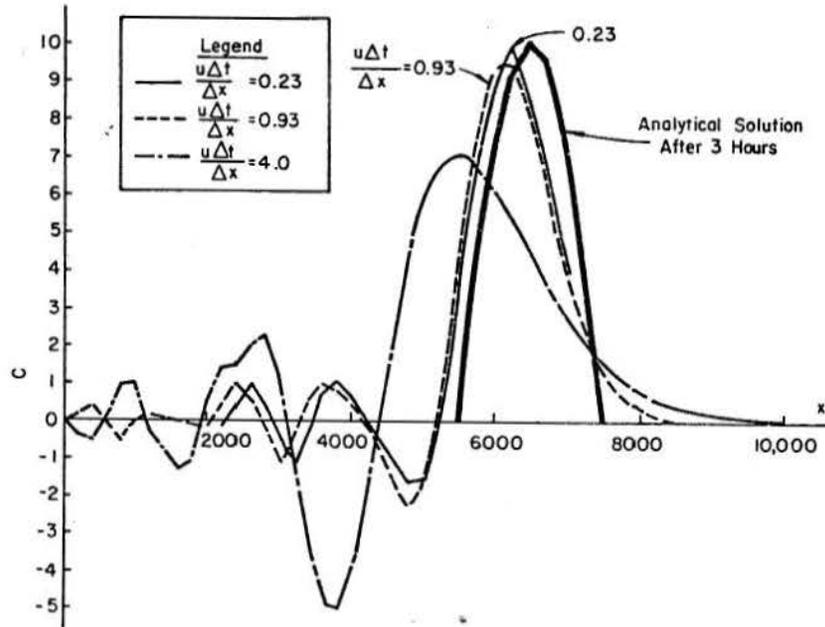
Fig. 2.4. Application of double-step implicit-explicit second order scheme to idealized channel
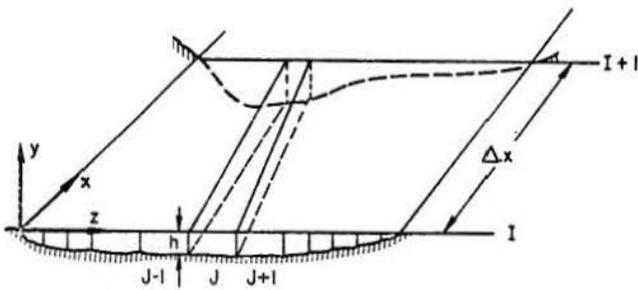
Fig. 2.5. Stream tube conceptualization of natural river
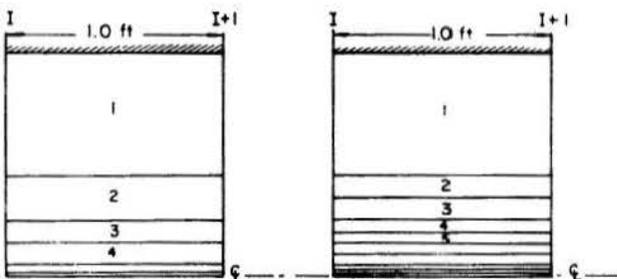
Fig. 2.6. Schematic sketch of rectangular channel model
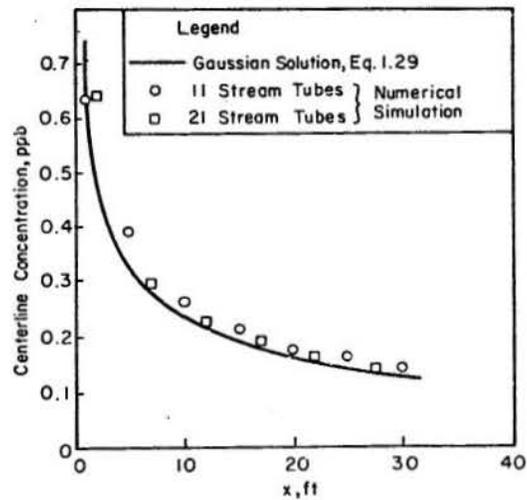
a) Longitudinal Concentration Profile at Centerline
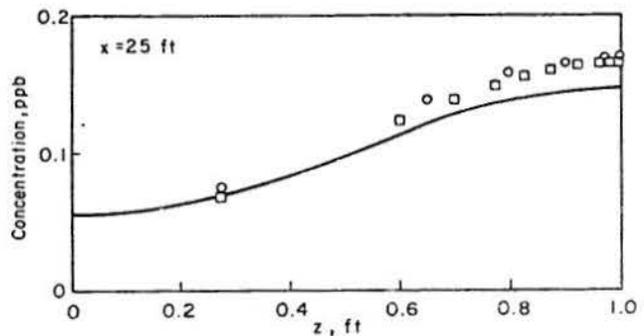
b) Transverse Concentration Profile at x = 25 ft

Fig. 2.7. Comparison of analytical and numerical predictions of continuous line source diffusion in a rectangular channel

43

a) The Physical Setting

b) 11-Tube Model
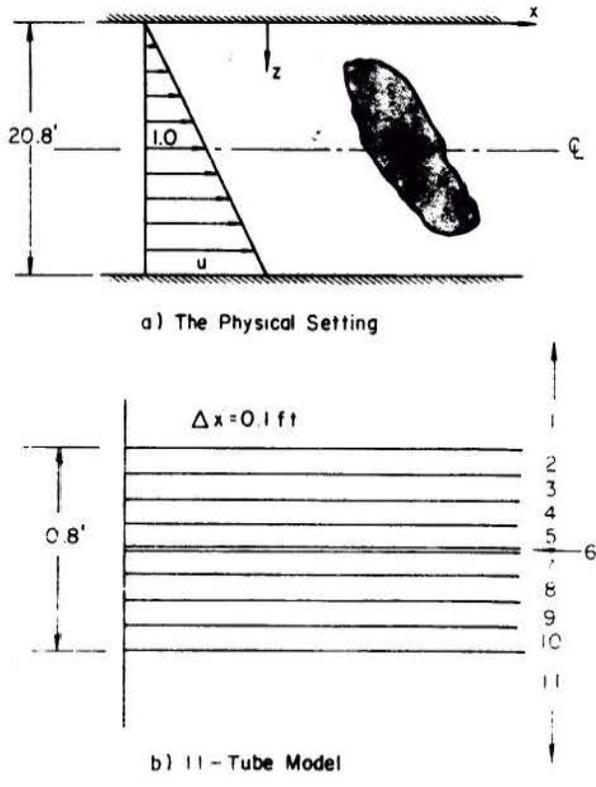
Fig. 2.8. Schematic sketch of uniform shear flow model

a) Longitudinal Concentration Profile at Centerline, $z = 10.4$ ft.

Legend
- O $\Delta t = 0.010$ sec
- □ $\Delta t = 0.0175$ sec
- △ $\Delta t = 0.005$ sec
- —— Jointly Gaussian Solution, Eq. 1.28

b) Transverse Concentration Profile at $x = 0.08$ ft.
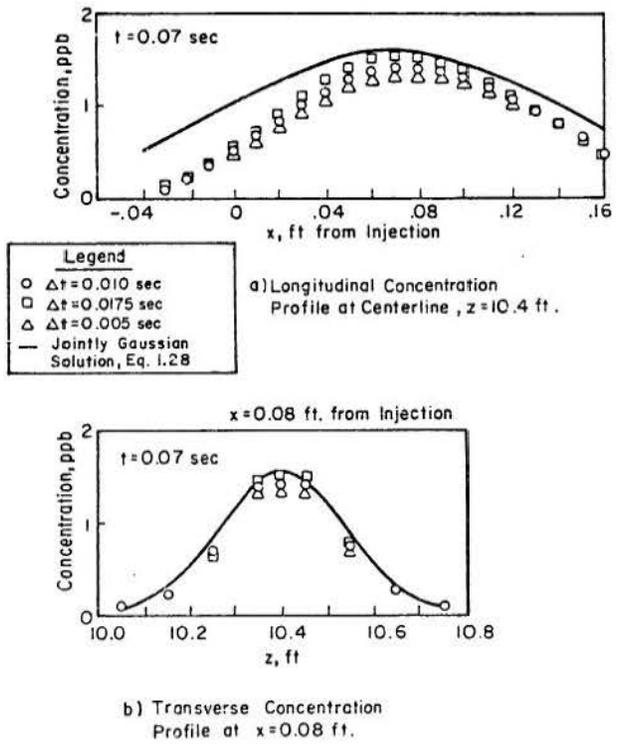
Fig. 2.9. Comparison of analytical and numerical predictions of instantaneous line source diffusion in a uniform shear flow

a) Detail of Gradient Computation

Legend
- O Measured Data
- --- 3-Pt. Linear Least Square Fits
- —— Averaged Linear Fits

b) Application to Missouri River Data
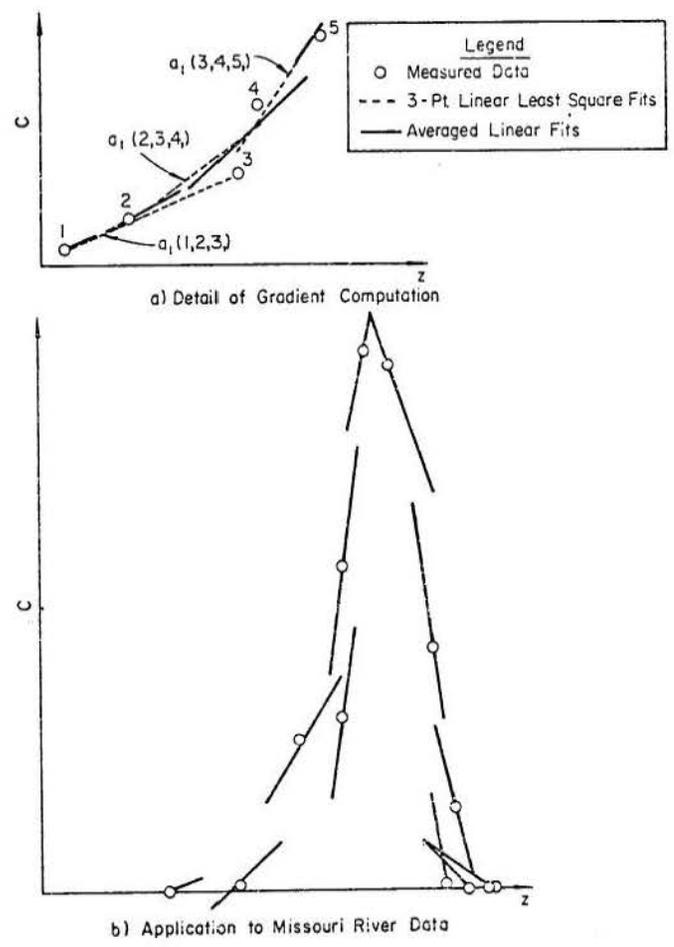
Fig. 3.1. Transverse gradient computation for GCM method

a) Flume Cross Section

b) Half and Full Roughness Models

c) Alternate Test-D Model
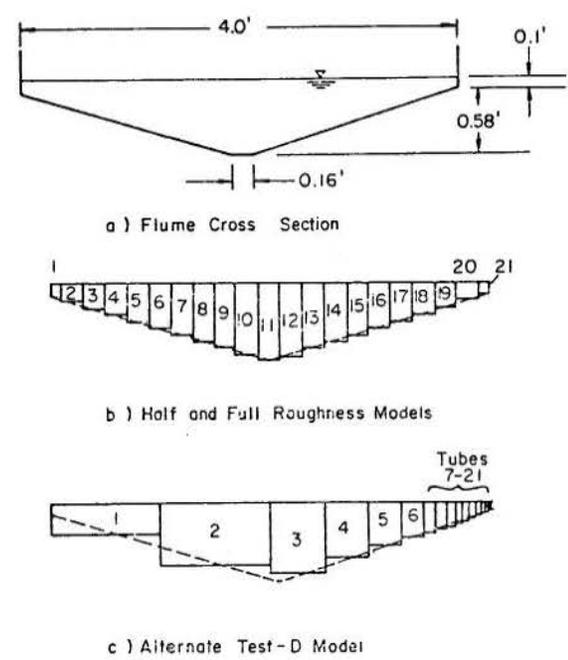
Fig. 4.1. Triangular channel and stream tube configurations

44
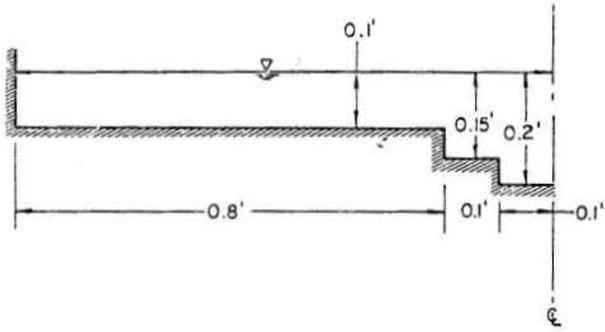
Fig. 4.2. Composite channel for investigation of continuous vs instantaneous tracer injection
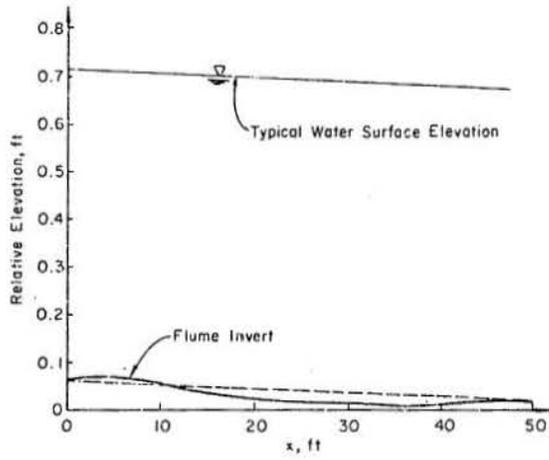
Fig. 4.4. Flume bottom contour

a) $\frac{\partial u}{\partial z} \neq 0$

b) $\frac{\partial u}{\partial z} = 0$
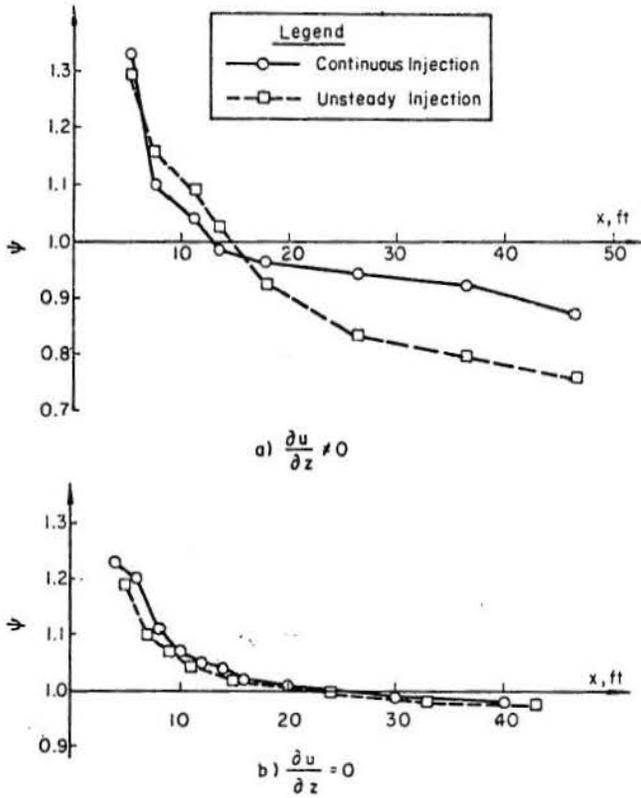
Fig. 4.3. Effects of transverse velocity gradient on injection method sensitivity to ε_z

a) False Bottom

b) Artificial Roughness
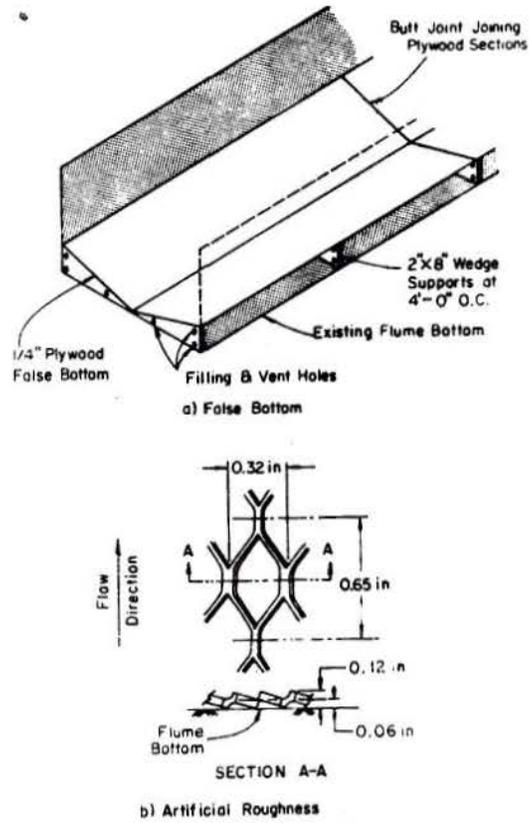
Fig. 4.5. Triangular false bottom and artificial roughness

a) Full Roughness, x = 40.0 ft

b) Half Roughness, x = 30.6 ft
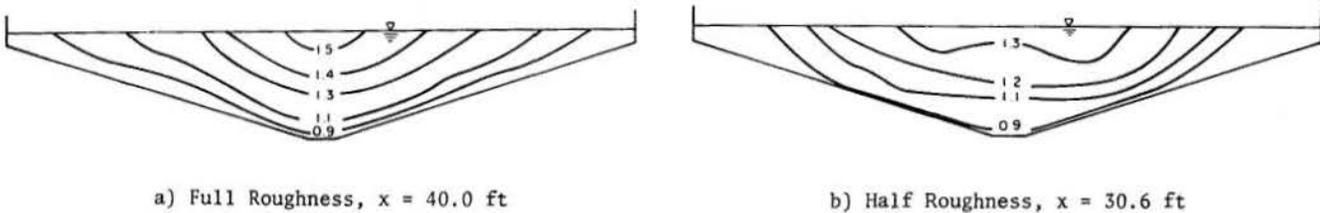
Fig. 4.6. Typical velocity contours for half and full-roughness flows, in ft/sec

45
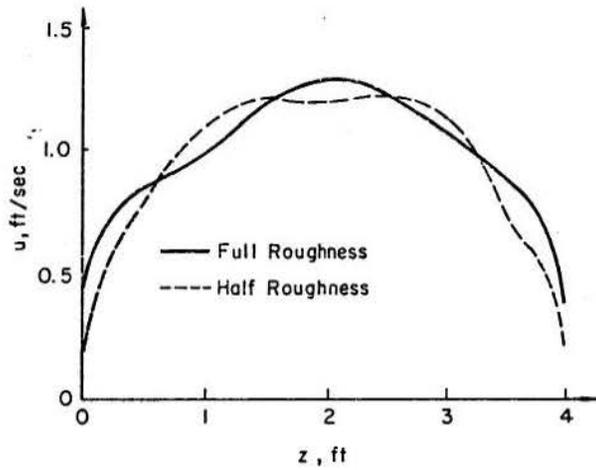
Fig. 4.7. Depth-averaged velocity distributions for half and full-roughness flows

a) Injection at x=18 ft, z=2.0 ft

b) Injection at x=18 ft, z=3.0 ft
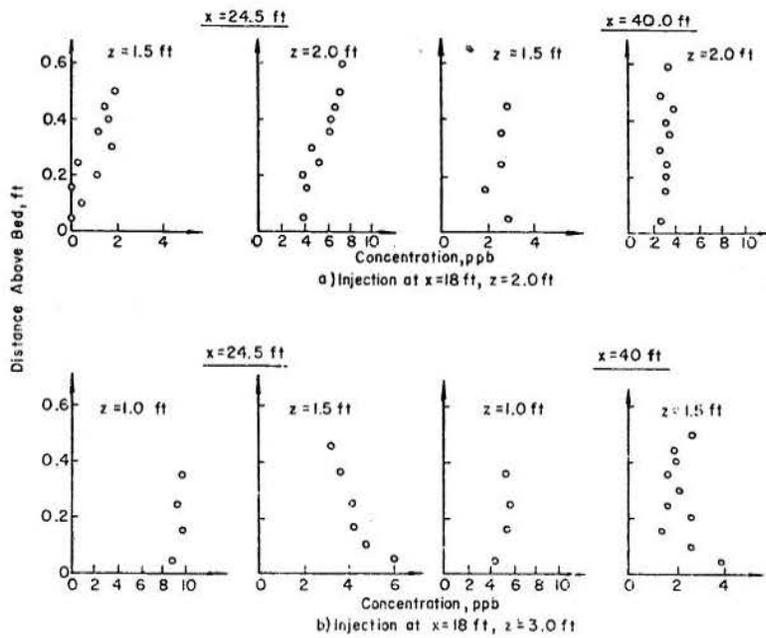
Fig. 4.8. Vertical concentration profiles, half-roughness flow

a) Tests A,B,C

b) Tests D,E,F,
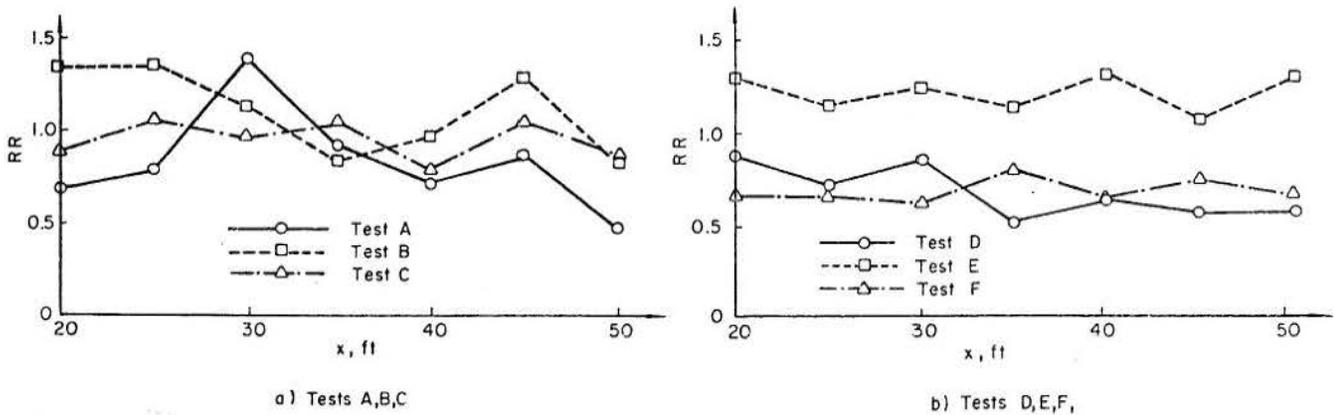
Fig. 4.9. Recovery ratios, tests A-F
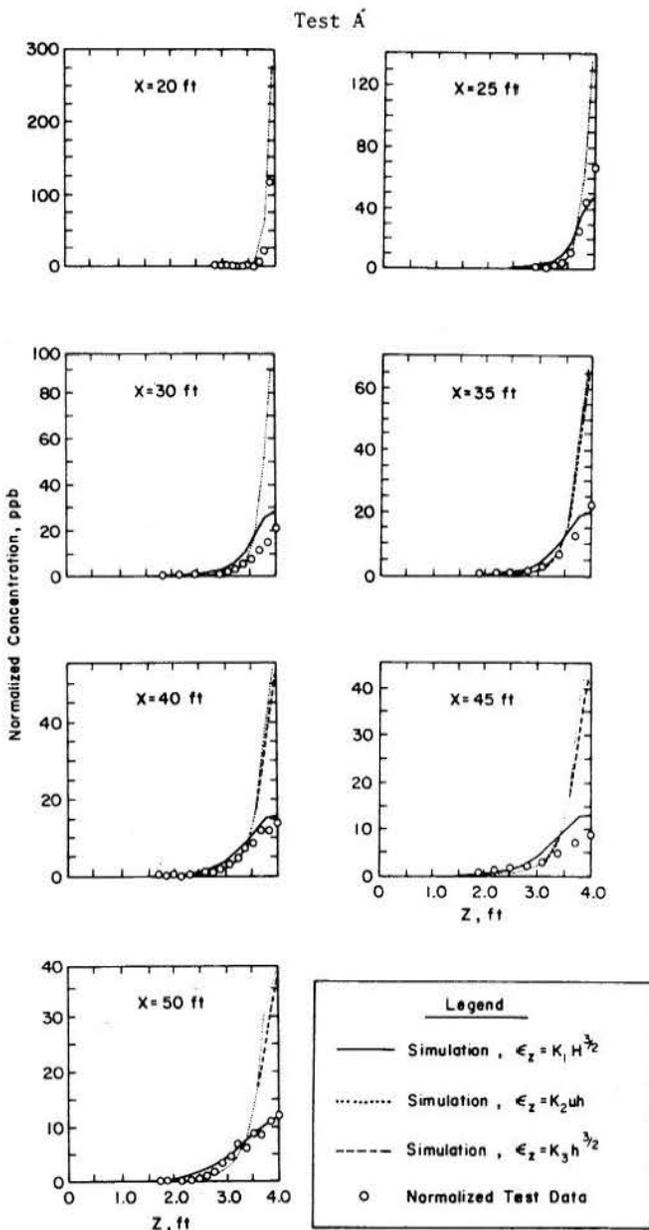
Test A

Fig. 4.10. Measured and computed concentration distributions, Test A
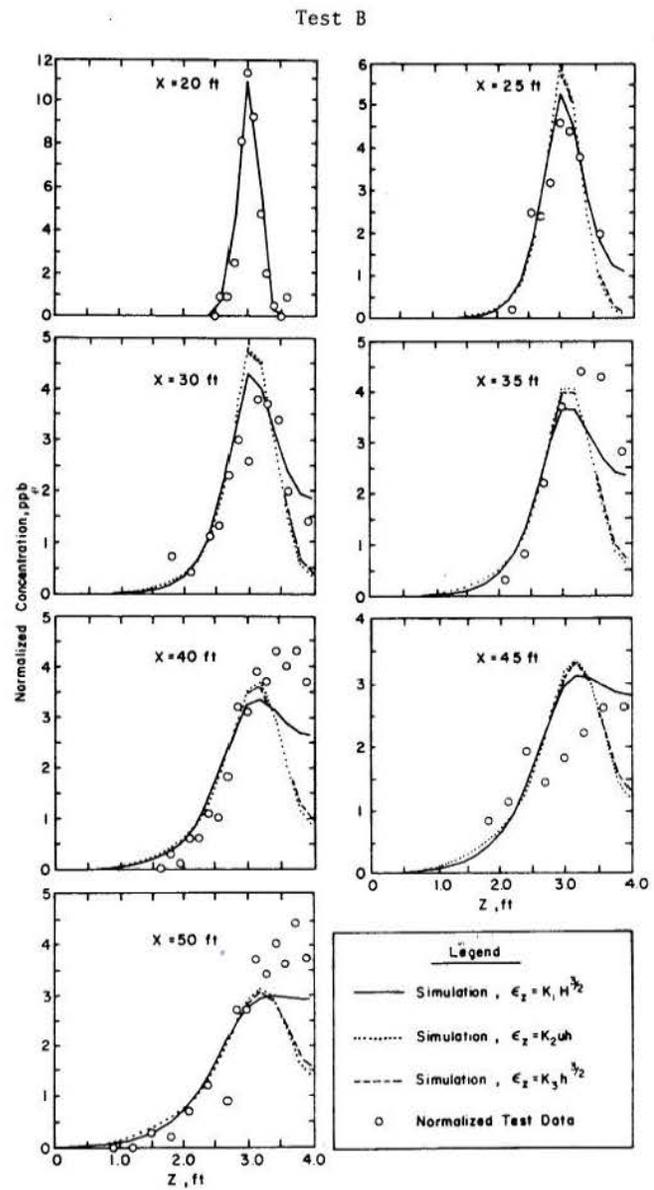
Test B

Fig. 4.11. Measured and computed concentration distributions, Test B

Test C   Test D
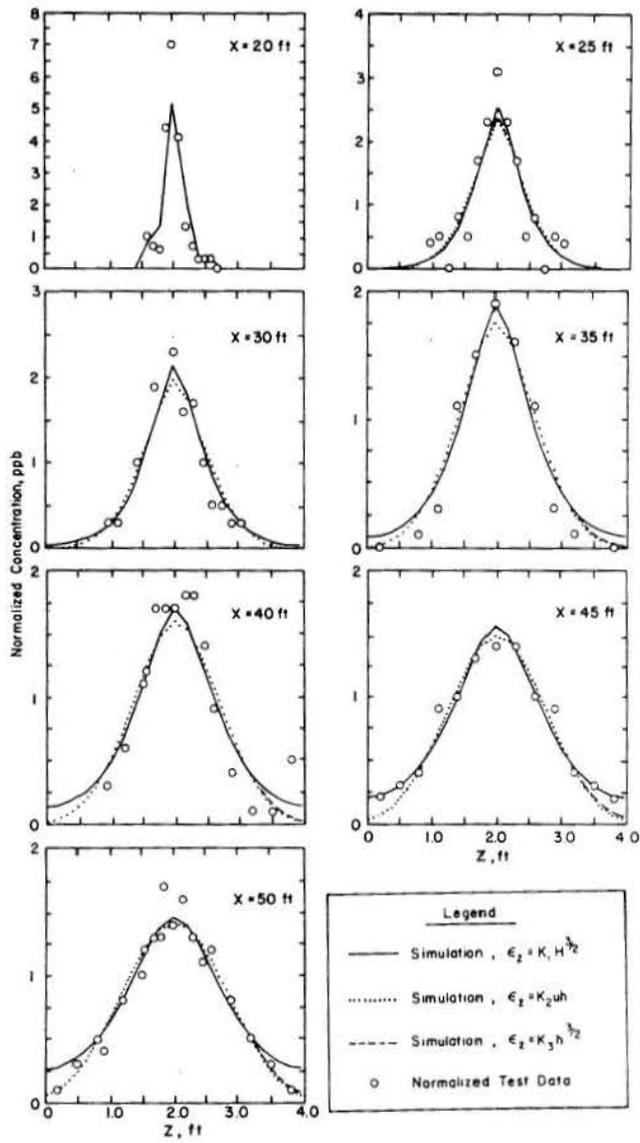
Fig. 4.12. Measured and computed concentration
distributions, Test C
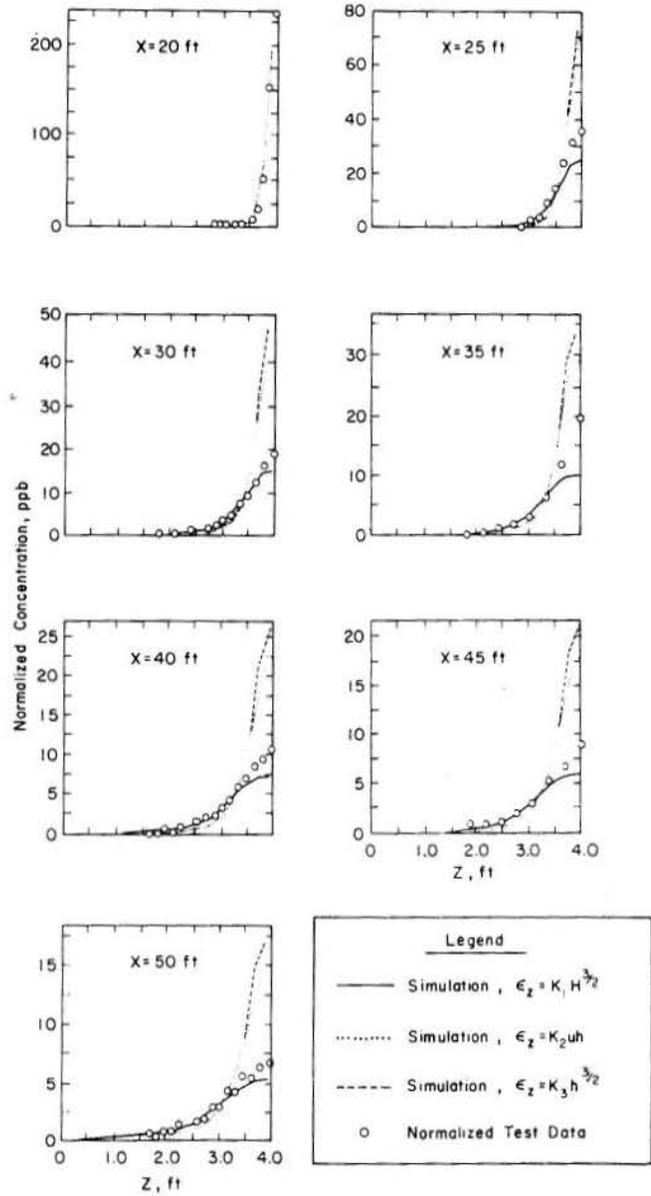
Fig. 4.13. Measured and computed concentration
distributions, Test D

48
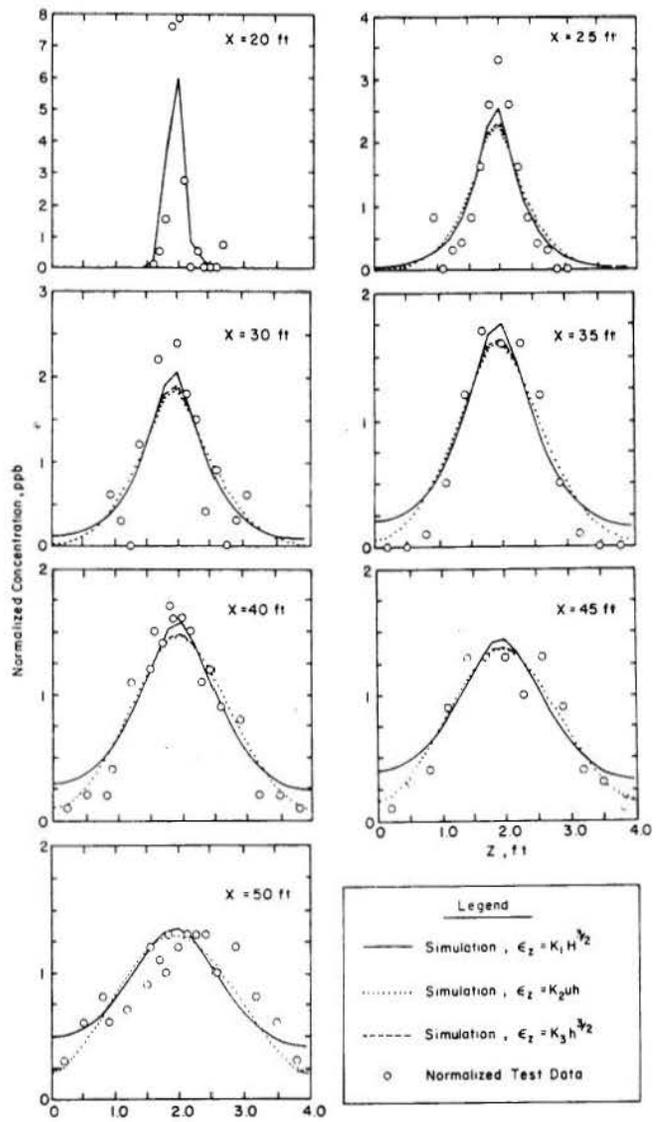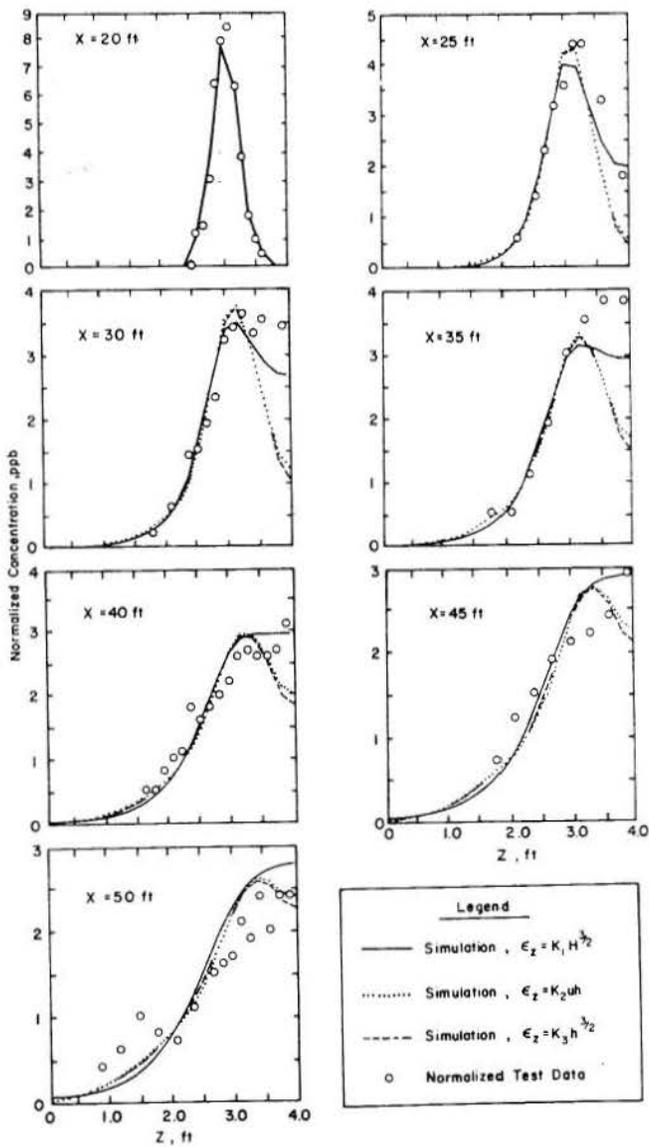
Test E

Test F

Fig. 4.14. Measured and computed concentration
distributions, Test E

Fig. 4.15. Measured and computed concentration
distributions, Test F
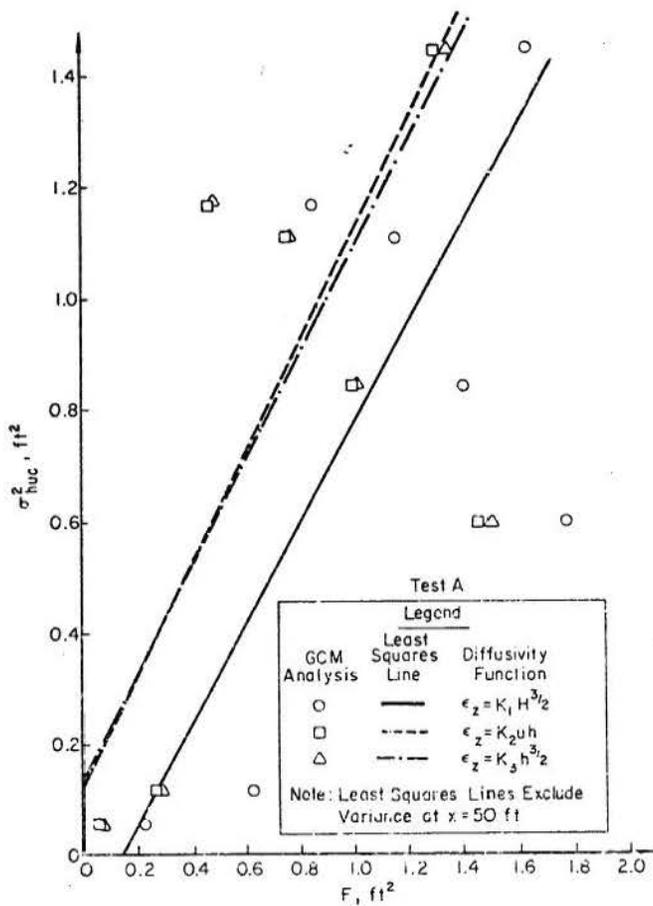
Fig. 4.16. Generalized Change of Moments analysis, Test A
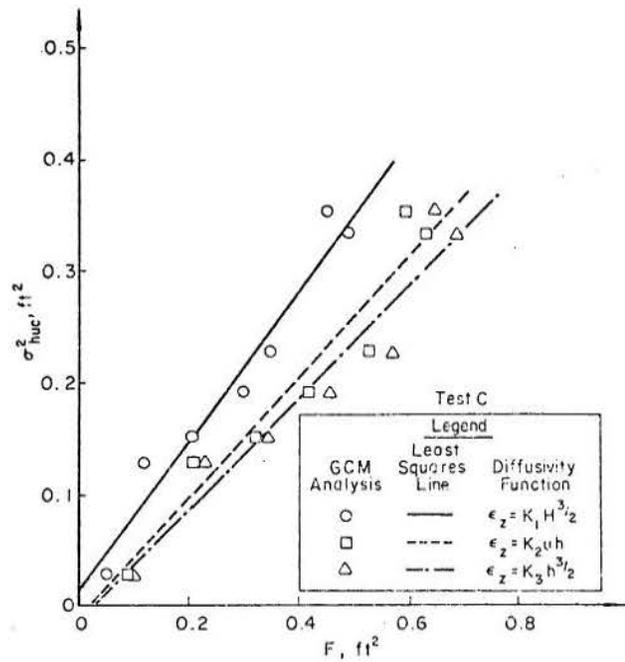
Fig. 4.18. Generalized Change of Moments analysis, Test C
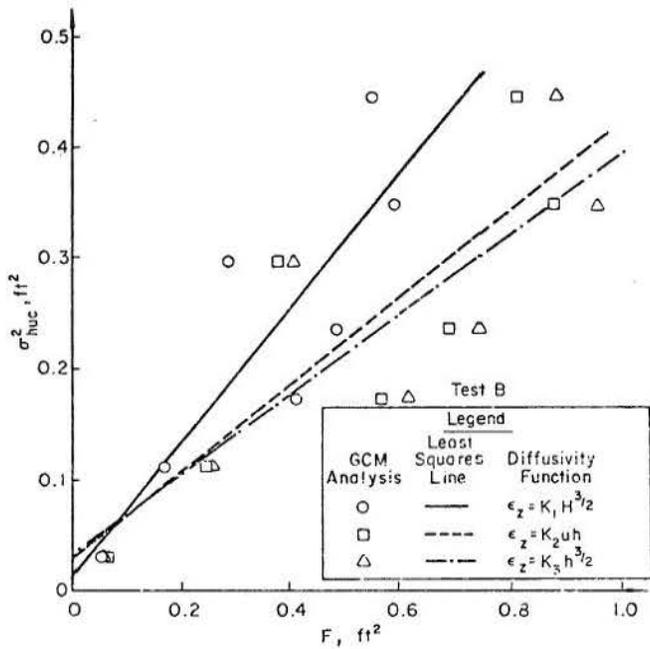
Fig. 4.17. Generalized Change of Moments analysis, Test B
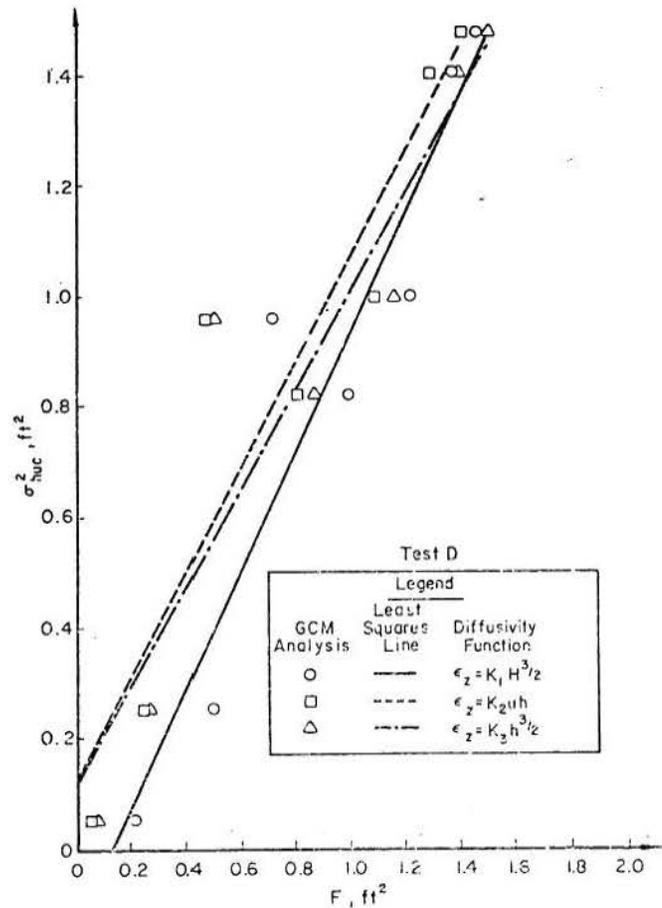
Fig. 4.19. Generalized Change of Moments analysis, Test D
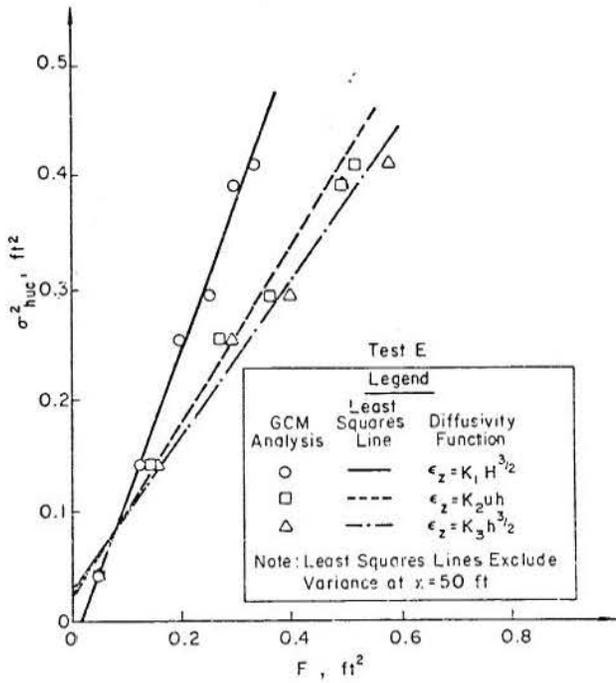
Fig. 4.20. Generalized Change of Moments analysis, Test E

Test E

Legend

GCM Analysis	Least Squares Line	Diffusivity Function
○	——	$\epsilon_z = K_1 H^{3/2}$
□	- - -	$\epsilon_z = K_2 uh$
△	—·—·	$\epsilon_z = K_3 h^{3/2}$

Note: Least Squares Lines Exclude Variance at $x = 50$ ft
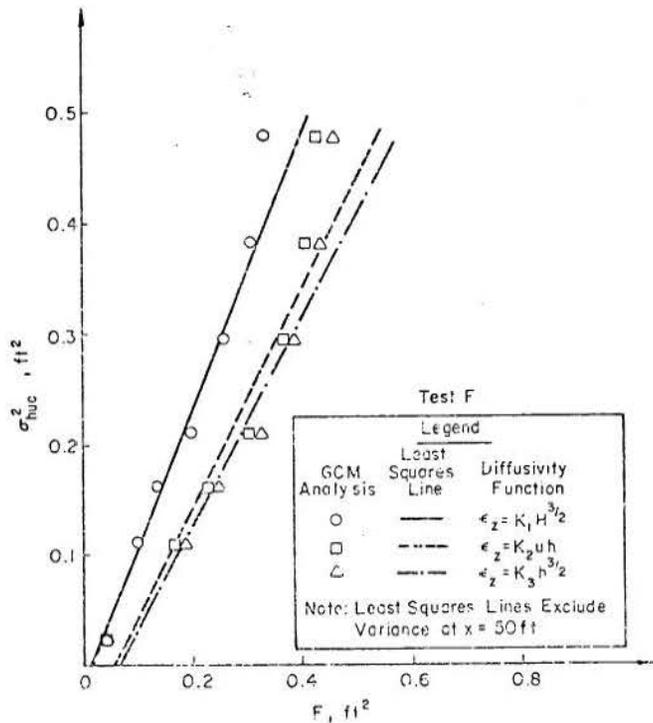
Fig. 4.21. Generalized Change of Moments analysis, Test F

Test F

Legend

GCM Analysis	Least Squares Line	Diffusivity Function
○	——	$\epsilon_z = K_1 H^{3/2}$
□	- - -	$\epsilon_z = K_2 uh$
△	—·—·	$\epsilon_z = K_3 h^{3/2}$

Note: Least Squares Lines Exclude Variance at $x = 50$ ft

Test D Modified

Legend

Simulation, $\epsilon_z = K_1 H^{3/2}$ ——
Simulation, $\epsilon_z = K_2 uh$ ········
Simulation, $\epsilon_z = K_3 h^{3/2}$ - - -
○ Normalized Test Data
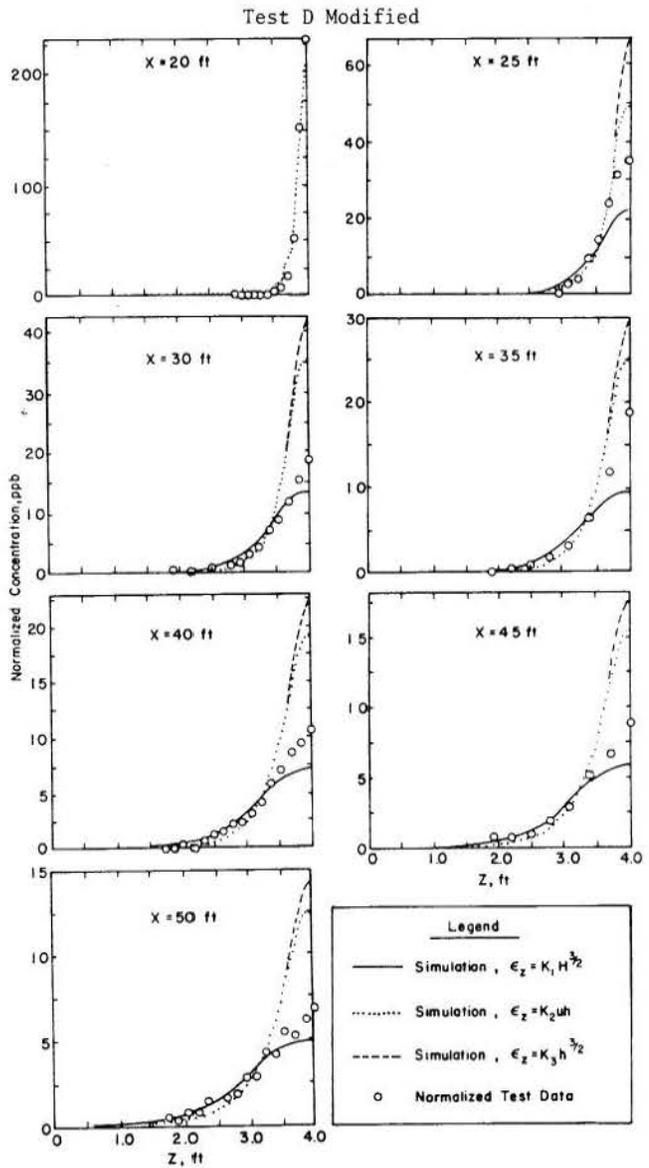
Fig. 4.22. Measured and computed concentration distributions, Test D modified
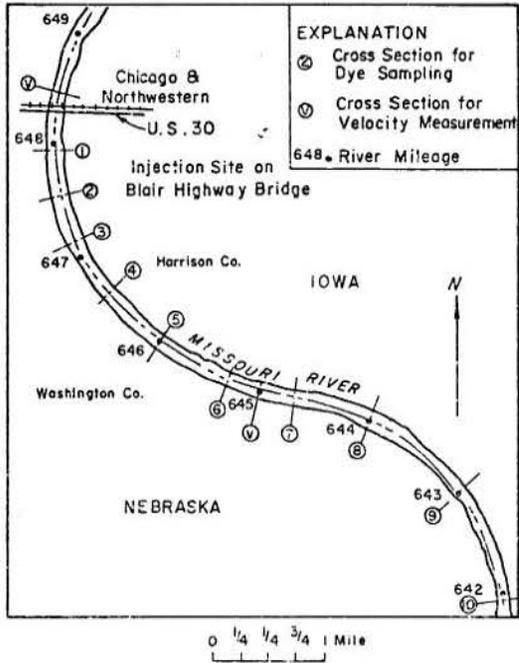
Fig. 5.1. Reach of the Missouri River for the transverse mixing test
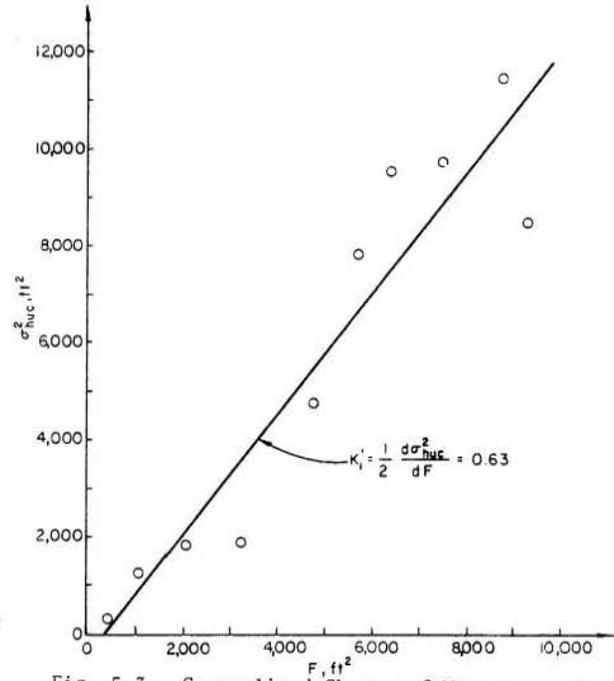
Fig. 5.3. Generalized Change of Moments analysis Missouri River

$$K_i' = \frac{1}{2} \frac{d\sigma_{huc}^2}{dF} = 0.63$$
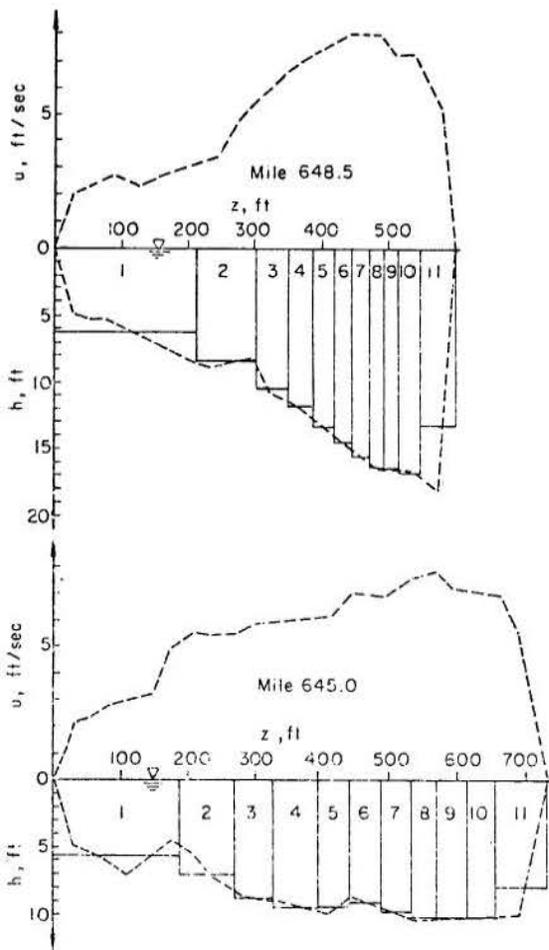
Fig. 5.2. Missouri River measured cross sections and stream tube configurations

Missouri River Simulation

Legend

Simulation, $\epsilon_z = 0.63\ U_* H$

○ Normalized Test Data
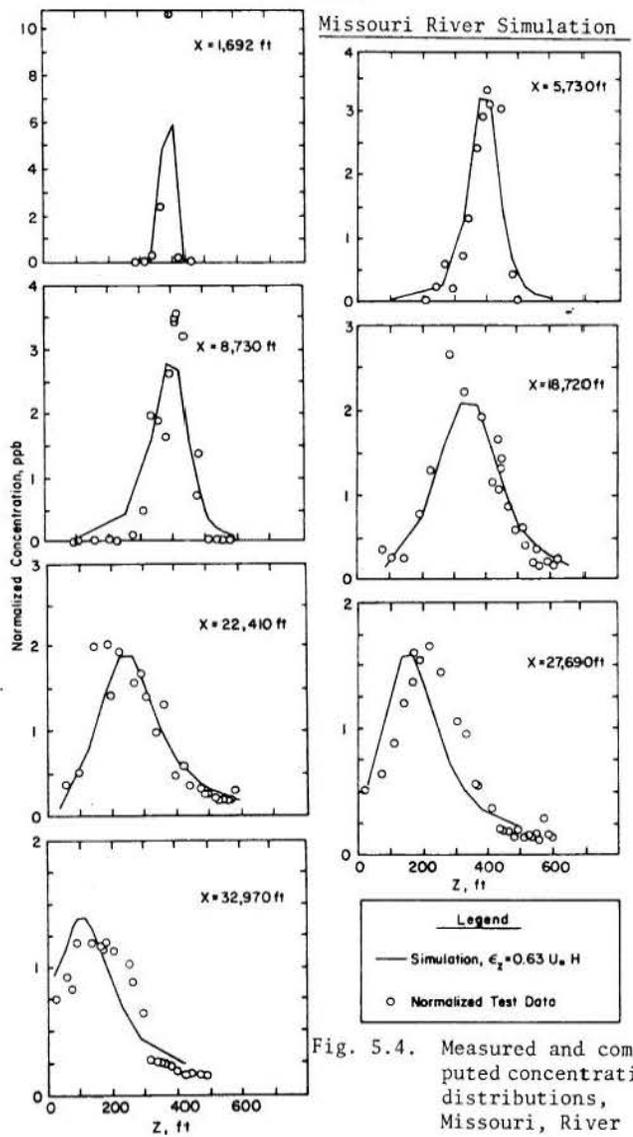
Fig. 5.4. Measured and computed concentration distributions, Missouri, River

52
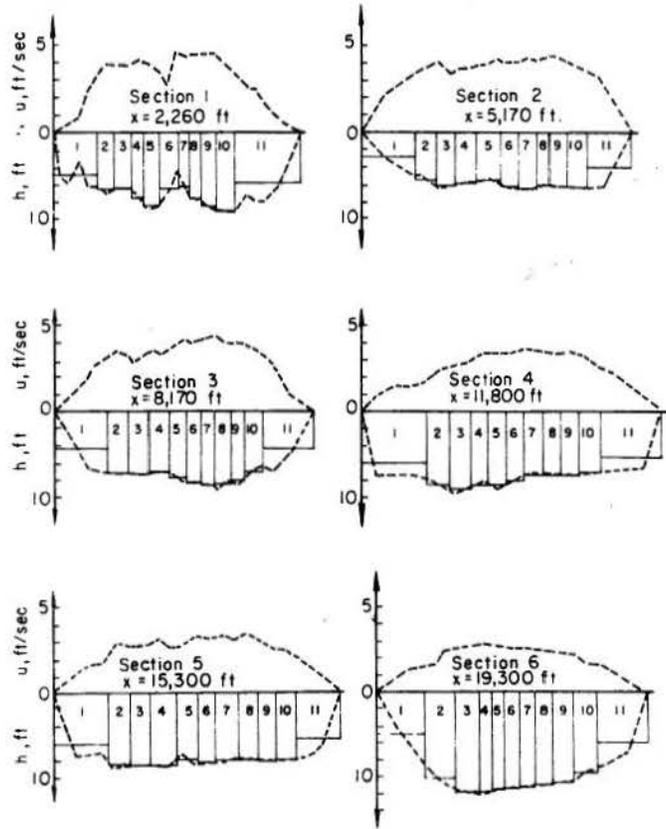
Fig. 6.1.   Clinch River measured cross sections
and stream tube configurations
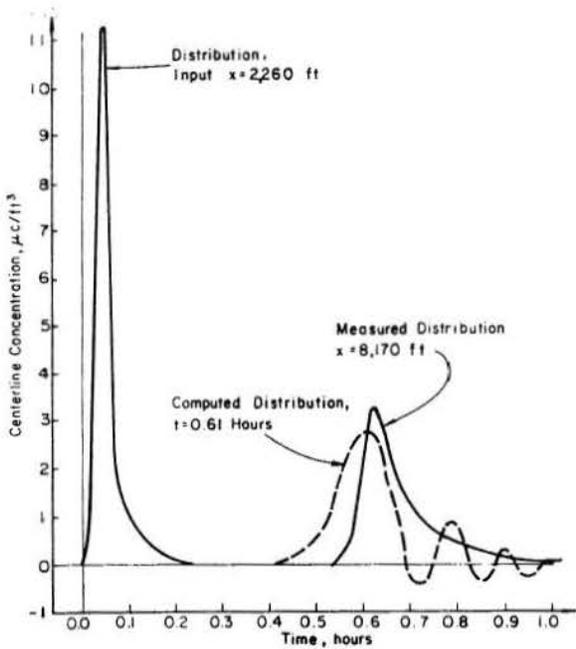
Fig. 6.2.   Measured and computed centerline
concentration distributions after
0.61 hours, Clinch River
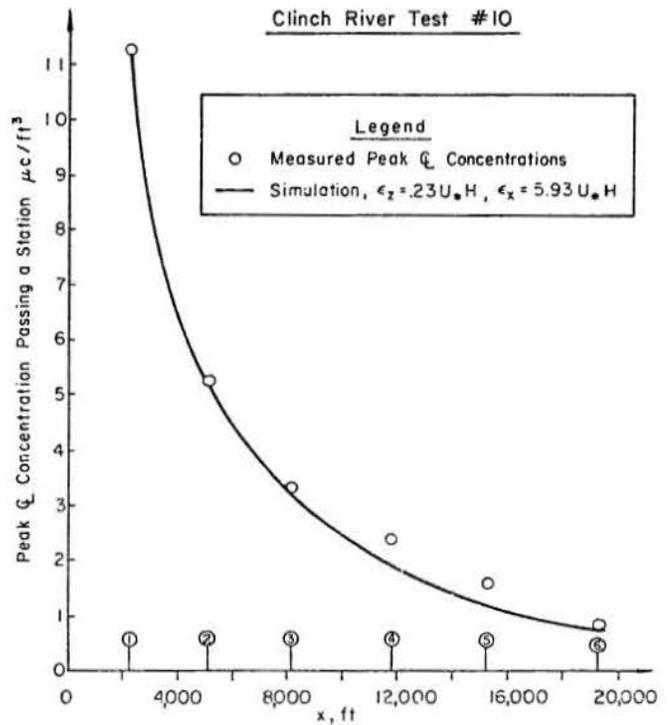
Fig. 6.3.   Longitudinal decay of peak
concentration, Clinch River
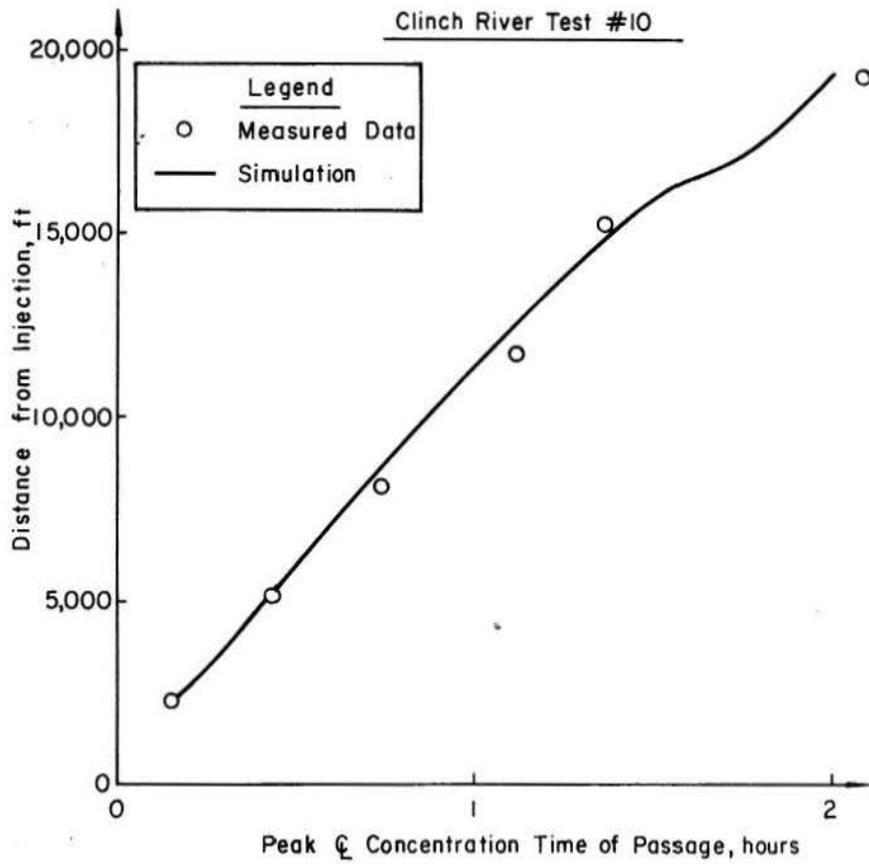
Fig. 6.4. Travel time of peak centerline concentration, Clinch River
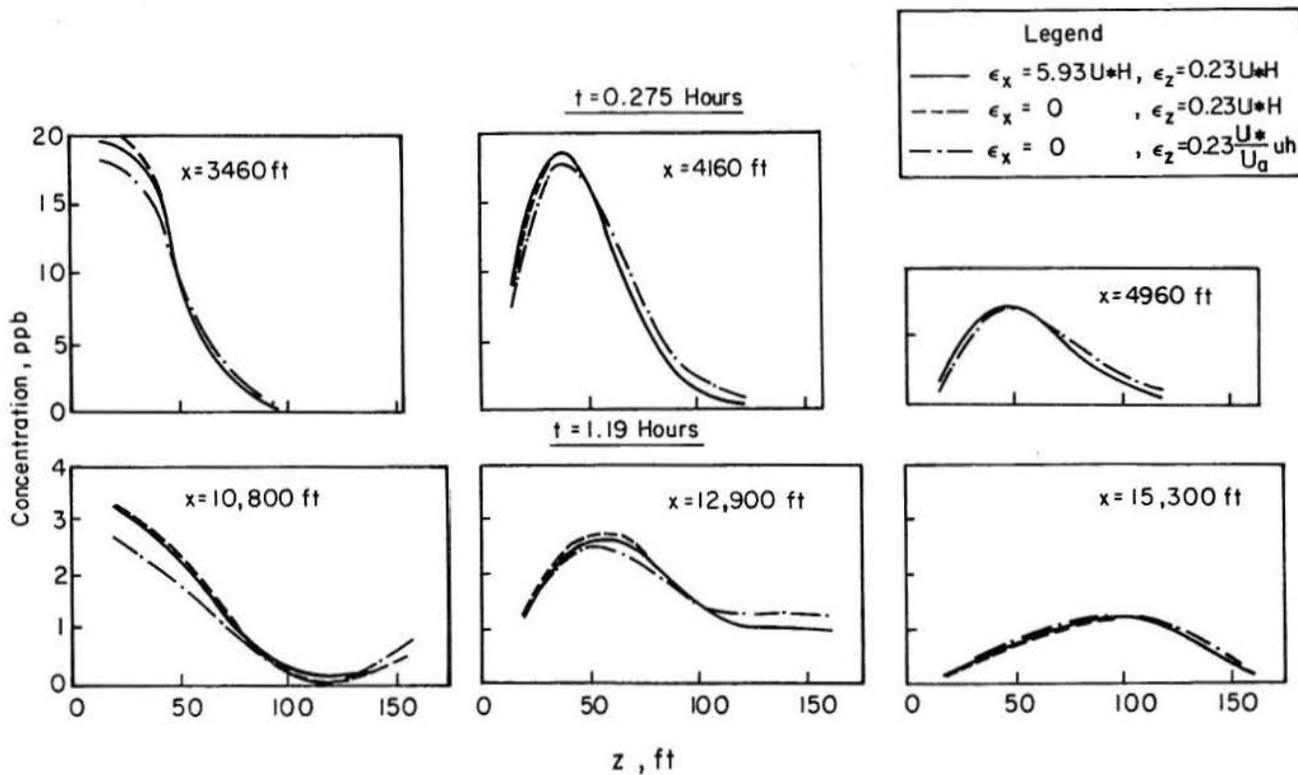
Fig. 6.5. Computed concentration distributions, Clinch River bank injection

APPENDIX C

ANALYSIS OF SEVEN ADDITIONAL FINITE DIFFERENCE
METHODS FOR THE COMPUTATION OF CONVECTION

The double-step implicit-explicit scheme described in Sect. 2.4 was chosen from eight schemes initially considered. In this Appendix the remaining schemes are presented, and their numerical characteristics are summarized without detailed derivation.

A. <u>Asymmetrical explicit scheme, first order</u>. This relatively simple scheme is used in Sect. 2.2 to demonstrate numerical diffusivity.
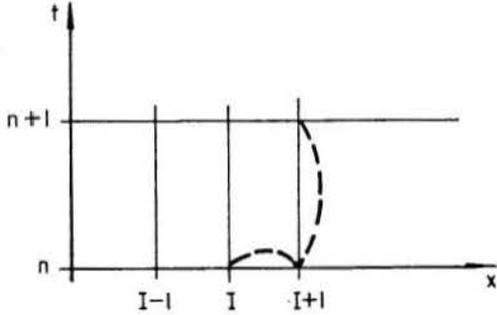
Fig. C.1. Scheme A Discretization

Figure C.1 shows the computational method, whereby Eq. 2.2 is written

$$\frac{C_{I+1}^{n+1} - C_{I+1}^{n}}{\Delta t} + \frac{u(C_{I+1}^{n} - C_{I}^{n})}{\Delta x} = 0. \qquad (C2)$$

For this scheme

$$R_1 = [1+2r(1-r)(\cos \sigma\Delta x-1)]^{1/2}$$

and

$$R_2 = \frac{\text{arctan}\left(\frac{r \sin \sigma\Delta x}{1-2r \sin^2 \frac{\sigma\Delta x}{2}}\right)}{u\sigma\Delta t}$$

The scheme is unstable for $r>1$, stable and non-diffusive for $r=1$, and introduces numerical diffusion for $r<1$. R_2 is equal to unity when $r=1$ and $\frac{L}{\Delta x} > 4$, but is generally less than unity for other values. The method is computationally attractive due to the possibility of a direct, single calculation for each concentration at each time step, but obviously suffers from numerical diffusion problems if $r<1$, as it must be at most locations in a natural channel.

B. <u>Asymmetrical implicit scheme, first order</u>.
Figure C.2 indicates
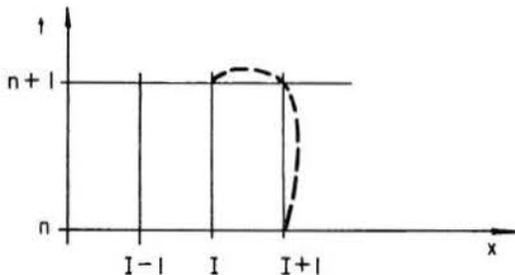
Fig. C.2. Scheme B Discretization

that this scheme is just an implicit version of Scheme A. Equation 2.2 is written

$$\frac{C_{I+1}^{n+1} - C_{I+1}^{n}}{\Delta t} + \frac{u(C_{I+1}^{n+1} - C_{I}^{n+1})}{\Delta x} = 0$$

and

$$R_1 = [1+2r(1+r)(1-\cos \sigma\Delta x)]^{-1/2}$$

$$R_2 = \frac{\text{arctan}\left[\frac{r \sin \sigma\Delta x}{1+r(1-\cos \sigma\Delta x)}\right]}{u\sigma\Delta t} \qquad (C3)$$

It may be noted that $R_1<1$, always, (unless $\Delta x=0$), so the scheme is unconditionally stable but diffusive. For all values of r and $\frac{L}{\Delta x}$, $R_2<1$, and numerical dispersion can be quite severe for $r>2$ and $\frac{L}{x} < 50$. Thus the method offers no major advantage in spite of the greater computational complexity demanded by the implicit discretization.

C. <u>Symmetrical implicit scheme, first order</u>. Some improvement over the first order implicit scheme can be gained by using a centered space
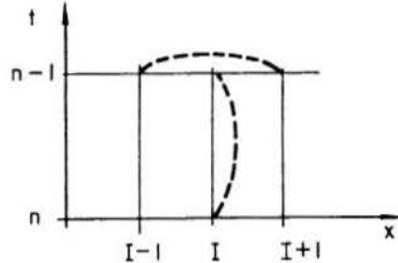
Fig. C.3. Scheme C Discretization

derivative as on Fig. C.3. Equation 2.2 is written

$$\frac{C_I^{n+1} - C_I^{n}}{\Delta t} + \frac{u(C_{I+1}^{n+1} - C_{I-1}^{n+1})}{2\Delta x} = 0$$

and

$$R_1 = (1+r^2 \sin^2 \sigma\Delta x)^{-1/2}$$

$$R_2 = \left[\frac{\text{arctan}(r \sin \sigma\Delta x)}{u\sigma\Delta t}\right]$$

Again the method is unconditionally stable but diffusive although R_1 tends to be closer to unity then for the asymmetrical method. The scheme is also dispersive, but R_2 tends to be closer to unity than for the asymmetrical method.

D. <u>Symmetrical explicit "leap frog" method, second order</u>. By stepping the time derivative backwards the centered explicit method can be made

55
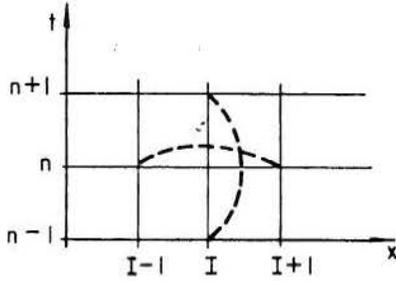
Fig. C.4. Scheme D Discretization

almost nondamping. As shown in Fig. C.4, Eq. 2.2 can be written

$$\frac{C_I^{n+1} - C_I^{n+1}}{2\Delta t} + \frac{u(C_{I+1}^n - C_{I-1}^n)}{2\Delta x} = 0$$

where for $r \leq 1$, $R_1 = 1$,

for $r > 1$, $R_1 = -r \sin \sigma \Delta x \pm (r^2 \sin^2 \sigma \Delta x - 1)^{1/2}$

and for $r \leq 1$, $R_2 = \dfrac{\arctan \dfrac{r \sin \sigma \Delta x}{\pm (1 - r^2 \sin^2 \sigma \Delta x)^{1/2}}}{u \sigma \Delta t}$.

Thus for $r > 1$ the method is unstable. But for $r \leq 1$ it is stable and nondamping; moreover, for $r \leq 1$, R_2 approaches unity rapidly as $\frac{L}{\Delta x}$ increases.

E. **Symmetrical explicit "leap frog" method, fourth order.** Fourth order accuracy can be added to the explicit leap frog method by extending the space derivatives. As suggested in Fig. C.5, Eq. 2.2 is written

$$\frac{C_I^{n+1} - C_I^{n-1}}{2\Delta t} + u\left[\frac{4}{3}\frac{(C_{I+1}^n - C_{I-1}^n)}{2\Delta x} - \frac{1}{3}\frac{(C_{I+2}^n - C_{I-2}^n)}{4\Delta x}\right] = 0.$$
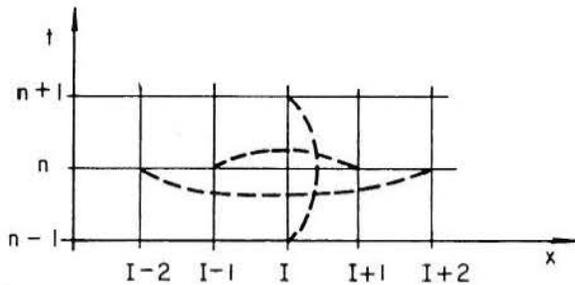
Fig. C.5. Scheme E Discretization

It turns out that

$$R_1 = 1 \quad \text{for} \quad r < 1, \text{ and}$$

$$R_2 > 1 \quad \text{for} \quad r \geq 1.$$

Also, for $r < 1$,

$$R_2 = \frac{\arctan\left[\dfrac{\dfrac{r}{3}(8 \sin \sigma \Delta x - \sin 2\sigma \Delta x)}{\pm 4 - \dfrac{r^2}{9}(8 \sin \sigma \Delta x - \sin 2\sigma \Delta x)^2{}^{1/2}}\right]}{u \sigma \Delta t}.$$

The method is stable and nondamping for $r < 1$, but R_2 can reach nearly 1.4 before converging back toward 1.0 as $\frac{L}{\Delta x}$ increases.

F. **Double-step implicit-explicit scheme, fourth order.** An extension of the space derivatives gives fourth order accuracy to the method first described in Sect. 2.4. As shown on Fig. C.6, Eq. 2.2 is written in two parts as

$$\frac{C_I^{n+1} - C_I^n}{\Delta t} + u\left[\frac{4}{3}\frac{(C_{I+1}^{n+\frac{1}{2}} - C_{I-1}^{n+\frac{1}{2}})}{2\Delta x} - \frac{1}{3}\frac{(C_{I+2}^{n+\frac{1}{2}} - C_{I-2}^{n+\frac{1}{2}})}{4\Delta x}\right] = 0$$

followed by

$$\frac{C_I^{n+1} - C_I^{n+\frac{1}{2}}}{\Delta t/2} + u\left[\frac{4}{3}\frac{(C_{I+1}^{n+\frac{1}{2}} - C_{I-1}^{n+\frac{1}{2}})}{2\Delta x} - \frac{1}{3}\frac{(C_{I+2}^{n+\frac{1}{2}} - C_{I-2}^{n+\frac{1}{2}})}{4\Delta x}\right] = 0.$$
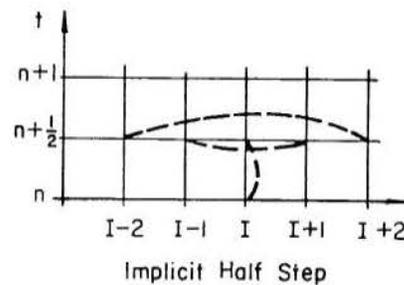
Implicit Half Step
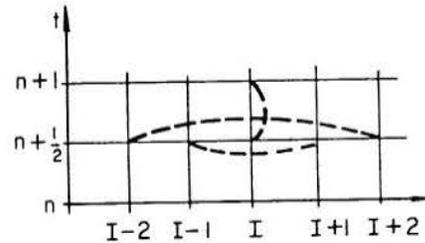
Explicit Half Step

Fig. C.6. Scheme F Discretization

A derivation similar to that of Sect. 2.4 shows that

$$R_1 = 1$$

and

$$R_2 = \frac{2 \arctan\left[\dfrac{r}{12}(8 \sin \sigma \Delta x - \sin 2 \sigma \Delta x)\right]}{\sigma u \Delta t}.$$

As is the case with its second-order counterpart, this method is unconditionally stable and nondamping. However the additional fourth-order complexity results in only a slight improvement in the numerical dispersion characteristics as displayed by R_2.

G. **Double-step predictor-corrector scheme.** A minor variation of the second-step time derivative in the double-step implicit-explicit scheme of Sect. 2.4 can reduce the numerical dispersion. With reference to Fig. C.7., the first half-step is applied to Eq. 2.2 to yield

$$\frac{C_I^{n+\frac{1}{2}} - C_I^n}{\Delta t/2} + u\frac{(C_{I+1}^{n+\frac{1}{2}} - C_{I-1}^{n+\frac{1}{2}})}{2\Delta x} = 0$$

56
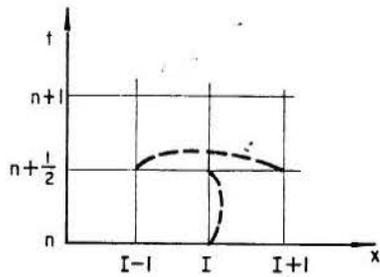
First Half Step
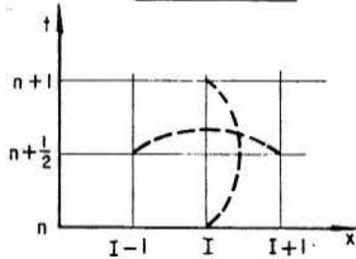
Second Half Step

Fig. C.7. Scheme G Discretization

and for the second step

$$\frac{C_I^{n+1} - C_I^{n}}{\Delta t} + u \frac{(C_{I+1}^{n+\frac{1}{2}} - C_{I-1}^{n+\frac{1}{2}})}{2\Delta x} = 0$$

The coefficients R_1 and R_2 must be computed for two conditions.

For $\quad r \sin \sigma \Delta x \leq 2$,

$$R_1 = \left(1 + \frac{r^2}{4} \sin^2 \sigma x \right)^{-1/2}$$

and

$$R_2 = \frac{\arctan \left(\frac{r}{2} \sin \sigma \Delta x\right) \pm \arctan \left[-r \sin \sigma \Delta x (4 - r^2 \sin^2 \sigma \Delta x)^{-1/2}\right]}{u \sigma \Delta t}.$$

For $\quad r \sin \sigma \Delta x > 2$,

$$R_1 = \frac{r \sin \sigma \Delta x \pm (r^2 \sin^2 \sigma \Delta x - 4)^{1/2}}{(2 + r^2 \sin^2 \sigma \Delta x)^{1/2}}$$

and

$$R_2 = \frac{\arctan \left(\frac{r}{2} \sin \sigma \Delta x\right) + \pi/2}{u \sigma \Delta t}$$

Here R_1 is less than unity always, so the method is unconditionally stable but also damping, compared to the nondamping characteristics of the parent scheme, Sect. 2.4. Thus the slight improvement in numerical dispersion characteristics is obtained at the expense of numerical damping.

APPENDIX D
DESCRIPTION OF DISPERSION MODEL COMPUTER PROGRAM

The dispersion model as described in Chapter 2 and Appendix E is programmed in Fortran IV, and as presented here is written for the CDC 6400 computer. The program consists of the following major elements:

SUBROUTINE GEOMIN - Reads stream tube data from permanent file.

SUBROUTINE DATAIN - Reads time history of source injection at upstream end of each tube; supplies appropriate injection concentration for each tube at any time during the simulation.

SUBROUTINE UANDDI - Computes longitudinal and transverse diffusivities for all stream tubes at all computational points.

SUBROUTINE CONCEN - Executes the dispersion simulation; revises time step, requests output.

SUBROUTINE CONVECM - Solves Eq. 2.38 for one time step using the second order implicit-explicit double step scheme.

SUBROUTINE DIFFUS - Solves Eq. 2.48 for one time step using the centered fully implicit scheme.

SUBROUTINE LODIFF - Solves Eq. 2.55 for one time step using the centered fully implicit scheme.

SUBROUTINES LABEL, EDIT, EDIT 3 - Print out complete concentration fields and stream tube data.

Included in this Appendix is a complete listing of the program and a generalized flow chart. The following list of important variables is by no means complete, but includes all input and most output variables:

Variable	Description
ALFA (real)	Dimensionless K'-coefficients, Eq. 3.12.
B (real)	Width of stream tube.
BWØUT (integer)	Number of computational points for which complete printout of stream tube specifications is desired.
C (real)	Concentration.
CINIT (logical)	If true, concentrations set equal to zero initially; if false, initial concentration field read in.
DTH (real)	Beginning simulation time step, in hours.
EPSLØC (integer)	Specifies the transverse diffusivity function to be used, keyed to K'-subscripts, Eq. 3.12.
G (real)	Gravitational acceleration.
IN (integer)	General subscript in columnwise variable array.

Variable	Description
INDEX (integer)	Number of iteration cycles between outputs of concentration field; if zero, output will be generated only at end of simulation.
LALFA (real)	Dimensionless longitudinal diffusivity coefficient.
LONGD (logical)	If true, longitudinal diffusion is computed.
NBPTS (integer)	Number of longitudinal computational points.
NCIN (integer)	Number of concentration-time pairs input for upstream end of each stream tube.
NCYCL (integer)	Number of simulation iteration cycle.
NDT (integer)	Number of times at which time step is changed; if zero, time step is constant.
NTUBE (integer)	Number of stream tubes.
Q (real)	Total stream discharge.
RDATA (logical)	If true, stream tube velocities and depths are read in, not computed.
STR (real)	If RDATA=true, velocity of stream tube; if RDATA=false, Strickler coefficient of stream tube.
T (real)	In DISPERS, the array in which all variables are stored columnwise; in subroutine DATAIN, the times (in decimal hours) at which input concentrations are specified.
TEND (real)	Decimal time, in hours, at which simulation ends.
TIME (real)	Decimal time, in hours at which simulation begins.
TITLE (alphanumeric)	User-specified title of run.
ZBOT (real)	If RDATA=true, depth of stream tube; if RDATA=false, bed elevation of stream tube.

The use of program DISPERS first requires that a permanent file be established on disk or tape storage containing stream tube data for the river being studied. These data, which are read by subroutine GEOMIN, are prepared by the user based on known data and the procedures described in Appendix E.

As presented here, the program is dimensioned and formatted for a maximum of 22 stream tubes. The restriction can be removed by revising subroutine EDIT to print out additional sets of 11 tubes each.

PROGRAM DISPERS

```
        ┌─────────┐
        │  Start  │
        └────┬────┘
             │
      ┌──────┴──────┐
      │    Read     │
      │  TITLE and  │
      │  control    │
      │    data     │
      └──────┬──────┘
             │
      ┌──────┴──────┐
      │  Compute    │
      │ locations of│
      │ variables in│
      │      T      │
      └──────┬──────┘
             │
      ┌──────┴──────┐
      │    Read     │
      │  time step  │
      │  revisions  │
      └──────┬──────┘
             │
      ┌──────┴──────┐
      │    Write    │
      │    TITLE    │
      └──────┬──────┘
             │
      ┌──────┴──────┐       ┌──────────────┐
      │    Call     │-------│    Loads     │
      │   GEOMIN    │       │ Stream tube  │
      └──────┬──────┘       │    data      │
             │              └──────────────┘
      ┌──────┴──────┐
      │    Write    │
      │   control   │
      │    data     │
      └──────┬──────┘
             │
      ╱──────┴──────╲
     ╱  Initialize   ╲
     ╲ concentration ╱
      ╲    field    ╱
       ╲────┬──────╱
             │
      ┌──────┴──────┐       ┌──────────────┐
      │    Call     │-------│    loads     │
      │   DATAIN    │       │    input     │
      └──────┬──────┘       │concentrations│
             │              └──────────────┘
           ( A )
             │
      ┌──────┴──────┐       ┌──────────────┐
      │    Call     │-------│   Computes   │
      │   UANDDI    │       │diffusivities │
      └──────┬──────┘       └──────────────┘
             │
      ┌──────┴──────┐       ┌──────────────┐
      │    Call     │-------│   Executes   │
      │   CONCEN    │       │  dispersion  │
      └──────┬──────┘       │  simulation  │
             │              └──────────────┘
        ┌────┴────┐
        │  Stop   │
        └─────────┘
```

SUBROUTINE GEOMIN

```
        ┌─────────┐
        │  Start  │
        └────┬────┘
             │
      ┌──────┴──────┐
      │ Read stream │
      │  tube data  │
      │  from disk  │
      │   storage   │
      └──────┬──────┘
             │
        ┌────┴────┐
        │  Stop   │
        └─────────┘
```

SUBROUTINE DATAIN

```
        ┌─────────┐
        │  Start  │
        └────┬────┘
             │
         ╱───┴───╲         ┌──────────┐
        ╱   If    ╲  yes   │   Read   │
       ╱ first iter-╲──────│ T,C pairs│
       ╲   ation   ╱       │ for each │
        ╲─────┬───╱        │stream tube│
          no  │            └────┬─────┘
             │                  │
            (  )───────────────┘
             │
      ┌──────┴──────┐
      │   Locate    │
      │  T,C pairs  │
      │ which bracket│
      │simulation time│
      └──────┬──────┘
             │
      ┌──────┴──────┐
      │ Interpolate │
      │  to obtain  │
      │input concentration,│
      │  each tube  │
      └──────┬──────┘
             │
        ┌────┴────┐
        │  Stop   │
        └─────────┘
```

SUBROUTINE CONCEN

```
        ┌─────────┐
        │  Start  │
        └────┬────┘
             │
           ( A )
             │
      ┌──────┴──────┐
      │  Increment  │
      │    time     │
      └──────┬──────┘
             │
      ┌──────┴──────┐       ┌──────────────┐
      │    Call     │-------│ Loads input  │
      │   DATAIN    │       │concentrations,│
      └──────┬──────┘       │  each tube   │
             │              └──────────────┘
      ┌──────┴──────┐       ┌──────────────┐
      │    Call     │-------│   Computes   │
      │   CONVECM   │       │  convection  │
      └──────┬──────┘       └──────────────┘
             │
      ┌──────┴──────┐       ┌──────────────┐
      │    Call     │-------│   Computes   │
      │   DIFFUS    │       │  transverse  │
      └──────┬──────┘       │  diffusion   │
             │              └──────────────┘
      ┌──────┴──────┐       ┌──────────────┐
      │    Call     │-------│   Computes   │
      │   LODIFF    │       │ longitudinal │
      │(if LONGD=T) │       │  diffusion   │
      └──────┬──────┘       └──────────────┘
             │
      ┌──────┴──────┐
      │    Write    │
      │concentration│
      │    field    │
      └──────┬──────┘
             │
         ╱───┴───╲         ┌──────────────┐
        ╱   If    ╲  no    │ Revise time  │
       ╱ TIME >TEND╲───────│  step when   │
       ╲           ╱       │ appropriate  │
        ╲─────┬───╱        └──────┬───────┘
         yes  │                   │
             │                  ( A )
        ┌────┴────┐
        │ Return  │
        └─────────┘
```

SUBROUTINE UANDDI

Start

Compute Q, A, B, U_a, U_* for each section

Compute $\varepsilon_x, \varepsilon_z$ for each tube, each section

- - - Diffusivity function specified by EPSLOC

Compute $(h\varepsilon_z)_{I;J,J-1}$ etc.

Write complete stream tube data

Stop

SUBROUTINE CONVECM

Start

Generate downstream boundary condition

If first iteration — yes → Compute and store all R,S values

no

Compute and store all E,F values

Compute concentrations by recurrence

⎱ Implicit half step for each stream tube

Generate downstream boundary condition

Compute concentrations directly

Return

⎱ Explicit half step for each stream tube

SUBROUTINE DIFFUS

Start

Compute D1,D2,D3, D2*,D2** values

Compute E,F values

Compute concentrations by recurrence

Return

SUBROUTINE LODIFF

Start

Compute G1,G2,G3 values

Compute E,F values

Compute concentrations by recurrence

Return

TWO-DIMENSIONAL MASS DISPERSION COMPUTER PROGRAM

```
      PROGRAM DISPERS (INPUT,OUTPUT,TAPE5=INPUT,TAPE6=OUTPUT,TAPE3)      DIS 10
C                                                                       DIS 20
C***************NUMERICAL MODEL OF TWO DIMENSIONAL MASS DISPERSION IN RIVDIS 30
C                                                                       DIS 40
      DIMENSION T(17500), INN(15), TITLE(20)                            DIS 50
      COMMON NRPTS,NTUBE,NCYCL,ZDOWNS,G,Q,TIME,TEND,DT,DTH,EPSLOC,ITMP,IDDIS 60
     1Z,IX,IF,IB,ISTR,IZB,IALF,IU,IDIF,ICON1,ICON2,ICON,ID,IE,ILDIFF,IETDIS 70
     2,IFT,INTCH,ICUPS1,ICUPS2,ISLOP,T                                  DIS 80
      EXTERNAL CONVECM                                                  DIS 90
      EQUIVALENCE (INN(1),IZ)                                           DIS 100
      LOGICAL CINIT,LONGD,RDATA                                         DIS 110
      INTEGER EPSLOC,BWOUT                                              DIS 120
      REAL LALFA                                                        DIS 130
C                                                                       DIS 140
C***************VARIABLE MEMORY MUST BE INITIALIZED WITHIN PROGRAM.      DIS 150
C***************GREATER THAN (NBPTS-1)(4+13*NTUBE)+4*NTUBE. VARIABLE T   DIS 160
C***************MUST BE DIMENSIONED T(MEMORY)                           DIS 170
C                                                                       DIS 180
      MEMORY=17500                                                      DIS 190
      NCYCL=0                                                           DIS 200
C                                                                       DIS 210
C***************READ TITLE AND CONTROL DATA                             DIS 220
C                                                                       DIS 230
      READ (5,250) (TITLE(I),I=1,20)                                    DIS 240
      READ (5,260) NBPTS,NTUBE,INDEX,NDT,TIME,TEND,DTH,LALFA,ZO,G,ALFA,CDIS 250
     1INIT,BWOUT,LONGD,RDATA,EPSLOC                                     DIS 260
      DT=DTH*3600.                                                      DIS 270
C                                                                       DIS 280
C***************COMPUTE LOCATIONS OF VARIABLES IN TABLE T               DIS 290
C                                                                       DIS 300
      N=(NRPTS-1)*NTUBE                                                 DIS 310
      IZ=0                                                              DIS 320
      DO 110 J=2,3                                                      DIS 330
  110 INN(J)=INN(J-1)+NRPTS+1                                           DIS 340
      DO 120 J=4,15                                                     DIS 350
  120 INN(J)=INN(J-1)+N                                                 DIS 360
      IET=ILDIFF+N                                                      DIS 370
      IFT=IET+NTUBE                                                     DIS 380
      INTCH=IFT+NTUBE                                                   DIS 390
      NDT=NDT+NDT                                                       DIS 400
      ICUPS1=INTCH+NDT                                                  DIS 410
      IN=INTCH+1                                                        DIS 420
C                                                                       DIS 430
C***************READ TIME STEP REVISIONS                                DIS 440
C                                                                       DIS 450
      IF (NDT.EQ.0) GO TO 130                                           DIS 460
      READ (5,270) (T(J),J=IN,ICUPS1)                                   DIS 470
      ITMP=1                                                            DIS 480
  130 ICUPS2=ICUPS1+NTUBE                                               DIS 490
      ISLOP=ICUPS2+NTUBE                                                DIS 500
C                                                                       DIS 510
C***************CHECK TOTAL COMMON BLOCK LENGTH                         DIS 520
C                                                                       DIS 530
      IF ((ISLOP+NRPTS).LT.MEMORY) GO TO 140                            DIS 540
      LIMIT=ISLOP+NBPTS                                                 DIS 550
      WRITE (6,280) LIMIT                                               DIS 560
      GO TO 240                                                         DIS 570
  140 CONTINUE                                                          DIS 580
C                                                                       DIS 590
C***************LOAD STREAM TUBE DATA                                   DIS 600
C                                                                       DIS 610
      CALL GEOMIN (T(IB+1),T(IZB+1),T(ISTR+1),T(IALF+1),T(IX+1),T(IZ+1),DIS 620
     1T(IF+1),T(ISLOP+1))                                               DIS 630
      IBEG=IALF+1                                                       DIS 640
      IEND=IBEG+N-1                                                     DIS 650
      DO 150 I=IBEG,IEND                                                DIS 660
  150 T(I)=ALFA                                                         DIS 670
C                                                                       DIS 680
C***************WRITE TITLE AND CONTROL DATA                            DIS 690
C                                                                       DIS 700
      WRITE (6,290) (TITLE(I),I=1,20)                                   DIS 710
      WRITE (6,350) NBPTS,NTUBE,DTH,INDEX,G,Q,ZDOWNS,T(IX+NBPTS),CINIT,LDIS 720
     1ONGD,T(IALF+1),LALFA                                              DIS 730
      GO TO (160,170,180,190), EPSLOC                                   DIS 740
  160 WRITE (6,300)                                                     DIS 750
      GO TO 200                                                         DIS 760
  170 WRITE (6,310)                                                     DIS 770
      GO TO 200                                                         DIS 780
  180 WRITE (6,320)                                                     DIS 790
      GO TO 200                                                         DIS 800
  190 WRITE (6,330)                                                     DIS 810
  200 NDTOUT=NDT/2                                                      DIS 820
      WRITE (6,340) NDTOUT,(T(J),J=IN,ICUPS1)                           DIS 830
      IN=ICON+1                                                         DIS 840
C                                                                       DIS 850
C***************INITIALIZE CONCENTRATION FIELD                          DIS 860
C                                                                       DIS 870
      IF (CINIT) GO TO 210                                              DIS 880
      READ (5,360) (T(J),J=IN,ID)                                       DIS 890
      GO TO 230                                                         DIS 900
  210 DO 220 J=IN,ID                                                    DIS 910
  220 T(J)=0.0                                                          DIS 920
  230 CONTINUE                                                          DIS 930
C                                                                       DIS 940
C***************LOAD INPUT CONCENTRATIONS                               DIS 950
C                                                                       DIS 960
      CALL DATAIN (T(ICUPS2+1))                                         DIS 970
C                                                                       DIS 980
C***************COMPUTE DIFFUSIVITIES                                   DIS 990
C                                                                       DIS 1000
      CALL UANDDI (T(IZ+1),T(IX+1),T(IF+1),T(IB+1),T(ISTR+1),T(IZB+1),T(DIS 1010
     1IALF+1),T(IU+1),T(IDIF+1),T(IET+1),BWOUT,T(ILDIFF+1),LALFA,RDATA) DIS 1020
C                                                                       DIS 1030
C***************EXECUTE SIMULATION                                      DIS 1040
C                                                                       DIS 1050
      CALL CONCEN (T(IX+1),T(IF+1),T(IU+1),T(IDIF+1),T(ICON1+1),T(ICON2+DIS 1060
     11),T(ICON+1),T(ID+1),T(IE+1),T(ICUPS1+1),T(ICUPS2+1),T(IET+1),T(IFDIS 1070
     2T+1),T(INTCH+1),NDT,T(IZ+1),T(IZB+1),INDEX,T(ISTR+1),CONVECDIS 1080
     3CM,T(ILDIFF+1),LONGD,T(ISLOP+1))                                  DIS 1090
      WRITE (6,370) TIME,NCYCL                                          DIS 1100
  240 STOP                                                              DIS 1110
C                                                                       DIS 1120
  250 FORMAT (20A4)                                                     DIS 1130
  260 FORMAT (4I10,,4F10.0,/,3F10.0,L10,I10,2L10,I10)                   DIS 1140
  270 FORMAT (8F10.0)                                                   DIS 1150
  280 FORMAT ( 1H0,T10, 20HINSUFFICIENT STORAGE,I10)                    DIS 1160
  290 FORMAT ( 1H1,T25,20A4)                                            DIS 1170
  300 FORMAT (1X, 60HLATERAL DIFFUSIVITY = ALFA X USTAR(MEAN) X D(MEAN))DIS 1180
  310 FORMAT (1X, 72HLATERAL DIFFUSIVITY = ALFA X USTAR(MEAN) X U(LOCAL)DIS 1190
     1 X D(LOCAL) / U(MEAN))                                            DIS 1200
  320 FORMAT (1X, 52HLATERAL DIFFUSIVITY = ALFA X USTAR(LOCAL) X D(LOCALDIS 1210
     1))                                                                DIS 1220
  330 FORMAT (1X, 39HLATERAL DIFFUSIVITY = ALFAXUMEANXD(LOCAL))         DIS 1230
  340 FORMAT (/,1X, 26HINITIAL TIME STEP CHANGED ,I5, 7H TIMES,/,1X, 80DIS 1240
     15HFOLLOWING ARE PAIRS OF TIMES AT WHICH DELTA T IS CHANGED, AND NEDIS 1250
     2W DELTA T ,(IN HOURS),/,1X,8F8.0)                                 DIS 1260
  350 FORMAT (20X, 46HNUMBER OF LONGITUDINAL COMPUTATIONAL POINTS = ,I5,DIS 1270
     1/,20X, 25HNUMBER OF STREAM TUBES = ,I5,//,20X, 20HINITIAL TIME STEDIS 1280
     2P = ,F8.6, 7H HOURS, 32H WITH CONCENTRATION OUPUT EVERY ,I2, 12HODIS 1290
     3 TIME STEPS,//,20X, 29HGRAVITATIONAL ACCELERATION = ,F6.3,//,20X,2DIS 1300
     4 18HRIVER DISCHARGE = ,F10.3, 15H M AT STATIODIS 1310
     5ION X = ,F10.3,//,20X, 64HIF TRUE INITIAL CONCENTRATIONS ARE SET TDIS 1320
     6O ZERO WITHIN PROGRAM ,L5,//,20X, 60HIF TRUE, LONGITUDINADIS 1330
     7L TURBULENT DIFFUSION HAS BEEN COMPUTED ,L5,//,20X, 37HUNIVERSAL LODIS 1340
     8ATERAL DIFFUSION FACTOR = ,F7.5,/,20X, 42HUNIVERSAL LONGITUDINAL DODIS 1350
     9FFUSION FACTOR = ,F6.3,///)                                       DIS 1360
  360 FORMAT ( 10F8.0)                                                  DIS 1370
  370 FORMAT ( 1H0,T10, 26HEND OF COMPUTATION AT TIME,E10.3, 13H HOURS, DIS 1380
     1 AFTER,I5, 8H CYCLES.)                                            DIS 1390
C                                                                       DIS 1400
      END                                                               DIS 1410
```

```
C                                                            GEO  20
        SUBROUTINE GEOMIN (B,ZBOT,STR,ALFFAC,X,Z,SLOPE,SLOP) GEO  30
C**************READ STREAM TUBE DATA FOR EACH SECTION FROM PERMANENT  GEO  40
C**************FILE                                          GEO  50
                                                            GEO  60
                                                            GEO  70
        DIMENSION B(2), ZBOT(2), STR(2), ALFFAC(2), X(2), Z(2), SLOPE(2), GEO  80
       1SLOP(2)                                              GEO  90
        COMMON NBPTS,NTUBE,NCYCL,ZDOWNS,G,Q,TIME,TEND,DT,DTM,EPSLOC,ITMP,I GEO  100
       1Z,IX,IF,IB,ISTR,IZB,IALF,IU,IDIF,ICON1,ICON2,ICON,ID,IE,ILDIFF,IE GEO  110
       2IFT,INTCH,ICUPS1,ICUPS2,ISLOP                        GEO  120
        IN=1                                                 GEO  130
        DO 140 I=1,NBPTS                                     GEO  140
        READ (3,180) X(I),Z(I),SLOPE(I)                      GEO  150
        IF (EOF(3)) 150,110,150                               GEO  160
110     CONTINUE                                             GEO  170
        SLOP(I)=SLOPE(I)                                     GEO  180
        DO 130 J=1,NTUBE                                     GEO  190
        READ (3,190) B(IN),ZBOT(IN),STR(IN),ALFFAC(IN)      GEO  200
        IF (EOF(3)) 160,120,160                               GEO  210
120     CONTINUE                                             GEO  220
130     IN=IN+NBPTS+1                                        GEO  230
140     IN=IN-NTUBE*(NBPTS+1)+1                              GEO  240
        RETURN                                               GEO  250
150     WRITE (6,200) I,X(I-1),Z(I-1),SLOPE(I-1)             GEO  260
        GO TO 170                                            GEO  270
160     WRITE (6,210) IN,B(IN-1),ZBOT(IN-1),STR(IN-1),ALFFAC(IN-1)  GEO  280
170     CONTINUE                                             GEO  290
        RETURN                                               GEO  300
C                                                            GEO  310
180     FORMAT (1X,2F13.4,F10.4)                             GEO  320
190     FORMAT (1X,4F10.4)                                   GEO  330
200     FORMAT (I10,3F20.10)                                 GEO  340
210     FORMAT (I10,4F20.10)                                 GEO  350
C                                                            GEO  360
        END                                                  GEO  370
C  ==========================================================DAT  10
C                                                            DAT  20
        SUBROUTINE DATAIN (CUPST)                            DAT  30
C**************READS INPUT CONCENTRATIONS AND GENERATES UPSTREAM  DAT  40
C**************CONCENTRATIONS                                DAT  50
                                                            DAT  60
                                                            DAT  70
        DIMENSION T(20,30), C(20,30), CUPST(2)               DAT  80
        COMMON NBPTS,NTUBE,NCYCL,ZDOWNS,G,Q,TIME,TEND,DT,DTM,EPSLOC,ITMP,IDAT  90
       1Z,IX,IF,IB,ISTR,IZB,IALF,IU,IDIF,ICON1,ICON2,ICON,ID,IE,ILDIFF,IEDAT  100
       2IFT,INTCH,ICUPS1,ICUPS2,ISLOP                        DAT  110
        IF (NCYCL) 110,110,130                                DAT  120
C                                                            DAT  130
C**************READ TIME-CONCENTRATION INPUT DATA PAIRS FOR EACH STREAM  DAT  140
C**************TUBE                                          DAT  150
                                                            DAT  160
110     READ (5,170) NCIN                                    DAT  170
        WRITE (6,180) NCIN                                   DAT  180
        NCINM1=NCIN-1                                        DAT  190
        DO 120 J=1,NTUBE                                     DAT  200
        READ (5,190) (T(I,J),I=1,NCIN)                       DAT  210
        READ (5,190) (C(I,J),I=1,NCIN)                       DAT  220
        WRITE (6,200) J                                      DAT  230
        WRITE (6,210) (T(I,J),C(I,J),I=1,NCIN)               DAT  240
120     CONTINUE                                             DAT  250
130     CONTINUE                                             DAT  260
C                                                            DAT  270
C**************LOCATE TIME-CONCENTRATION PAIRS WHICH BRACKET THE  DAT  280
C**************SIMULATION TIME                               DAT  290
                                                            DAT  300
        DO 160 J=1,NTUBE                                     DAT  310
        DO 140 N=1,NCINM1                                    DAT  320
        IF ((TIME.LT.T(N+1,J)).AND.(TIME.GE.T(N,J))) GO TO 150  DAT  330
140     CONTINUE                                             DAT  340
C                                                            DAT  350
C**************LINEARLY INTERPOLATE TO OBTAIN APPROPRIATE INPUT  DAT  360
C**************CONCENTRATION FOR ANY TIME                    DAT  370
                                                            DAT  380
150     CUPST(J)=C(N,J)+(TIME-T(N,J))*(C(N+1,J)-C(N,J))/(T(N+1,J)-T(N,JDAT  390
       1                                                     DAT  400
160     CONTINUE                                             DAT  410
        RETURN                                               DAT  420
C                                                            DAT  430
170     FORMAT (I10)                                         DAT  440
180     FORMAT (//,1X,I5, 66H  PAIRS OF (TIME,CONC) DATA INPUT FOR UPSTREADAT  450
       1M  END OF EACH TUBE.//)                              DAT  460
190     FORMAT (10F8.0)                                      DAT  470
200     FORMAT (/,1X,  5HTUBE ,I5, 17H  TIME      CONC,/)     DAT  480
210     FORMAT (11X,2E10.3)                                  DAT  490
C                                                            DAT  500
        END                                                  DAT  510
C  ==========================================================UAN  10
C                                                            UAN  20
        SUBROUTINE UANDDI (Z,X,SLOPE,B,STR,ZBOT,ALFFAC,U,DIFF,H,BWOUT,LDIFUAN  30
       1F,LALFA,RDATA)                                       UAN  40
C**************COMPUTES DIFFUSIVITIES, TRANSVERSE AND LONGITUDINAL  UAN  50
                                                            UAN  60
                                                            UAN  70
        DIMENSION Z(2), X(2), SLOPE(2), B(2), STR(2), ZBOT(2), ALFFAC(2),UAN  80
       1U(2), DIFF(2), H(2), LDIFF(2)                        UAN  90
        COMMON NBPTS,NTUBE,NCYCL,ZDOWNS,G,Q,TIME,TEND,DT,DTM,EPSLOC,ITMP,IUAN  100
       1Z,IX,IF,IB,ISTR,IZB,IALF,IU,IDIF,ICON1,ICON2,ICON,ID,IE,ILDIFF,IEUAN  110
       2IFT,INTCH,ICUPS1,ICUPS2,ISLOP                        UAN  120
        LOGICAL RDATA                                        UAN  130
        INTEGER EPSLOC,BWOUT                                 UAN  140
        REAL LALFA,LDIFF                                     UAN  150
        IN=1                                                 UAN  160
C                                                            UAN  170
C**************IF RDATA=TRUE, THE VALUES OF STR, ZBOT READ FROM PF  UAN  180
C**************ARE ACTUALLY U AND H, RESPECTIVELY.  BUT Z, ZBOT ARE  UAN  190
C**************USED IN OTHER ROUTINES TO COMPUTE THE DEPTH H.  UAN  200
C**************CONSEQUENTLY ARTIFICIAL VALUES OF Z (WATER SURFACE) AND  UAN  210
C**************ZBOT (TUBE BOTTOM ELEVATION) ARE GENERATED HERE.  UAN  220
C**************IF RDATA=TRUE                                 UAN  230
C**************COMPUTE DISCHARGE, WIDTH, AREA, MEAN VELOCITY, SHEAR  UAN  240
C**************VELOCITY                                      UAN  250
                                                            UAN  260
        DO 240 I=1,NBPTS                                     UAN  270
        W=0.                                                 UAN  280
        A=0.                                                 UAN  290
        Q=0.                                                 UAN  300
        S=SLOPE(I)                                           UAN  310
        ALF=ALFFAC(I)                                        UAN  320
        IF (RDATA) Z(I)=1000.                                UAN  330
        DO 110 J=1,NTUBE                                     UAN  340
        H(J)=Z(I)-ZBOT(IN)                                  UAN  350
        IF (RDATA) H(J)=ZBOT(IN)                             UAN  360
        IF (RDATA) ZBOT(IN)=Z(I)-H(J)                        UAN  370
        U(IN)=STR(IN)*(H(J)**0.666667)*SQRT(S)               UAN  380
        IF (RDATA) U(IN)=STR(IN)                             UAN  390
        A=A+H(J)*B(IN)                                       UAN  400
        W=W+B(IN)                                            UAN  410
        Q=Q+B(IN)*U(IN)*H(J)                                 UAN  420
110     IN=IN+NBPTS+1                                        UAN  430
        IF (I.LE.BWOUT) CALL LABEL3                          UAN  440
        UMEAN=Q/A                                            UAN  450
        USTAR=SQRT(G*S*A/W)                                  UAN  460
C                                                            UAN  470
C**************COMPUTE DIFFUSIVITY FOR EPSLOC=1               UAN  480
                                                            UAN  490
        GO TO (120,130,130,130), EPSLOC                      UAN  500
120     EPS=ALF*((A/W)**1.5)*SQRT(G*S)                       UAN  510
        OLDIFF=LALFA*((A/W)**1.5)*SQRT(G*S)                  UAN  520
110     J=NTUBE                                              UAN  530
140     IN1=IN                                               UAN  540
        IN=IN-NBPTS-1                                        UAN  550
        IF (J.LT.NTUBE) GO TO 150                            UAN  560
        DIFF(IN)=0.0                                         UAN  570
        OLDIFF=LALFA*H(J)*SQRT(G*S*H(J))                     UAN  580
        GO TO 230                                            UAN  590
C                                                            UAN  600
C**************COMPUTE MIXING DEPTH                          UAN  610
                                                            UAN  620
150     DMIX=AMIN1(H(J),H(J+1))                              UAN  630
        GO TO (220,180,160,200), EPSLOC                      UAN  640
```

```
C                                                                    UAN  650
C***********COMPUTE DIFFUSIVITY FOR EPSLOC=3                          UAN  660
                                                                     UAN  670
    160   EPS=ALFFAC(IN)*H(J)*SQRT(G*S*H(J))                          UAN  680
          DLDIFF=LALFA*H(J)*SQRT(G*S*H(J))                            UAN  690
          IF (J-NTUBE) 170,220,220                                    UAN  700
    170   EPS=EPS/2.+ALFFAC(IN+NBPTS+1)*H(J+1)*SQRT(G*S*H(J+1))/2.    UAN  710
          GO TO 220                                                   UAN  720
C                                                                    UAN  730
C***********COMPUTE DIFFUSIVITY FOR EPSLOC=2                          UAN  740
                                                                     UAN  750
    180   EPS=ALFFAC(IN)*H(J)*U(IN)*USTAR/UMEAN                       UAN  760
          DLDIFF=LALFA*H(J)*SQRT(G*S*H(J))                            UAN  770
          IF (J-NTUBE) 190,220,220                                    UAN  780
    190   EPS=EPS/2.+ALFFAC(IN+NBPTS+1)*H(J+1)*U(IN+NBPTS+1)*USTAR/UMEAN/UAN  790
         12.                                                          UAN  800
          GO TO 220                                                   UAN  810
C                                                                    UAN  820
C***********COMPUTE DIFFUSIVITY FOR EPSLOC=4                          UAN  830
                                                                     UAN  840
    200   EPS=ALFFAC(IN)*UMEAN*H(J)                                   UAN  850
          DLDIFF=LALFA*H(J)*SQRT(G*S*H(J))                            UAN  860
          IF (J-NTUBE) 210,220,220                                    UAN  870
    210   EPS=EPS/2.+ALFFAC(IN+NBPTS+1)*H(J+1)*UMEAN/2.               UAN  880
    220   DIFF(IN)=2.0*DMIX*EPS/(B(IN)+B(IN))                         UAN  890
    230   LDIFF(IN)=DLDIFF                                            UAN  900
C                                                                    UAN  910
C***********WRITE COMPLETE STREAM TUBE DATA                           UAN  920
                                                                     UAN  930
      1   IF (I.LE.BWOUT) CALL EDIT3 (X(I),J,DMIX,EPS,DIFF(IN),H(J),U(IN)UAN  940
         1,A,W,S,B(IN),LDIFF(IN))                                    UAN  950
          J=J-1                                                       UAN  960
          IF (J.GT.0) GO TO 140                                       UAN  970
          IN=IN+1                                                     UAN  980
    240 CONTINUE                                                      UAN  990
        RETURN                                                        UAN 1000
C                                                                    UAN 1010
        END                                                           UAN 1020
C       ==============================================================CON   10
                                                                     CON   20
        SUBROUTINE CONCEN (X,F,U,DIFF,CCON1,CCON2,C,D,E,CUPS12,CUPST,ET,FTCON   30
       1,TCHG,NDT,Z,ZBOT,B,INDEX,STR,CONVEC,LDIFF,LONGD,SLOPE)        CON   40
C                                                                    CON   50
C***********EXECUTES DISPERSION SIMULATION                            CON   60
                                                                     CON   70
        DIMENSION X(2), F(2), U(2), DIFF(2), CCON1(2), CCON2(2), C(2), D(2CON   80
       1), E(2), STR(2), CUPS12(2), CUPST(2), ET(2), FT(2), TCHG(2), Z(2)CON   90
       2 ZBOT(2), B(2), LDIFF(2), SLOPE(2)                            CON  100
        COMMON NBPTS,NTUBE,NCYCL,ZDOWNS,G,Q,TIME,TEND,DT,DTH,EPSLOC,ITMP,ICCON 110
       1,IX,IF,IB,ISTR,IZB,IALF,IU,IDIF,ICON1,ICON2,ICON,ID,IE,ILDIFF,IETCON 120
       2,IFT,INTCH,ICUPS1,ICUPS2,ISLOP                                CON  130
        LOGICAL FIRST,LONGD                                           CON  140
        REAL LDIFF                                                    CON  150
        RINDEX=INDEX                                                  CON  160
        FIRST=.TRUE.                                                  CON  170
        NCYCL=1                                                       CON  180
        ICHECK=0                                                      CON  190
C                                                                    CON  200
C***********INCREMENT TIME BY HALF THE TIME STEP                      CON  210
                                                                     CON  220
    110 TIME=TIME+DTH/2.0                                             CON  230
        IN=0                                                          CON  240
C                                                                    CON  250
C***********LOAD INPUT CONCENTRATIONS FOR FIRST HALF STEP             CON  260
                                                                     CON  270
        CALL DATAIN (CUPS12(1))                                       CON  280
C                                                                    CON  290
C***********INCREMENT TIME BY HALF THE TIME STEP                      CON  300
                                                                     CON  310
        TIME=TIME+DTH/2.0                                             CON  320
C                                                                    CON  330
C***********LOAD INPUT CONCENTRATIONS FOR SECOND HALF STEP            CON  340
                                                                     CON  350
        CALL DATAIN (CUPST(1))                                        CON  360
C                                                                    CON  370
C***********WRITE CONCENTRATION FIELD BEFORE STARTING SIMULATION      CON  380
                                                                     CON  390
        IF (NCYCL.EQ.1) CALL EDIT (X,C)                               CON  400
C                                                                    CON  410
C***********COMPUTE CONVECTION                                        CON  420
                                                                     CON  430
        CALL CONVEC (X,F,U,DIFF,CCON1,CCON2,C,D,E,CUPS12,CUPST,ET,FT,TCHG,CON  440
       1Z,ZBOT,B,FIRST,STR)                                           CON  450
C                                                                    CON  460
C***********COMPUTE TRANSVERSE DIFFUSION                              CON  470
                                                                     CON  480
        CALL DIFFUS (X,F,U,DIFF,CCON1,CCON2,C,D,E,CUPS12,CUPST,ET,FT,TCHG,CON  490
       1Z,ZBOT,B)                                                     CON  500
C                                                                    CON  510
C***********COMPUTE LONGITUDINAL DIFFUSION IF LONGD IS TRUE           CON  520
                                                                     CON  530
        IF (.NOT.LONGD) GO TO 120                                     CON  540
        CALL LODIFF (X,F,U,DIFF,CCON1,CCON2,C,D,E,CUPS12,CUPST,ET,FT,TCHG,CON  550
       1Z,ZBOT,B,LDIFF)                                               CON  560
    120 IN=0                                                          CON  570
C                                                                    CON  580
C***********WRITE CONCENTRATION FIELD IF NUMBER OF ITERATIONS IS A     CON  590
C***********MULTIPLE OF INDEX                                         CON  600
                                                                     CON  610
        IF (INDEX) 160,160,130                                        CON  620
    130 IF (ICHECK.EQ.INDEX.OR.NCYCL.EQ.1) GO TO 140                  CON  630
        GO TO 150                                                     CON  640
    140 CONTINUE                                                      CON  650
        CALL EDIT (X,C)                                               CON  660
        CHECK=TIME+RINDEX*DTH                                         CON  670
        ICHECK=0                                                      CON  680
    150 ICHECK=ICHECK+1                                               CON  690
        GO TO 170                                                     CON  700
C                                                                    CON  710
C***********WRITE CONCENTRATION FIELD AT END OF SIMULATION IF INDEX=0CON  720
                                                                     CON  730
    160 IF (TIME.GE.TEND) CALL EDIT (X,C)                             CON  740
    170 CONTINUE                                                      CON  750
C                                                                    CON  760
C***********INCREMENT ITERATION COUNTER                               CON  770
                                                                     CON  780
        NCYCL=NCYCL+1                                                 CON  790
C                                                                    CON  800
C***********RETURN TO MAIN PROGRAM IF TIME GREATER THAN TEND          CON  810
                                                                     CON  820
        IF (TIME.GE.TEND) GO TO 180                                   CON  830
C                                                                    CON  840
C***********REVISE TIME STEP IF TIME HAS EXCEEDED A CHANGE POINT       CON  850
                                                                     CON  860
        IF (NDT.EQ.0) GO TO 110                                       CON  870
        IF (TIME.LT.TCHG(ITMP).OR.ITMP.GT.NDT) GO TO 110              CON  880
        DTH=TCHG(ITMP+1)                                              CON  890
        DT=DTH*3600.                                                  CON  900
        ITMP=ITMP+2                                                   CON  910
C                                                                    CON  920
C***********BEGIN ANOTHER TIME INCREMENT                              CON  930
                                                                     CON  940
        GO TO 110                                                     CON  950
    180 RETURN                                                        CON  960
C                                                                    CON  970
        END                                                           CON  980
C       ==============================================================CNV   10
                                                                     CNV   20
        SUBROUTINE CONVECH (X,F,U,DIFF,CCON1,CCON2,C,R,E,CUPS12,CUPST,ET,FCNV   30
       1T,TCHG,Z,ZBOT,B,FIRST,S)                                      CNV   40
C                                                                    CNV   50
C***********SECOND ORDER IMPLICITY-EXPLICIT DOUBLE-STEP SCHEME FOR     CNV   60
C***********CONVECTION                                                CNV   70
                                                                     CNV   80
        DIMENSION X(2), F(2), U(2), DIFF(2), CCON1(2),CCON2(2), C(2), R(2CNV   90
       1), E(2), S(2), CUPS12(2), CUPST(2), ET(2), FT(2), TCHG(2), Z(2), ZCNV  100
       2BOT(2), B(2)                                                  CNV  110
        COMMON NBPTS,NTUBE,NCYCL,ZDOWNS,G,Q,TIME,TEND,DT,DTH,EPSLOC,ITMP,ICNV  120
       1,IX,IF,IB,ISTR,IZB,IALF,IU,IDIF,ICON1,ICON2,ICON,ID,IE,ILDIFF,IETCNV  130
       2,IFT,INTCH,ICUPS1,ICUPS2,ISLOP                                CNV  140
        LOGICAL FIRST                                                 CNV  150
```

```
C***************FIRST IMPLICIT HALF STEP                           CNV 160
C                                                                  CNV 170
      IN=0                                                         CNV 180
C                                                                  CNV 190
C***************GENERATE DOWNSTREAM BOUNDARY CONDITION             CNV 200
C                                                                  CNV 210
      DO 170 J=1,NTUBE                                             CNV 220
      CCON1(IN+NBPTS+1)=C(IN+NBPTS)                                CNV 230
      U(IN+NBPTS+1)=U(IN+NBPTS)                                    CNV 240
      X(NBPTS+1)=X(NBPTS)+0.5*DT*U(IN+NBPTS)                       CNV 250
      DO 150 I=1,NBPTS                                            CNV 260
      IN=IN+1                                                      CNV 270
      IF (I.GT.1) GO TO 120                                        CNV 280
      AIP1=(Z(I+1)-ZBOT(IN+1))*B(IN+1)                             CNV 290
      AI=(Z(I)-ZBOT(IN))*B(IN)                                     CNV 300
C                                                                  CNV 310
C***************APPLY UPSTREAM BOUNDARY CONDITION                  CNV 320
C                                                                  CNV 330
      F(I)=CUPS12(J)                                               CNV 340
      IF (.NOT.FIRST) GO TO 110                                    CNV 350
      E(IN)=0.0                                                    CNV 360
      GO TO 140                                                    CNV 370
  110 CONTINUE                                                     CNV 380
C                                                                  CNV 390
C***************COMPUTE R,S,E,F                                    CNV 400
C                                                                  CNV 410
  120 IF (I.EQ.NBPTS) GO TO 130                                    CNV 420
      AIP1=(Z(I+1)-ZBOT(IN+1))*B(IN+1)                             CNV 430
  130 CONTINUE                                                     CNV 440
      DX=X(I+1)-X(I-1)                                             CNV 450
      R(IN)=0.5*DT*U(IN-1)*AIM1/AI/DX                              CNV 460
      S(IN)=0.5*DT*U(IN+1)*AIP1/AI/DX                              CNV 470
      DEN=1.0-R(IN)*E(IN-1)                                        CNV 480
      E(IN)=-S(IN)/DEN                                             CNV 490
      F(I)=(C(IN)+R(IN)*F(I-1))/(1.0-R(IN)*E(IN-1))                CNV 500
  140 AIM1=AI                                                      CNV 510
      AI=AIP1                                                      CNV 520
  150 CONTINUE                                                     CNV 530
      I=NBPTS                                                      CNV 540
C                                                                  CNV 550
C***************COMPUTE CONCENTRATIONS BY RECURRENCE               CNV 560
C                                                                  CNV 570
  160 CCON1(IN)=E(IN)*CCON1(IN+1)+F(I)                             CNV 580
      I=I-1                                                        CNV 590
      IN=IN-1                                                      CNV 600
      IF (I.GT.0) GO TO 160                                        CNV 610
      IN=IN+NBPTS+1                                                CNV 620
  170 CONTINUE                                                     CNV 630
C***************SECOND EXPLICIT HALF STEP                          CNV 640
C***************GENERATE DOWNSTREAM BOUNDARY CONDITION             CNV 660
C                                                                  CNV 670
      IN=0                                                         CNV 680
      DO 200 J=1,NTUBE                                             CNV 690
      X(NBPTS+1)=X(NBPTS)+0.5*DT*U(IN+NBPTS)                       CNV 700
C                                                                  CNV 710
C***************APPLY UPSTREAM BOUNDARY CONDITION                  CNV 720
C                                                                  CNV 730
      DO 190 I=1,NBPTS                                            CNV 740
      IN=IN+1                                                      CNV 750
      IF (I.NE.1) GO TO 180                                        CNV 760
      CCON2(IN)=CUPST(J)                                           CNV 770
      C(IN)=CCON2(IN)                                              CNV 780
      GO TO 190                                                    CNV 790
C***************COMPUTE CONCENTRATIONS DIRECTLY                    CNV 810
C                                                                  CNV 820
  180 CCON2(IN)=CCON1(IN)-S(IN)*CCON1(IN+1)+R(IN)*CCON1(IN-1)      CNV 830
  190 CONTINUE                                                     CNV 840
      IN=IN+1                                                      CNV 850
  200 CONTINUE                                                     CNV 860
      IF (FIRST) FIRST=.FALSE.                                     CNV 870
      RETURN                                                       CNV 880
C                                                                  CNV 890
      END                                                          CNV 900
======================================================================
C                                                                  DIF 10
      SUBROUTINE DIFFUS (X,F,U,DIFF,CCON1,CCON2,C,D,E,CUPS12,CUPST,ET,FTDIF 20
     1,TCHG,Z,ZBOT,B,FIRST)                                        DIF 30
C                                                                  DIF 40
C***************IMPLICIT SCHEME FOR TRANSVERSE DIFFUSION           DIF 50
C                                                                  DIF 60
C                                                                  DIF 70
      DIMENSION X(2),F(2),U(2),DIFF(2),CCON1(2),CCON2(2),C(2),D(2 DIF 80
     1),E(2),CUPS12(2),CUPST(2),ET(2),FT(2),TCHG(2),Z(2),ZBOT(2)  DIF 90
     2,B(2)                                                        DIF 100
      COMMON NBPTS,NTUBE,NCYCL,ZDOWNS,Q,Q,TIME,TEND,DT,DTH,EPSLOC,ITMP,IDDIF 110
     1Z,IX,IF,IB,ISTR,IZB,IALF,IU,IDIF,ICON1,ICON2,ICON,ID,IE,ILDIFF,IETDIF 120
     2,IFT,INTCH,ICUPS1,ICUPS2,ISLOP                               DIF 130
      LOGICAL FIRST                                                DIF 140
      IN=1                                                         DIF 150
C                                                                  DIF 160
C***************COMPUTE DIFFUSION SEPARATELY AT EACH LONGITUDINAL  DIF 170
C***************COMPUTATIONAL POINT                                DIF 180
C                                                                  DIF 190
      DO 160 I=1,NBPTS                                            DIF 200
      N=NTUBE-1                                                    DIF 210
C                                                                  DIF 220
C***************COMPUTE D,E,F COEFFICIENTS FOR EACH STREAM TUBE,   DIF 230
C***************LEFT TO RIGHT                                      DIF 240
C                                                                  DIF 250
      AJM1=1.                                                      DIF 260
      DO 110 J=1,N                                                DIF 270
      AJ=(Z(I)-ZBOT(IN))*B(IN)                                     DIF 280
      IF (J.EQ.1) D3=0.0                                           DIF 290
      D1=D3*AJM1/AJ                                                DIF 300
      D3=DIFF(IN)*DT/AJ                                            DIF 310
      D2=1.0+D3+D1                                                 DIF 320
      AUX1=D2                                                      DIF 330
      IF (J.NE.1) AUX1=D2-D1*ET(J-1)                               DIF 340
      ET(J)=D3/AUX1                                                DIF 350
      AUX2=CCON2(IN)                                               DIF 360
      IF (J.NE.1) AUX2=AUX2+D1*FT(J-1)                             DIF 370
      FT(J)=AUX2/AUX1                                              DIF 380
      IN=IN+NBPTS+1                                                DIF 390
      AJM1=AJ                                                      DIF 400
  110 CONTINUE                                                     DIF 410
      D3=D3*AJ/((Z(I)-ZBOT(IN))*B(IN))                             DIF 420
      C(IN)=(CCON2(IN)+D3*FT(N))/(1.0+D3*(1.0-ET(N)))              DIF 430
C                                                                  DIF 440
C***************DO NOT COMPUTE DIFFUSION AT FIRST COMPUTATIONAL POINT DIF 450
C                                                                  DIF 460
      IF (I.LT.2) C(IN)=CCON2(IN)                                  DIF 470
      J=N                                                          DIF 480
  120 IN1=IN-NBPTS-1                                               DIF 490
      IF (I-1) 140,140,130                                         DIF 500
C                                                                  DIF 510
C***************COMPUTE CONCENTRATIONS BY RECURRENCE               DIF 520
C                                                                  DIF 530
  130 C(IN1)=C(IN)*ET(J)+FT(J)                                     DIF 540
      GO TO 150                                                    DIF 550
  140 C(IN1)=CCON2(IN1)                                            DIF 560
  150 IN=IN1                                                       DIF 570
      J=J-1                                                        DIF 580
      IF (J.GT.0) GO TO 120                                        DIF 590
C                                                                  DIF 600
C***************REPEAT LOOP FOR NEXT COMPUTATIONAL POINT           DIF 610
C                                                                  DIF 620
      IN=IN+1                                                      DIF 630
  160 CONTINUE                                                     DIF 640
      RETURN                                                       DIF 650
C                                                                  DIF 660
      END                                                          DIF 670
```

```
C     ***********************************************************LOD  10
C                                                                LOD  20
      SUBROUTINE LODIFF (X,N,U,DIFF,M,CCON2,C,D,E,CUPS12,CUPST,ET,FT,TCHLOD  30
     16,Z,ZBOT,B,FIRST,LDIFF)                                    LOD  40
C                                                                LOD  50
C**************IMPLICIT SCHEME FOR LONGITUDINAL DIFFUSION         LOD  60
C                                                                LOD  70
      DIMENSION X(2), N(2), U(2), DIFF(2), M(2), CCON2(2), C(2), D(2), ELOD  80
     1(2), CUPS12(2), CUPST(2), ET(2), FT(2), TCHG(2), Z(2), ZBOT(2), B(LOD  90
     22), LDIFF(2)                                               LOD 100
      COMMON NBPTS,NTUBE,NCYCL,ZDOWNS,G,Q,TIME,TEND,DT,DTH,EPSLOC,ITMP,ILOD 110
     1Z,IX,IF,IB,ISTR,IZB,IALF,IU,IDIF,ICON1,ICON2,ICON,ID,IE,ILDIFF,IETLOD 120
     2,IFT,INTCH,ICUPS1,ICUPS2,ISLOP                             LOD 130
      REAL LDIFF,M,N                                             LOD 140
      LOGICAL FIRST                                              LOD 150
      IN=0                                                       LOD 160
C                                                                LOD 170
C**************GENERATE DOWNSTREAM BOUNDARY CONDITIONS            LOD 180
C                                                                LOD 190
      DO 180 J=1,NTUBE                                           LOD 200
      X(NBPTS+1)=X(NBPTS)+U(IN+NBPTS)*DT                         LOD 210
      IF (U(IN+NBPTS).LE.0.0) X(NBPTS+1)=2.0*X(NBPTS)-X(NBPTS-1) LOD 220
      I=0                                                        LOD 230
  110 I=I+1                                                      LOD 240
      IN=IN+1                                                    LOD 250
      IF (I.NE.1) GO TO 120                                      LOD 260
C**************APPLY UPSTREAM BOUNDARY CONDITION                  LOD 270
C                                                                LOD 280
      M(IN)=0.0                                                  LOD 290
      N(I)=CUPST(J)                                              LOD 300
      DX=2.*(X(I+1)-X(I))                                        LOD 310
C                                                                LOD 320
C**************COMPUTE G,M,N VALUES                               LOD 330
C                                                                LOD 340
      G1=0.0                                                     LOD 350
      GO TO 130                                                  LOD 360
  120 G1=G2*DX*AT/(X(I+1)-X(I-1))/B(IN)/(Z(I)-ZBOT(IN))          LOD 370
      IF (I.EQ.NBPTS) GO TO 140                                  LOD 380
      DX=X(I+1)-X(I-1)                                           LOD 390
  130 AI=B(IN)*(Z(I)-ZBOT(IN))                                   LOD 400
      AIP1=AI+B(IN+1)*(Z(I+1)-ZBOT(IN+1))                        LOD 410
      DXP1=X(I+1)-X(I)                                           LOD 420
      G2=DT*AIP1*(LDIFF(IN+1)+LDIFF(IN))/2./AI/DX/DXP1           LOD 430
      GO TO 150                                                  LOD 440
  140 G2=2.*DT*LDIFF(IN)/(X(I+1)-X(I-1))/(X(I+1)-X(I))           LOD 450
  150 IF (I.EQ.1) GO TO 160                                      LOD 460
      M(IN)=G2/(1.0-G2*G1*(1.0-M(IN-1)))                         LOD 470
      N(I)=(G1*N(I-1)+C(IN))/(1.0+G2+G1*(1.0-M(IN-1)))           LOD 480
  160 IF (I.NE.NBPTS) GO TO 110                                  LOD 490
C                                                                LOD 500
C**************COMPUTE CONCENTRATIONS BY RECURRENCE               LOD 510
C                                                                LOD 520
      C(IN)=M(IN)*C(IN)+N(I)                                     LOD 530
  170 C(IN-1)=M(IN-1)*C(IN)+N(I-1)                               LOD 540
      I=I-1                                                      LOD 550
      IN=IN-1                                                    LOD 560
      IF (I.EQ.1) GO TO 180                                      LOD 570
      GO TO 170                                                  LOD 580
C                                                                LOD 590
C**************REPEAT LOOP FOR NEXT STREAM TUBE                   LOD 600
C                                                                LOD 610
  180 IN=IN+NBPTS                                                LOD 620
      RETURN                                                     LOD 630
C                                                                LOD 640
      END                                                        LOD 650
C     ===========================================================EDI  10
      SUBROUTINE EDIT (X,C)                                      EDI  20
C                                                                EDI  30
C**************WRITE OUT CONCENTRATION FIELDS                     EDI  40
C                                                                EDI  50
      DIMENSION X(2), C(2)                                       EDI  60
      COMMON NBPTS,NTUBE,NCYCL,ZDOWNS,G,Q,TIME,TEND,DT,DTH,EPSLOC,ITMP,IEDI  70
     1Z,IX,IF,IB,ISTR,IZB,IALF,IU,IDIF,ICON1,ICON2,ICON,ID,IE,ILDIFF,IETEDI  80
     2,IFT,INTCH,ICUPS1,ICUPS2,ISLOP                             EDI  90
      N=(NTUBE-1)*(NBPTS+1)                                      EDI 100
      ISKIP=NBPTS+1                                              EDI 110
      ISTART=1                                                   EDI 120
      K=1                                                        EDI 130
      IF (NTUBE.GT.11) N=10*(NBPTS+1)                            EDI 140
      NDUM=10*(NBPTS+1)                                          EDI 150
      WRITE (6,160) TIME,DT                                      EDI 160
  110 DO 120 I=1,NBPTS                                           EDI 170
      IEND=ISTART+N                                              EDI 180
      WRITE (6,150) X(I),(C(J),J=ISTART,IEND,ISKIP)              EDI 190
      ISTART=ISTART+1                                            EDI 200
  120 CONTINUE                                                   EDI 210
      IF (NTUBE.GT.11.AND.K.EQ.1) GO TO 130                      EDI 220
      GO TO 140                                                  EDI 230
  130 N=(NTUBE-1)*(NBPTS+1)-NDUM                                 EDI 240
      ISTART=(NBPTS+1)*11+1                                      EDI 250
      K=2                                                        EDI 260
      WRITE (6,170) TIME,DT                                      EDI 270
      GO TO 110                                                  EDI 280
  140 CONTINUE                                                   EDI 290
      RETURN                                                     EDI 300
C                                                                EDI 310
  150 FORMAT (10X,12E10.3)                                       EDI 320
  160 FORMAT (10X,7HTIME = ,E15.5,7H HOURS.,16H    TIME STEP = ,E14.6,  EDI 330
     1 8H SECONDS.//,10X,6M   X,,M,8X,  4HC(1),8X, 93HC(2)      C(3)     EDI 340
     2  C(4)      C(5)      C(6)      C(7)      C(8)      C(9)      C(10)EDI 350
     3  C(11),/)                                                 EDI 360
  170 FORMAT (10X,7HTIME = ,E15.5,7H HOURS.,16H    TIME STEP = ,E14.6,  EDI 370
     1 8H SECONDS.//,10X,6M   X,,M,8X,  5HC(12),8X, 93HC(13)     C(14)   EDI 380
     2  C(15)     C(16)     C(17)     C(18)     C(19)     C(20)     C(21)EDI 390
     3  C(22),/)                                                 EDI 400
C                                                                EDI 410
      END                                                        EDI 420
      SUBROUTINE LABEL3                                          LAB  10
C                                                                LAB  20
C**************LABEL STREAM TUBE DATA                             LAB  30
C                                                                LAB  40
      WRITE (6,110)                                              LAB  50
      RETURN                                                     LAB  60
C                                                                LAB  70
  110 FORMAT (/,127H                                             LAB  80
     1 U                 M       X     S      DMIX      B      EPS     H LAB  90
     2    LDIFF,//)                                              LAB 100
C                                                                LAB 110
      END                                                        LAB 120
C     ===========================================================ED3  10
      SUBROUTINE EDIT3 (X,J,DMIX,EPS,DIFF,H,U,A,W,S,R,LDIFF)     ED3  20
C                                                                ED3  30
C**************WRITE OUT COMPLETE STREAM TUBE DATA                ED3  40
C                                                                ED3  50
      WRITE (6,110) X,J,R,H,U,A,W,S,DMIX,EPS,DIFF,LDIFF          ED3  60
      RETURN                                                     ED3  70
C                                                                ED3  80
  110 FORMAT (10X,F10.2,I5,5X,5F10.3,F10.8,/3F10.5,F10.6)        ED3  90
C                                                                ED3 100
      END                                                        ED3 110
```

65

RECOMMENDED PROCEDURE FOR THE COMPUTATION OF STREAM TUBE WIDTHS, DEPTHS, AND VELOCITIES

Stream tube dimensions must be chosen so as to satisfy continuity in each. The derivation of Eq. 2.57 requires that there be no flow of water across transverse stream tube boundaries; consequently the discharge in each tube must be the same at all longitudinal computational points. Topographical and hydraulic information are generally available at only a few cross sections in a typical study reach; stream tube dimensions are determined at each of these "reference" sections, and then assigned to intermediate longitudinal computational points by linear interpolation. The computations at a reference section require the cross-sectional geometry and transverse distribution of longitudinal velocity; if only the cross-sectional geometry is known, the velocities may be estimated by a gradually-varied flow computation, described below.

<u>Optional computation of transverse distribution of longitudinal velocity.</u> If velocities must be estimated, topographic information for the reach must be sufficient to describe the cross-sectional geometry at each reference section in terms of bed elevations referenced to a common datum. Once these cross sections have been plotted, each one may be divided into an equal number of rectangular elements, not to be confused with stream tubes. The element widths are chosen to coincide with zones of roughly constant bed elevation as shown on Fig. E.1. The elements at the banks must be chosen so that their bed elevations are below the expected water surface elevation. The computations begin with a straightforward backwater computation, by which the loss of total energy head, i.e., water surface elevation plus velocity head, is balanced by an equivalent friction loss. The friction slope S may be expressed by Manning's equation,

$$S = (\frac{Q}{K_i})^2$$

where Q is the total discharge, and K_i is the total conveyance at the ith reference section. Between any two reference sections i-1 and i the energy equation is

$$y_i + (\frac{Q}{A_i})^2 \frac{1}{2g} + \frac{(x_i - x_{i-1})}{2}[(\frac{Q}{K_i})^2 + (\frac{Q}{K_{i-1}})^2]$$

$$= y_{i-1} + (\frac{Q}{A_{i-1}})^2 \frac{1}{2g} \qquad (E.1)$$

where the friction slope applicable to the reach between i-1 and i has been taken as the average of the slope at the end points, and

y_i = the water surface elevation at point i,

A_i = the cross-sectional area at point i, and

g = gravitational acceleration.

The computation is started with the known water surface elevation at the furthest downstream reference section, L. Then an estimate of the water surface elevation is made for point L-1, and the total conveyance for each cross section is computed as the sum of the conveyances of each element, or
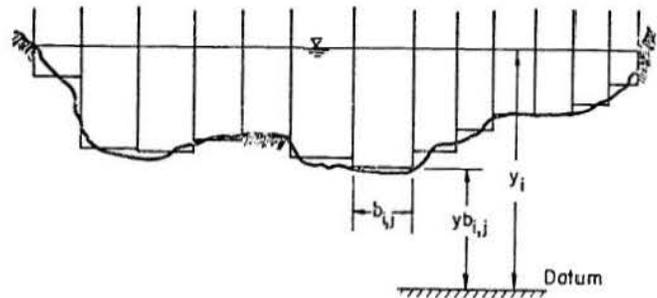
Fig. E.1. Discrete elements for estimation of longitudinal velocities.

$$K_i = \sum_j \frac{1.49}{n_{i,j}} b_{i,j} (y_i - yb_{i,j})^{5/3} \qquad (E.2)$$

where $n_{i,j}$ is the estimated Manning roughness coefficient for the jth element at the ith reference section, and $yb_{i,j}$ is the corresponding bed elevation. The water surface elevation y_{L-1} which satisfies Eq. E.1 is found by a Newton-Raphson iterative computation; once the proper value is found (usually in less than ten iterations) the water surface elevation and the energy slope are stored, and the entire computation repeated at successive upstream sections.

The above procedure establishes the water surface elevations and energy slope for a given discharge Q. Assuming that the Manning equation can be written for each element using the overall energy slope at section i, the longitudinal velocity in each element may be estimated as

$$u_{i,j} = \frac{1.49}{n_{i,j}} (y_i - yb_{i,j})^{2/3} (\frac{Q}{K_i}). \qquad (E.3)$$

It must be emphasized that the velocities estimated by Eq. E.3 are no more valid than the roughness estimates $n_{i,j}$. An estimate of the cross-sectional average Manning coefficient may be based on experience and methods described by Barnes (1967). But transverse variations of depth in Eq. E.3 do not fully account for observed velocity distributions; transverse variations in bed material size and bed forms in alluvial channels, and bank roughness all contribute to an apparent transverse variation of Manning's coefficient. Nonetheless, there is no basis for a computation of this transverse variation, which must therefore be estimated based on the engineer's experience and knowledge of typical transverse velocity distributions. As a first approximation, the estimated cross-sectional average roughness should be decreased slightly in the center of the stream, and increased slightly near the banks.

<u>Stream tube dimensioning by graphical integration.</u> At each reference section i the transverse variations of depth and velocity at the desired discharge must be available either from direct measurements or from an estimate such as that described above. The depth h, velocity u, and the partial discharge hu, are all plotted versus the transverse position z referenced from the left bank (see Fig. E.2). The cumulative partial discharge, defined as

$$q = \int_0^z hu\,dz \qquad (1.32)$$

is then obtained by graphical integration (planimetering) of the partial discharge curve. Since the total discharge at each reference section i may not exactly equal the assumed discharge Q, denote the discharge at each reference section as

$$Q_i = \int_0^B hu\,dz \qquad (E.4)$$

The number of stream tubes, and their individual widths or discharges, must be chosen for the furthest upstream reference section. If the dispersion process to be modeled is expected to occur over the entire cross section, it is usually best to use tubes of equal discharge in each. If, on the other hand, the
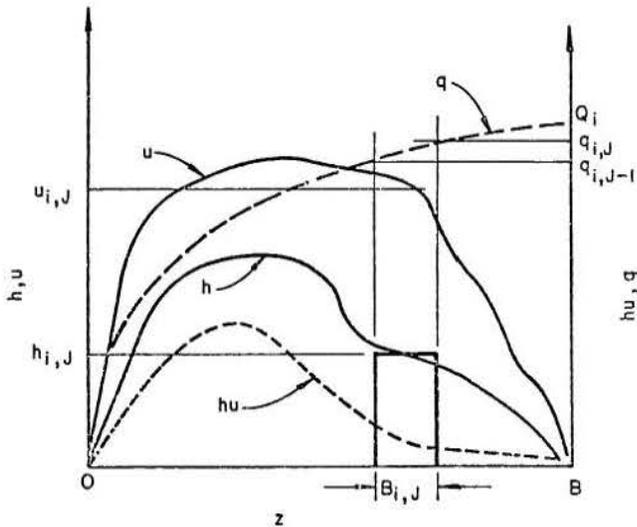
Fig. E.2. Definition sketch for dimensioning of stream tubes.

dispersion is expected to take place primarily near one bank, it is best to use tubes of smaller discharge (narrower width) in that region. The cumulative partial discharge at the right hand boundary of each chosen stream tube J is denoted by q_J. The following procedure is then followed at each reference section i: (see Fig. E.2)

a) Compute the cumulative partial discharge at the right hand boundary of each tube J at reference section i as

$$q_{i,J} = q_J \left(\frac{Q_i}{Q}\right)$$

b) Locate the right hand boundary of each tube J at reference section i by entering the cumulative partial discharge curve for that section with $q_{i,J}$; compute the stream tube widths $B_{i,J}$ by subtraction.

c) Estimate the appropriate stream tube velocity $u_{i,J}$ for each tube using the transverse velocity distribution already plotted.

d) Compute the required depth for each stream tube J as

$$\frac{1}{(Bu)_{i,J}} (q_{i,J} - q_{i,J-1})$$

where $(q_{i,J} - q_{i,J-1})$ is simply the desired discharge in tube J.

e) Adjust the velocity in each stream tube so as to obtain the desired total discharge:

$$u_{i,J} = u_{i,J} \frac{Q}{\displaystyle\sum_J hub}$$

The computation outlined above is best done by hand, since it relies upon the user's judgment as to the appropriate velocity to be assigned to each stream tube. Note that step d) requires a computation of stream tube depth, ensuring that the discrete depths and velocities satisfy the continuous cumulative partial discharge curve at the tube boundaries. Depths thus computed must always be checked against the measured depths falling within that stream tube. The final velocity adjustment e) is required to ensure that continuity is satisfied in each stream tube as well as between overall reference sections.

Once the stream tube dimensions and velocities have been established at the reference sections, the tube depths and widths are established at the computational points by linear interpolation between reference sections. Then tube velocities are determined by dividing the desired tube discharge by the interpolated tube area, thus ensuring that continuity is satisfied.

67

Key Words: Mass Dispersion, Dispersion of Pollutants in
            Channels, Transverse Mixing, Unsteady Mixing

Abstract: The design of waste treatment facilities and the
establishment of effluent standards for rivers require that
the dilution attributable to turbulence be estimated for
particular rivers and particular disposal sites. The ob-
jective of this research was to develop an efficient com-
putational model for the prediction of time-dependent mass
dispersion in natural streams by using the results of
transverse diffusivity in laboratory channels.

   The computational model is a partial differential
equation expressing conservation of pollutant mass in a
control volume. The computational model developed is
based on a finite-difference solution to the depth-
averaged dispersion equation, for predicting concentrations
resulting from a pollutant source of arbitrary time and

space configuration in a stream of any geometry with non-uniform steady flow. Problems of numerical instability and damping in the convective stage of the computation are avoided through the use of a half-implicit and half-explicit second order differencing scheme for the space derivative. The result is a model which is unconditionally stable with accuracy not dependent on the time and distance steps.

The triangular-channel tests performed indicate that the transverse diffusivity is constant within a cross section. This suggests an interaction between bed shear and transverse shear. The applicability of the model is demonstrated through simulation of dispersion experiments for the Missouri River and Clinch River.

Hydrology Paper #78 - "Two-Dimensional Mass Dispersion in Rivers," by Forrest M. Holly, Jr.